Seasonal Dynamics of Organic Matter Turnover in the Arctic Ocean

Dissertation

zur Erlangung des Doktorgrades

– Dr. rer. nat –

der Mathematisch-Naturwissenschaftlichen Fakultät

der Christian-Albrechts-Universität zu Kiel

vorgelegt von

Anabel Charlott von Jackowski

Kiel, Februar 2022

Die vorliegende Doktorarbeit wurde in der Zeit von April 2018 bis Februar 2022 im Forschungsbereichs 2 Marine Biogeochemie, in der Abteilung Biologische Ozeanographie und der Arbeitsgruppe Mikrobielle Biogeochemie am GEOMAR Helmholz Zentrum für Ozeanforschung Kiel angefertigt.

Gutachterin 1:	Prof. Dr. Anja Engel
Gutachterin 2:	Prof. Dr. Ute Hentschel Humeida
Abgabe beim Promotionsbüro:	22.02.2022
Tag der mündlichen Prüfung:	10.05.2022
Genehmigt zum Druck:	17.05.2022

"With
every drop
of water you drink,
every breath you take,
you're connected to the sea.
No matter where you live."
-Sylvia Earle

Summary

The Arctic Ocean is extremely susceptible to climate change, which has led to warmer air temperatures, accelerated sea ice loss, and an intensified inflow of Atlantic water masses into the Arctic. Furthermore, the reduction in sea ice has been linked to a prolonged phytoplankton growth season. Fewer days of sea ice cover and thinner sea ice increases the light availability for ice algae and expands the habitat for pelagic phytoplankton. An extension of the growth season prolongs the release of phytoplankton-derived organic matter with consequences for the seasonal carbon cycle. However, the seasonal carbon stock and microbial processes are largely unexplored because many parameters require *in situ* sampling. A systematic strategy to enhance microbial observations is through time series stations. The long-term ecological research observatory HAUSGARTEN was established in 1999 and is the only pelagic microbial observatory in the Arctic to date. The observatory is sampled annually during the summer months, which limits its explanatory power to assess the seasonal carbon cycling and microbial dynamics. To close this gap, the goals of this doctoral project were to *(a)* investigate the seasonal variability of organic matter, *(b)* explore seasonal organic matter turnover and the microbial community, and *(c)* evaluate the inter-annual variability in the Fram Strait.

Organic matter is the dominant seasonal control on microbial dynamics (Manuscript 1) and shifts in the microbial community (Manuscript 2) in the eastern Fram Strait between summer and fall 2018. Our efforts to extend the summertime sampling frequency at HAUSGARTEN unprecedentedly provide a baseline for dissolved organic carbon, dissolved combined carbohydrates, dissolved hydrolyzable amino acids, and gel particles during fall. This is the first study to highlight a decoupling in the major classes of gel particles, namely transparent exopolymer particles and Coomassie stainable particles. Discovering the uncoupled seasonal variability shows that different classes of particles have a unique significance in marine biogeochemical processes. Moreover, the availability of organic matter controlled bacterial production, microbial abundances, and the microbial community. Identifying the microbial community composition revealed a low diversity with a dominance of polysaccharide-degrading bacteria in summer, which shifted to wider diversity including microbes that assimilate refractory biopolymers in fall. Our aim to combine the available organic matter pool and taxonomy of microbes is a novel approach in order to understand microbial substrate regimes.

To showcase the spatial and temporal variability of microbial organic matter turnover, we generated a high-resolution analysis for Fram Strait from 2009 to 2019 (Manuscript 3). Our study combines year-round remote sensing approaches with *in situ* biogeochemical and microbial parameters from

HAUSGARTEN during summer, which revealed a fundamental link of microbial dynamics to the regional oceanography. The remotely sensed bloom dynamics contextualized the inter-annual *in situ* variability of organic matter bioavailability, bacterial production, and microbial abundances of the HAUSGARTEN time series dataset. In the northward flowing Atlantic waters, the slowly terminating pelagic phytoplankton bloom releases organic matter that stimulates rapid microbial turnover. In the southward flowing polar waters, the remote sensing analysis revealed a phytoplankton bloom peak around May, which is prior to our *in situ* sampling period, resulting in relatively low concentrations of organic matter. In addition to organic matter, the cold temperatures co-limit bacterial production and microbial abundances. Our approach to combine the remote sensing with microbial observations contextualizes the inter-annual variability observed at HAUSGARTEN.

This thesis contributes to a better understanding of the seasonal biogeochemical and microbial coupling in the Arctic. Our collected data provides a baseline for microbial observations during fall, contributes to a better understanding of seasonal gel particle dynamics, and explores the spatio-temporal microbial substrate regimes. Applying a multi-disciplinary approach has advanced the understanding of seasonality in biogeochemical and microbial processes across the Fram Strait. This newly acquired knowledge highlights current seasonal dynamics in the Arctic microbial loop that are essential to accurately assess the transformations in a rapidly changing Arctic Ocean.

Zusammenfassung

Der Arktische Ozean ist extrem anfällig für den Klimawandel. Der Klimawandel erwärmt die Lufttemperaturen, beschleunigt die Abschmelzung des Meereises und verstärkt den Zufluß atlantischen Meerwassers in die Arktis. Des Weiteren wird der drastische Rückgang des Meereises mit einer Verlängerung der Wachstumssaison des Phytoplanktons in Verbindung gebracht. Zeitlich verkürzte Meereisbedeckung und dünneres Meereis erhöhen die Lichtverfügbarkeit für Eisalgen und erweitern den Lebensraum für pelagisches Phytoplankton. Eine verlängerte Wachstumssaison erhöht die Freisetzung von organischer Masse durch das Phytoplankton, was sich auf den saisonalen Kohlenstoffkreislauf auswirkt. Der Kohlenstoffbestand und die mikrobiellen Prozesse waren bisher weitgehend unerforscht, da viele Parameter nur durch *in situ* Proben erfaßt werden können. Eine Strategie zur Verbesserung der mikrobiellen Beobachtungen sind Zeitreihen. Die einzige arktische Zeitreihe „HAUSGARTEN“ existiert seit 1999 in der Framstraße. HAUSGARTEN wird jährlich während der Sommermonate beprobt, was jedoch nur eine begrenzte Aussagekraft hat, um die saisonale Dynamik des Kohlenstoffkreislaufes und der Mikroben zu erfassen. Zur Schließung dieser Wissenslücke waren die Ziele dieses Promotionsprojekts *(a)* die Untersuchung der saisonalen Variabilität des Kohlenstoffkreislaufes, *(b)* die Erforschung des saisonalen Umsatzes von organischer Masse und der mikrobiellen Gemeinschaft und *(c)* die Bewertung der zwischenjährlichen Variabilität in der Framstraße.

Die organische Masse ist der wichtigste saisonale Kontrollfaktor für die mikrobielle Dynamik (Artikel 1) und die Veränderungen in der mikrobiellen Gemeinschaft (Artikel 2) in der östlichen Framstraße während Sommer und Herbst 2018. Unsere zusätzlichen Einsätze im Herbst, statt der bisher einmal jährlichen Messung in den Sommermonaten, liefern eine einzigartige Datenbasis an gelösten organischen Kohlenstoffanteilen, gelösten kombinierten Kohlenhydraten, gelösten hydrolisierbaren Aminosäuren und Gel-Partikel. Obwohl Gel-Partikel in vorherigen Studien schon in der Framstraße nachgewiesen wurden, hat unsere Publikation als Erste, eine noch bisher nicht nachgewiesene saisonale Entkopplung zwischen den transparenten exopolymeren Partikeln und den Coomassie-färbbaren Partikeln gezeigt. Dabei ist hervorzuheben, dass die nachgewiesene saisonale Entkopplung der Partikelklassen eine einzigartige Bedeutung für biogeochemischen Prozesse im Meer hat. Darüber hinaus kontrollierte die Verfügbarkeit von organischen Substraten die bakterielle Produktion, die Zellzahlen und die Verschiebung der Zusammensetzung der Mikroben. Deutliche Veränderungen in der Zusammensetzung der Mikroben wurden mit einer Dominanz von Polysaccharid-abbauenden Bakterien im Sommer und einer Verlagerung zu einer höheren mikrobiellen Diversität einschließlich

Mikroben welche refraktäre Biopolymere verarbeiten, nachgewiesen. Unser neuartiger Ansatz, den verfügbaren Pool an organischer Masse und die Taxonomie der Mikroben zu kombinieren erweitert unser Verständnis mikrobieller Substratverhältnisse.

Weiterführend wurde erstmalig eine hochauflösende räumliche und zeitliche Analyse der organischen Substanzen in der gesamten Framstraße von 2009 bis 2019 vorgestellt (Artikel 3). Der Einsatz von durchgehenden Satelliten-Fernerkundungsmethoden in Kombination mit *in situ* biogeochemischen und mikrobiellen Analysen zeigte, dass die mikrobielle Dynamik grundlegend mit der regionalen Ozeanographie verbunden ist. In der nördlich fließenden atlantischen Strömung setzt die langsam abklingende pelagische Phytoplanktonblüte im Sommer organische Masse frei, das den schnellen mikrobiellen Umsatz anregt. Hingegen wird in der nördlich fließenden polaren Strömung der Höhepunkt der Phytoplanktonblüte schon im Mai erreicht, also vor unserem Probenentnahmezeitraum, was zu relativ geringen Konzentrationen an nachgewiesener organischer Masse führt. Zusätzlich zur organischen Masse scheinen auch die niedrigen Temperaturen die bakterielle Produktion und die Zellzahlen im Sommer zu begrenzen. Die per Satelliten-Fernerkundungsbeobachtungen ermittelte Blütendynamik stellt die interannuelle In-situ-Variabilität der Bioverfügbarkeit organischer Stoffe, der bakteriellen Produktion und der Zellzahlen des HAUSGARTEN-Zeitreihendatensatzes in einen Zusammenhang. Unser Ansatz, die Fernerkundung mit mikrobiellen Beobachtungen zu kombinieren, ermöglicht es, die bei HAUSGARTEN beobachtete interannuelle Variabilität in einen Kontext zu bringen.

Die im Rahmen dieser Arbeit gewonnenen Erkenntnisse tragen zu einem besseren Verständnis der saisonalen biogeochemischen und mikrobiellen Kopplung in der Arktis bei. Die von uns gesammelten Daten liefern eine Grundlage für mikrobielle Beobachtungen im Herbst, tragen zu einem besseren Verständnis der saisonalen Gelpartikeldynamik bei und erforschen die räumlich-zeitlichen mikrobiellen Substratregime. Der multidisziplinäre Ansatz hat das Verständnis der saisonalen biogeochemischen und mikrobiellen Prozesse in der Framstraße verbessert. Dieses neu erworbene Wissen hebt die aktuelle saisonale Dynamik in der arktischen mikrobiellen Schleife hervor, die für eine genaue Bewertung der Umwandlungen in einem sich schnell verändernden Arktischen Ozean entscheidend ist.

Table of Contents

List of Abbreviations

ANOSIM ..... analysis of similarity
ASV ..... amplicon sequence variant
AW ..... Atlantic water
BDCM ..... below deep chlorophyll maximum
Chl-*a* ..... chlorophyll-*a*
C:N ..... carbon to nitrogen ratio
C:N:P ..... carbon to nitrogen to phosphate ratio
CSP ..... Coomassie stainable particles
CTD ..... conductivity temperature depth profiler
Da ..... Dalton
DCCHO ..... dissolved combined carbohydrates
DCM ..... deep chlorophyll maximum
DIC ..... dissolved inorganic carbon
DHAA ..... dissolved hydrolyzable amino acids
DNA ..... deoxyribonucleic acid
DOM ..... dissolved organic matter
DOC ..... dissolved organic carbon
DON ..... dissolved organic nitrogen
DOP ..... dissolved organic phosphorus
EGC ..... East Greenland Current
ESD ..... equivalent spherical diameter
HMW ..... high-molecular-weight
HNA ..... high nucleic acids
HPAEC ..... high-performance anion-exchange chromatography
HPLC ..... high-performance liquid chromatography
kDa ..... kilodaltons
LDOC ..... labile DOC
LMW ..... low-molecular-weight
LNA ..... low nucleic acids
LTER ..... long-term ecological research
NMDS ..... non-metric multidimensional scaling
PAD ..... pulsed amperometric detection
PCA ..... principal component analysis
PgC ..... petagram carbon
POM ..... particulate organic matter
POC ..... particulate organic carbon
PW ..... polar water
RDA ..... redundancy analysis
RNA ..... ribonucleic acid
rRNA ..... ribosomal RNA
TEP ..... transparent exopolymer particles
TEP-C ..... transparent exopolymer particle carbon content
SLDOC ..... semi-labile DOC
WSC ..... West Spitsbergen Current

List of Figures

List of Tables

Chapter 1

General Introduction

Marine Carbon Cycle

The ocean plays a vital role in the global carbon cycle and therewith the regulation of Earth's climate. In recent decades, the Earth's climate has been progressively impacted by anthropogenic emissions of greenhouse gases into the atmosphere, like carbon dioxide (CO_2) and methane (CH_4). The atmosphere is in permanent exchange with the surface layer of the ocean and increasing CO_2 concentrations in the atmosphere also increase the amount of dissolved CO_2 in the surface ocean. Accordingly, the oceans play a key role in CO_2 uptake via physicochemical and biological processes.

The solubility pump is the physiochemical transport of carbon from the euphotic zone (surface-200 m) to the meso- and bathypelagic zones (200-4000 m). In the euphotic zone, atmospheric CO_2 dissolves and reacts with water molecules to form carbonic acid (H_2CO_3), carbonate ions (HCO_3^{2-}), or bicarbonate (HCO_3^-; Fig. 1.1). These ionic and non-ionic species, collectively known as dissolved inorganic carbon (DIC), account for the largest carbon reservoir of ~38,000 PgC on Earth (Ciais et al., 2013). The dissolution of atmospheric CO_2 is temperature-dependent, which results in a higher relative net export of DIC to the meso- and bathypelagic zones in polar regions and a lower net export in equatorial regions. Hence, the temperature-dependency of the solubility pump makes it sensitive to climate change. Once the exported DIC reaches the meso- and bathypelagic zones, it can be stored for many thousands of years, during which carbon is not exchanged with the atmosphere (Sabine et al., 2004).

The biological carbon pump is driven by the export of organic carbon into the ocean interior. In the euphotic zone, phytoplankton fix an estimated ~45 PgC yr^{-1} into organic carbon through photosynthesis (Behrenfeld & Falkowski, 1997). Phytoplankton-derived organic carbon can be categorized into dissolved organic carbon (DOC) or particulate organic carbon (POC; Fig. 1.1). A large fraction of DOC supports microbes (here, archaea and bacteria) and is rapidly mineralized back into CO_2, while a small fraction is stored in the ocean for hundreds to millions of years (Azam et al., 1983; Sarmiento & Gruber, 2006). POC predominately contributes to the flux of detritus to the seafloor that accounts for ~10 PgC yr^{-1} (Fig. 1.1). Furthermore, DOC and POC cycling is coupled to heteroatoms, such as nitrogen (N) and phosphorus (P), that are major constituents of organic matter and together form the basis of marine food webs.

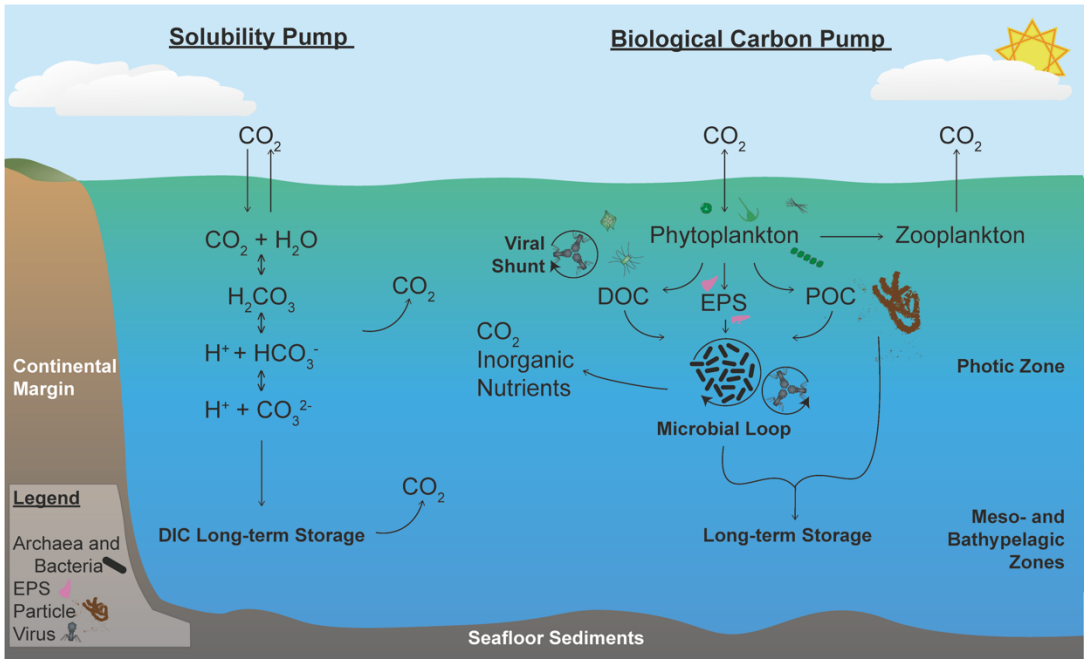

Figure 1.1 | Schematic illustrating the transport of carbon in the ocean. The solubility pump (left) transports atmospheric carbon dioxide (CO_2) that reacts to form carbonic acid (H_2CO_3), bicarbonate (HCO_3^-), and carbonate (CO_3^{2-}) as dissolved inorganic carbon (DIC) for long-term storage in the meso- and bathypelagic zones. The biological carbon pump (right) involves the photosynthetic production of phytoplankton-derived dissolved organic carbon (DOC), and particulate organic carbon (POC). DOC can be remineralized by archaea and bacteria as part of the microbial loop, which releases CO_2. POC, extracellular polymeric substances (EPS) and larger particles eventually sink to provide long-term storage in the meso- and bathypelagic zones or through burial. The figure is based on Buchan et al. (2014) and Arnosti et al. (2021).

Marine Primary Production

Primary production is the conversion of inorganic CO_2 into organic matter. Marine primary production typically refers to the synthesis of organic matter by phytoplankton (here, eukaryotic algae and cyanobacteria) via photosynthesis, which is limited by light and nutrient conditions. Light availability can vary globally from diurnal cycles in equatorial regions to a strong seasonality in polar regions. Additionally, polar regions are subjected to a low solar angle and sea ice, which can severely reduce the light availability in the euphotic zone (Arrigo, 2014; Lee et al., 2015; Popova et al., 2012). Moreover, phytoplankton are strongly dependent on macronutrients that prompt their relative biomolecule composition. Under optimal nutrient replete conditions, phytoplankton synthesize amino acids, proteins, nucleotides, and membrane lipids (Table 1.1). In contrast, nutrient limiting conditions prompt phytoplankton to invest in the synthesis of carbon-rich compounds such as carbohydrates and storage lipids (Table 1.1; Granum et al., 2002; Janse et al., 1996). Overall, light and nutrient conditions delegate

phytoplankton growth and can give rise to a phytoplankton bloom under cumulative conditions.

Phytoplankton blooms are highly dynamic phenomena that include groups such as Bacillariophyta and Haptophyta. In terms of biomass, blooms tend to be largely dominated by bacillariophytes like diatoms (Lampe et al., 2021; Teeling et al., 2012). Diatoms are a diverse taxonomic group with over 1,000 species that have cell sizes of an equivalent spherical diameter (or ESD) ~5-50 µm and a high nutrient demand (Lampe et al., 2021; Smetacek, 2000). However, in terms of cell numbers, phytoplankton blooms tend to be largely dominated by haptophytes like *Phaeocystis* species (Lampe et al., 2021; Teeling et al., 2012). *Phaeocystis* species feature small cells of an ESD ~2 µm that facilitate a high surface-to-volume ratio and enables an efficient metabolism under nutrient-depleted conditions (Lampe et al., 2021; Reid et al., 1990). As the bloom terminates, phytoplankton become increasingly constrained by nutrient depletion, predator grazing, and viral infections resulting in organic matter release. Phytoplankton exudate between 10-50% of organic matter, which generates a unique fingerprint of compounds available to microbes (Baines & Pace, 1991; Biddanda & Benner, 1997; Teira et al., 2001, 2003; Thornton, 2014).

Table 1.1 | Elemental composition of biomolecules in phytoplankton. The table is adapted from Geider & La Roche (2002).
Abbreviations: *R* refers to a side-chain and possible elements include carbon (C); hydrogen (H); nitrogen (N); oxygen (O); phosphorus (P); sulfur (S).

	Major Elements	Elemental Composition
Carbohydrates	CHO	$C_6H_{12}O_6$
Amino acids	*R*-CHNO	-
Protein[a]	R-CHNO	$C_{4\cdot43}H_7O_{1\cdot44}N_{1\cdot16}S_{0\cdot19}$
Storage Lipids [b]	CHOP(N)	$C_{40}H_7O_{74}N_5$
Membrane Lipids [c]	CHOP(N)	$C_{37\cdot9}H_{72\cdot5}O_{9\cdot4}N_{0\cdot43}P_1$
DNA[d]	CHONP	$C_{9\cdot75}H_{14\cdot25}O_8N_{3\cdot75}P$
RNA[e]	CHONP	$C_{9\cdot5}H_{13\cdot75}O_8N_{3\cdot75}P$

[a]Based on Laws (1991).
[b]This excludes phosphoglycerides.
[c]Assumes equal moles of phosphorus in phophatidylinositol, phophatidic acid, phophatidylglycerol, diphosphatidylglycerol, phosphatidylethanolamine, phosphatidylcholine and phosphatidylserine.
[d]Assumes equal moles of adenylic, cytidylic, guanylic and uridylic acids.
[e]Assumes equal moles of deoxyadenylic, deoxycytidylic, deoxyguanylic and deoxythymidic acids.

Marine Secondary Production

Secondary production is the conversion of organic matter to produce heterotrophic biomass. In the ocean, microbes remineralize phytoplankton-derived organic matter into cellular biomass and produce CO_2 through respiration. Microbial transformed organic matter has several possible fates in the ocean: direct remineralization, continual recycling in the microbial loop, resist degradation and storage in the ocean or transfer to higher trophic levels as a result of microbial predation (Fig. 1.1; Azam et al., 1983; Pomeroy, 1974).

Microbes are opportunistic in their assimilation of organic matter, which has allowed a high degree of niche specialization among closely related taxa. The niche adaptation classify microbes as free-living or particle-associated (Crump et al., 1998, 1999; Stocker, 2012). Free-living microbes reside in the water column and are commonly linked to phytoplankton blooms that include phylotypes of *Bacteroidia* (*Formosa*, *Polaribacter*, and *Ulvibacter*), *Alphaproteobacteria* (*Roseobacter*-related), and *Gammaproteobacteria* (Table 1.1; McCarren et al., 2010; Teeling et al., 2012). Only around 3-5% of microbial taxa colonize organic particles that provide niches for *Alphaproteobacteria* (*Rhodobacterales*), and *Gammaproteobacteria* (*Alteromonadales;* Buchan et al., 2005; Fadeev et al., 2018). In addition to the microbial niche, particles also transport microbes out of the euphotic zone. As the particles sink, microbes release organic matter into the surrounding water and provide important resources for the microbes in meso- and bathypelagic zones and seafloor sediments. Interestingly, the microbial community shows a relative shift from bacteria in the euphotic zone to archaea, like *Thaumarchaeota*, in the mesopelagic zone (Table 1.2; Acinas et al., 2021; González et al., 2008; Karner et al., 2001; Zhong et al., 2020). However, despite major advances in molecular approaches and sequencing technologies, i.e., universal marker gene 16S rRNA and metagenomics, relatively little is known about the specific roles that microbes play in shaping organic matter or vice versa.

Continuum from dissolved to particulate organic matter

Traditionally, organic matter has been classified as either dissolved organic matter (DOM) or particulate organic matter (POM) based on the filtration behavior (Verdugo et al., 2004). DOM passes through a filter with a pore size of 0.7 µm, while POM is retained on a filter with a pore size of 0.7 µm.

Table 1.2 | Key taxonomic groups and their function in the pelagic microbial community.
Abbreviations: dimethyl sulfide (DMS); dimethylsulfoniopropionate (DMSP)

Taxonomy (Domain / Phylum / Class)	Distinct Function	Literature
Bacteria/Bacteroidetes/ Bacteroidia	degradation of various organic biopolymers	Teeling et al. (2012)
Bacteria/Proteobacteria/ Alphaproteobacteria	specialized in DMS/DMSP turnover	Giovannoni et al. (2014) Giovannoni (2017)
Bacteria/Proteobacteria/ Deltaproteobacteria	oxidize sulfur and methylated compounds	Swan et al. (2011)
Bacteria/Proteobacteria/ Gammaproteobacteria	associated to particles	Buchan et al. (2014)
Bacteria/Verrucomicrobia/ Verrucomicrobiae	degradation of glycopolymers	Spring et al. (2016)
Archaea/Thaumarchaeota/ Nitrososphaeria	chemolithoautotrophs and specialized in ammonia-oxidation	González et al. (2008) Karner et al. (2001)

DOM is a complex mixture of truly dissolved compounds to colloidal fractions that are continually reshaped in the ocean (Fig. 1.2; Benner et al., 1992). The reshaping of DOM is largely performed by microbes that dynamically interact with their surroundings and alter the composition and availability of DOC. To simplify the range of DOC availability, researchers have defined five subfractions: labile DOC (LDOC), semi-labile DOC (SLDOC), semi-refractory DOC (SRDOC), refractory DOC (RDOC), and ultra-refractory DOC (URDOC). LDOC is the most reactive pool and supports the microbial loop resulting in a short residence time of minutes to hours (Keil & Kirchman, 1999). SLDOC is the supplemental material for the microbial loop and can resist rapid microbial turnover that allows it to accumulate in the photic zone during the productive season with residence times of weeks to months (Carlson & Ducklow, 1995; Hansell et al., 2009). SRDOC, RDOC, and URDOC resist microbial turnover resulting in an accumulation in the meso- and bathypelagic zones with residence times from decades to millennia (Hansell et al., 2009).

DOM polymers are also excreted as extracellular polymeric substances (EPS). EPS have a three-dimensional porous polymer matrices that spontaneously disperse or assemble into nanogels and further anneal into more stable micro- and macrogels (Fig. 1.2; Chin et al., 1998). The porous polymer matrices are transparent but can be visualized using compound-specific stains. Alcian Blue is a cationic copper-phthalocyanine dye that

reacts with the carboxyl and sulfate half ester functional groups of mucopolysaccharides and glycosaminoglycans to stain polysaccharide-containing gels, referred to as transparent exopolymer particles (TEP; Alldredge et al., 1993; Parker & Diboll, 1966; Schuster & Herndl, 1995). Another dye, Coomassie Brilliant Blue is a disulfonated triphenylmethane dye that binds proteins and peptides to stain proteinaceous-containing gels, referred to as Coomassie stainable particles (CSP; Chial & Splittgerber, 1993; Long & Azam, 1996). The polymer matrices of TEP and CSP represent substrates for microbes but also provide the sticky glue for the particle coagulation, e.g., marine snow, and enhance the POM export towards the seafloor (Chow et al., 2015; Engel, 2000; Logan et al., 1995).

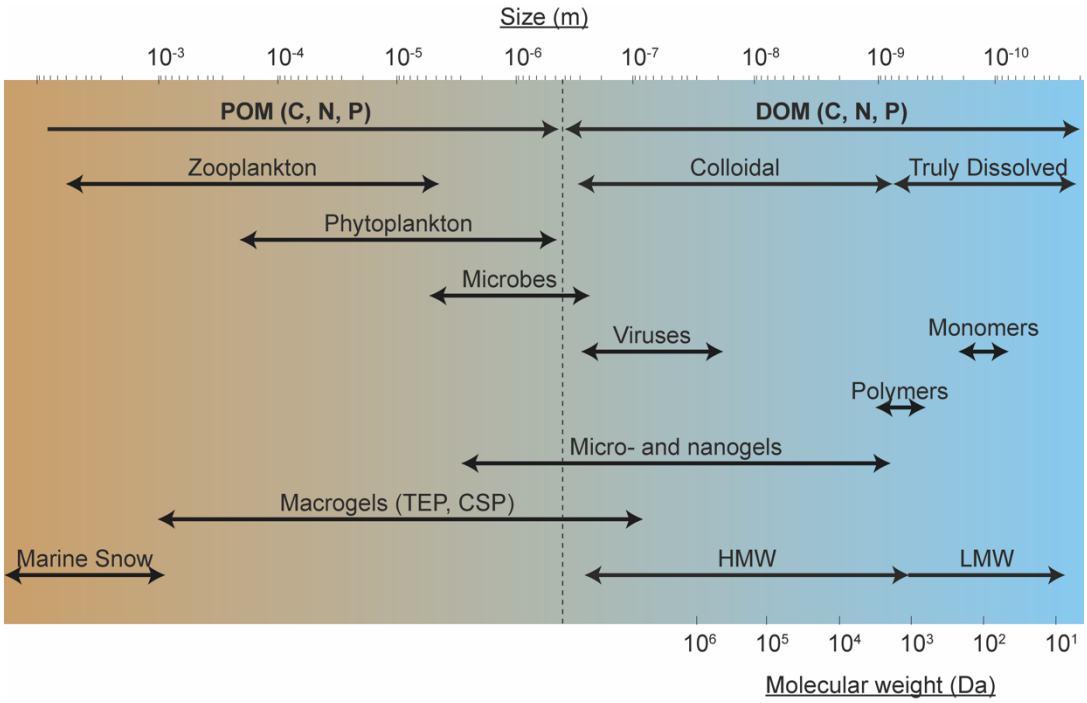

Figure 1.2 | Size continuum organic matter in seawater and ecology. Organic matter that is retained on a 0.7 µm pore-sized filter is categorized as particulate organic matter (POM), while the fraction percolates through the filter is categorized as dissolved organic matter (DOM). DOM is subcategorized into truly dissolved (<1 nm) colloidal (1-1000 nm) fractions or low-molecular-weight (LMW, <1000 Dalton) and high-molecular-weight (HMW, >1000 Dalton) fractions. DOM maintains a reversible assembly/dispersion equilibrium that forms nano-, microgels that eventually form macrogels. Macrogels like transparent exopolymer particles (TEP) and Coomassie stainable particles (CSP) form the matrix or “glue” of marine snow and larger particles in the POM range. The figure is adapted from Verdugo et al. (2004) and Verdugo (2012). Note: Monomer range only includes carbohydrate and amino acid monomers.

POM contains suspended and sinking particles that include the biomass from living and dead cells, gel particles, marine snow, fecal pellets, and other aggregated material. Furthermore, microplastics are a new anthropogenic addition to the POC pool (Law, 2017). Altogether, the sinking material is a key component of the biological carbon pump by exporting around 10%POC to the bathypelagic zones and eventually around 1%POC to the seafloor (Boyd & Trull, 2007; Cavan et al., 2015; Eppley & Peterson, 1979; J. H. Martin et al., 1987; Le Moigne, 2019; Volk & Hoffert, 1985).

Molecular Composition of Organic Matter

The bioavailability and turnover of DOM and POM is strongly dependent on the molecular composition (Arnosti, 2004). Molecular indicators of bioavailability include carbohydrates, amino acids, and fatty acids. These molecular indicators exist in variable sizes of monomers, oligomers, and polymers that can be size-fractionated according to their bioreactivity. In the conceptual size-reactivity framework, the bioreactivity increases from low-molecular-weight DOM (LMW DOM, <1 kDa) compounds, i.e., monomers, to high-molecular-weight DOM (HMW DOM, >1 kDa) compounds, i.e., oligomers and polymers (Fig. 1.2; Amon & Benner, 1994, 1996; Benner & Amon, 2015)

Carbohydrates constitute approximately 15-50% of DOC and 8-10% of suspended POC (Benner et al., 1992; McCarthy et al., 1996; Pakulski & Benner, 1994; Panagiotopoulos & Sempéré, 2005). Carbohydrates are structurally diverse with a size range from individual monosaccharides to oligosaccharides (~10 monosaccharides) and polysaccharides (>10 monosaccharides) that are linked via hydroxyl groups. Monosaccharides comprise around one-third of the total carbohydrate pool and are a relatively consistent fraction of LMW DOM (Lin & Guo, 2015; Myklestad & Børsheim, 2007). The largest characterizable carbohydrate fraction, with 10-35% of DOC, is composed of dissolved combined carbohydrates (DCCHO) that show a spatial and seasonal variability (Aluwihare et al., 1997; Benner et al., 1992; Borch & Kirchman, 1997; Kirchman et al., 2001; Skoog & Benner, 1997). Efforts to fully characterize the carbohydrate composition have been constrained by analytical challenges of polysaccharide solubility, size, and spectroscopic characteristics (Arnosti et al., 2021). Ideally, established analytical methods would characterize the monomer identity and polymer associated branches, branch position, and functional groups. However, none of the established methods provide all of the information (Panagiotopoulos & Sempéré, 2005).

For example, high-performance anion-exchange chromatography with pulsed amperometric detection (HPAEC-PAD) uses acid hydrolysis to chemically break the polymers into quantifiable monomer concentrations (Borch & Kirchman, 1997; K. Kaiser & Benner, 2000). HPAEC-PAD is extremely advantageous because it allows for the derivatization and differentiation of neutral sugars, amino sugars, and acidic sugars at the nanomolar level (Engel & Händel, 2011). Further developing analytical techniques with high accuracy and precision minimizes the gap to the uncharacterized compounds in organic matter.

Another widely studied component of organic matter are amino acids. Amino acids consist of individual units and peptides (>2 amino acids) linked via peptide bonds. Amino acids constitute a large fraction of bacterial carbon demand but also supply microbes with nitrogen (Jorgensen et al., 1993). Taking advantage of the bacterial carbon demand of amino acids has been used to quantify compositional changes of bulk DOC using degradation indices and carbon-normalized yields to quantify the bioavailability of DOC (Dauwe et al., 1999; Davis et al., 2009; K. Kaiser & Benner, 2009). A common method to quantify amino acid concentrations uses acid hydrolysis to chemically break peptides, followed by ortho-phthaldialdehyde derivatization and high-performance liquid chromatography (HPLC) analysis (Dittmar et al., 2009; Lindroth & Mopper, 1979).

Lipids constitute <0.1% of DOC and a minor component of POC (Kharbush et al., 2020; Liu et al., 1998; Ogawa & Tanoue, 2003). Nonetheless, the diversity of lipid compounds are commonly employed as biomarkers to elucidate novel carbon cycling and export pathways (Becker et al., 2018; Laber et al., 2018). Furthermore, microbial conversion of organic carbon can also be traced using various isotope labeling techniques that are new adaptations of routine labeling techniques (Dippold & Kuzyakov, 2013; Dong et al., 2017, 2019; Evans et al., 2018, 2019; Kellermann et al., 2016; Wegener et al., 2012).

Microbial processing constantly alters the bioavailability of substrates leaving behind more recalcitrant DOC. To quantify the bulk DOC pool, the scientific community has begun to generate organic matter inventories for the Atlantic Ocean (e.g., Aminot and Kérouel, 2004; Piontek et al., 2011; Engel et al., 2017b), Pacific Ocean (e.g., Kaiser and Benner, 2009; Loginova et al., 2019; Maßmig et al., 2020), Indian Ocean (e.g., Doval and Hansell, 2000; Krishna et al., 2015), Southern Ocean (e.g., Norman et al., 2011; Bercovici and Hansell, 2016), and Arctic Ocean (e.g., Amon, 2003; Engel et al., 2019;

Nöthig et al., 2020). A global organic matter inventory is particularly valuable to assess the feedback between climate systems, nutrient regimes, and microbial community structure that alter DOC bioavailability on seasonal and decadal time scales (Wagner et al., 2020). However, the global inventories lack a seasonal component for regions that are experiencing rapid environmental transformations, like the Arctic Ocean due to climate change. This data gap needs to be addressed in order to successfully assess the extent of climate change on biogeochemical cycles.

Microbial Dynamics in the Arctic Ocean

Arctic marine ecosystems are rapidly changing as a consequence of climate change (Wassmann et al., 2011). Climate change is the main factor for the staggering decrease in the sea ice minima from 6.9 million km^2 in 1979 to 4.7 million km^2 in 2021 (National Snow and Ice Data Center/NASA, USA). A reduction in sea ice creates a positive feedback loop that further reduces the planetary albedo and reinforces melting processes, amplifies under-ice light, and water column stratification (Arrigo & van Dijken, 2015; Beszczynska-Moller et al., 2012; Serreze et al., 2007). The plethora of environmental transformations could have far-reaching implications for the primary and secondary production in the Arctic Ocean.

Estimates of primary production in the Arctic basins are among the lowest worldwide (Sakshaug, 2004). Arctic primary production is constrained by the solar irradiance and nutrient stocks from winter mixing (Ardyna et al., 2011; Popova et al., 2010). When the light becomes available for primary production, the conditions facilitate pelagic phytoplankton blooms in the water column but also coupled to sea ice (Fig. 1.3). Sea ice facilitates ice-attached blooms, under-ice blooms, and ice-edge blooms in marginal ice zones (Arrigo, 2014; Arrigo et al., 2012; Barber et al., 2015). In particular, ice-attached *Melosira arctica* can develop dense blooms that, if released from the ice, rapidly sink to the seafloor and contribute to the vertical flux (Fig. 1.3; Boetius et al., 2013; Fernández-Méndez et al., 2014; Poulin et al., 2014). The ice algal aggregates provide niches and transport microbes to the seafloor (Rapp et al., 2018). The microbial niche specialization is likely to be lost from an Arctic Ocean, devoid of sea ice.

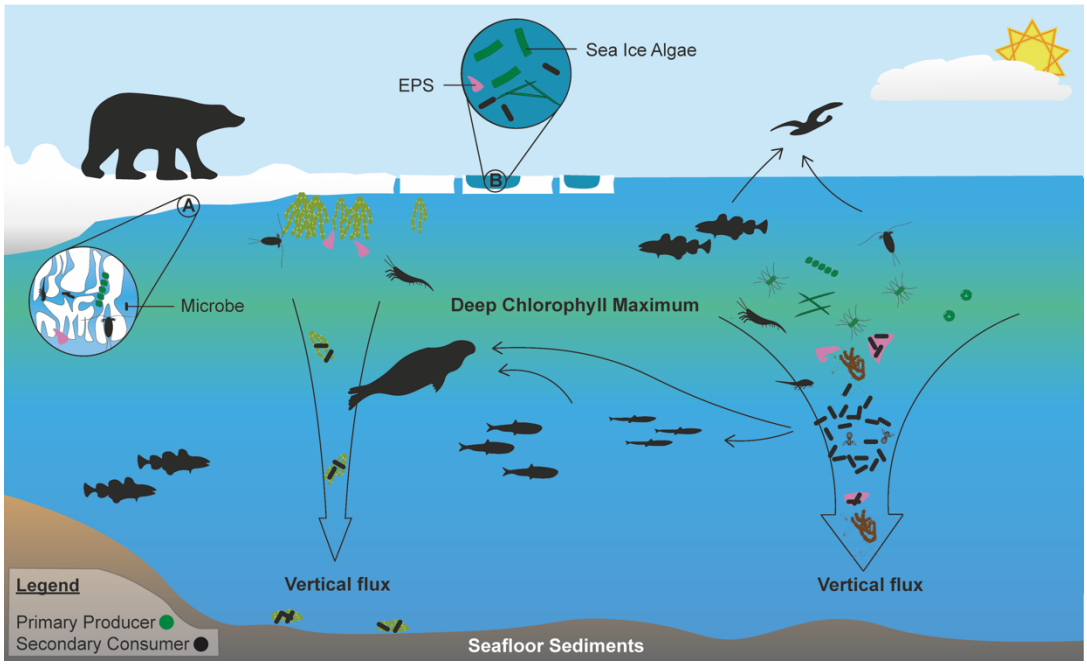

Figure 1.3 | Conceptual pelagic Arctic food web. This illustration shows a vertically-structured concept of sea ice and the underlying water column in the Atlantic basin. (A) shows the brine channels within the ice matrix that provide niches for phytoplankton, microbes, and zooplankton. (B) Melt ponds provide niches for sea ice, diatoms like *Pseudonituschia sp. and Fragilariopsis*, microbes, and extracellular polymeric substances (EPS). Below the sea ice, under ice algal mats form that occasionally sinks to the seafloor and contribute to the vertical flux. In the open water column, the phytoplankton release organic matter that is remineralized by microbes but also aggregates into EPS and particles that eventually contribute to the vertical flux. The primary producers are colored in green and the consumers in black. The figure was based on Boetius et al. (2015) and Wassmann et al. (2020).

Microbial secondary production tends to be controlled by temperature and the availability of DOM in the Arctic Ocean (Kirchman, Morán, et al., 2009; Ortega-Retuerta et al., 2014; Piontek et al., 2014; Sala et al., 2010; Wiebe et al., 1992). Temperature affects biological rate processes by lowering the activation energy of enzymes. In microbes, the temperature affects the processing of carbon (Hall et al., 2008; Pomeroy & Deibel, 1986; Pomeroy & Wiebe, 2001). However, the stand-alone effect of temperature may be overestimated given that the bioavailability of DOM is of equal importance, if not greater, than that of temperature for microbes in polar regions (Ducklow et al., 2012; Piontek et al., 2015).

Ongoing changes in marine ecosystems are best detected and tracked by establishing time series. To monitor food web structures and ecosystem functioning in the Arctic Ocean, the Alfred Wegener Institute Helmholtz Centre for Polar and Marine Research (AWI) established the Long-Term Ecological Research (LTER) observatory “HAUSGARTEN” in the

Fram Strait in 1999 (Fig. 1.4). Since 1999, summer expeditions have regularly sampled for phytoplankton biomass and organic matter in the water column along with a wide array of parameters in benthos in the eastern Fram Strait (Nöthig et al., 2020; Soltwedel et al., 2005, 2016). The pelagic sampling efforts were extended by researchers who established the *Plankton Ecology and Biogeochemistry in a Changing Arctic Ocean* (PEBCAO) group in 2009. The sampling strategy of PEBCAO targets biogeochemical parameters coupled with microbiological, microscopical, molecular biological, and physiological methods to investigate the bacterio-, phyto- and zooplankton composition and biodiversity in the water column at HAUSGARTEN ("PEBCAO," 2020). To continue assessing the ecological and biogeochemical stocks, HAUSGARTEN has been gradually extended westward to account for retreating ice conditions. As of 2016, the HAUSGARTEN observatory encompasses 21 permanent stations from the ice-free and marginal ice zones in the eastern Fram Strait to the typically sea-ice-covered areas in the western Fram Strait.

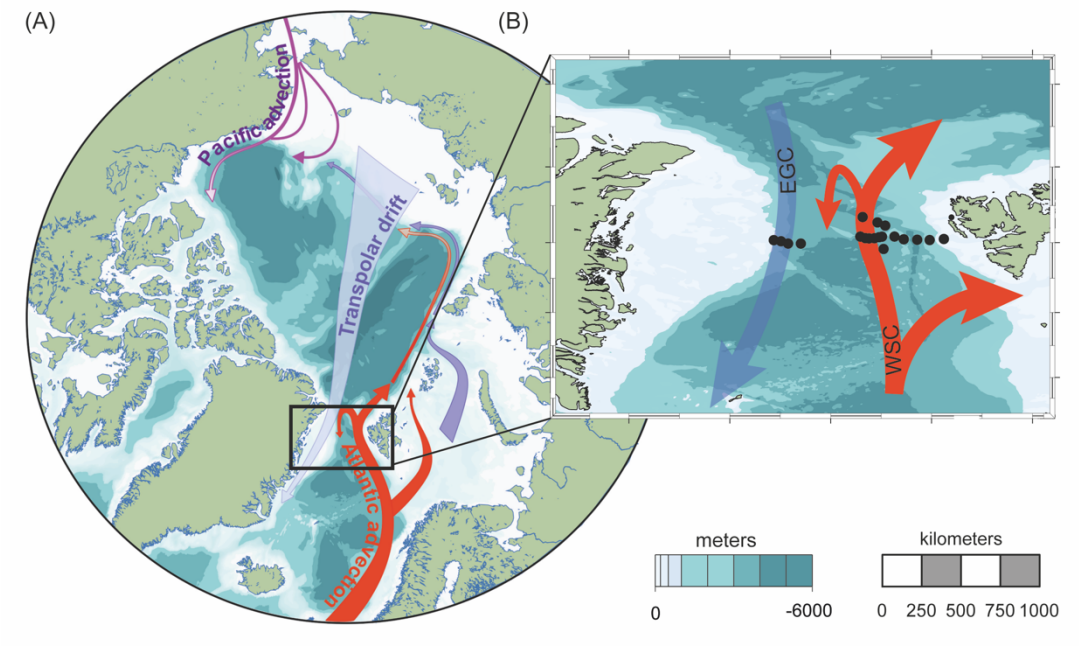

Figure 1.4 | Sampling sites of the LTER observatory HAUSGARTEN. (A) The arrows show the major advective domains of the Arctic Ocean with the Atlantic (red), pacific (pink), and transpolar drift (light purple). (B) The Fram Strait has an inflow and outflow on opposite sides of the 450 km wide strait with 21 permanent stations of the Long-Term Ecological Research (LTER) observatory HAUSGARTEN. The figure was modified from Wassmann et al. (2020). Abbreviations in (B): West Spitsbergen Current, WSC (red); Eastern Greenland Current, EGC (blue).

The Fram Strait is characterized by two currents, which stipulate its biogeochemistry and ecology. The West Spitzbergen Current (WSC) in the eastern Fram Strait and the East Greenland Current (EGC) in the western Fram Strait (Fig. 1.4). North Atlantic water masses enter the central Arctic Ocean as part of the WSC carrying relatively warm, saline waters (Beszczynska-Moller et al., 2012; Torres-Valdés et al., 2013). As the water circulates in the Arctic basin, additional inputs from the Bering Strait and rivers, i.e., Ob, Lena, and Mackenzie, are mixed into the water masses. Eventually, the water exits through the western Fram Strait as part of the EGC into the North Atlantic (de Steur et al., 2009). The EGC exports half of the total freshwater flux and almost the entire sea-ice flux out of the Arctic (Kwok, 2009; Serreze et al., 2006). The oceanographic conditions across the Fram Strait drive the spatial variability in phytoplankton biomass and ESD (Lampe et al., 2021; Nöthig et al., 2015, 2020), organic matter concentration (Engel et al., 2019; Grosse et al., 2021; Piontek et al., 2014), gel particle concentration (Busch et al., 2017; Engel, Piontek, et al., 2017), and microbial community (Cardozo Mino et al., 2021; Fadeev et al., 2018, 2021) across the HAUSGARTEN observatory. However, for the majority of the sampled parameters of PEBCAO, HAUSGARTEN only provides snapshots of the biogeochemical processes during summer. Unfortunately, the seasonal data bias is similar for other oligotrophic regions of the Arctic Ocean, which impede predictions about the natural variability and human impact through climate change (Maranger et al., 2015). This thesis provides the necessary baseline to improve the understanding of seasonal organic matter turnover in the Fram Strait and offers important perspectives on the present and future of biogeochemical processes in the Arctic Ocean.

Chapter 2

Scope of the Thesis

Objectives of this Thesis

Microorganisms play a critical role in biogeochemical cycles but large observational gaps exist for several Arctic regions. For example, primary production and zooplankton communities are monitored along the Russian shelf, while microbial dynamics are assessed along the Northern American shelf (Maranger et al., 2015). Truly understanding ecosystem dynamics requires a systematic sampling strategy over space and/or time. Many studies cover the spatial variability, while temporal sampling is limited in consistent observations that can be addressed using time series. Time series are rare around the world and HAUSGARTEN is the only pelagic time series in the Arctic Ocean to date (Buttigieg et al., 2018). Despite the invaluable microbial observatory established for HAUSGARTEN, the annual sampling frequency prohibits quantifying seasonal microbial dynamics.

In this thesis, I set out to investigate the seasonal variability of microbial organic matter turnover at HAUSGARTEN in the Fram Strait. I specifically want to combine biogeochemical and ecological approaches to investigate whether, and to what extent, the bioavailability of DOC shapes the microbial community composition. This thesis will help contribute to the understanding of how microbial carbon turnover influences the seasonal CO_2 storage in the Arctic. Additionally, the acquired knowledge will help to integrate seasonal fluxes within the microbial loop into models in order to predict carbon cycling in a changing Arctic.

The specific objectives were to:

- **Measure the seasonal changes in DOM, gel particles, and microbial processes in the euphotic zone.**
  Seasonal biogeochemical cycling and microbial turnover in the Arctic remain largely unexplained owed to the logistical difficulties of obtaining *in situ* samples in polar regions. Measuring the seasonal microbial processes in the Arctic Ocean will allow for a comprehensive analysis of concentration and composition of DOM and gel particles as well as microbial abundances and production rates in the Fram Strait. This contributes to the baseline dependencies needed for model applications in particular those incorporating seasonal DOM degradation under continuous light availability to dark periods.

- **Analyze the seasonal microbial community and possible links to bioavailability of DOM in the euphotic zone.**
  Seasonal biogeochemical cycling is likely to induce changes in the microbial community. However, the interactions between DOM and microbes are seldomly explored although they are important to understand the spatial and temporal variability of biogeochemical cycles in the Arctic Ocean. Analyzing the microbe-substrate relationships will allow to gain an insight into the seasonal associations in the Arctic microbial loop. This multi-disciplinary approach provides an important contribution to the previous culture studies focusing on taxa-specific DOM degradation strategies.

- **Assess the inter-annual trends of microbial organic matter cycling throughout the water column.**
  Temperature and bioavailability of DOM co-limit microbial activity in the Arctic Ocean. This is particularly relevant in the Fram Strait, where temperatures vary spatially from east to west and DOM bioavailability varies temporally. Hence, I want to use a targeted molecular analysis of DCCHO and DHAA to assess the inter-annual variability of semi-labile DOC at the HAUSGARTEN. Investigating the variability at an established time series will help to understand the physical and biological controls on microbial processes entering and exiting the Arctic through the Fram Strait.

List of Manuscripts

The objectives were addressed in the following chapters:

- **Chapter 3**
  Dynamics of organic matter and bacterial activity in the Fram Strait during summer and autumn.
  Anabel von Jackowski, Julia Grosse, Eva-Maria Nöthig, Anja Engel
  Manuscript published in *Philosophical Transactions of the Royal Society A (RSTA)*. Accepted in July 2020 and printed in August 2020.
  DOI: 10.1098/rsta.2019.0366

- **Chapter 4**
  Contrasting microbial communities and substrate regimes in the eastern Fram Strait between summer and fall.
  Anabel von Jackowski, Kevin W. Becker, Matthias Wietz, Christina Bienhold, Birthe Zäncker, Eva-Maria Nöthig, Anja Engel
  Manuscript in review with *Environmental Microbiology (EM)*.

- **Chapter 5**
  Summertime trends of semi-labile DOC across the Fram Strait
  Anabel von Jackowski, Vanessa Lampe, Judith Piontek, Anja Engel
  Manuscript in preparation for *Journal of Geophysical Research Biogeosciences (JGR Biogeosciences)*.

Chapter 3

Dynamics of organic matter and bacterial activity in the Fram Strait during summer and autumn

Declaration on the contribution of the doctoral researcher to the chapter

Title of the thesis:	Seasonal Dynamics of Organic Matter Turnover in the Arctic Ocean
Title of the chapter:	**Dynamics of organic matter and bacterial activity in the Fram Strait during summer and autumn**
Chapter is published in:	*Philosophical Transactions of the Royal Society A (RSTA)*
Authors of the chapter:	Anabel von Jackowski, Julia Grosse, Eva-Maria Nöthig, Anja Engel
Keywords of the chapter:	Arctic Ocean, seasonality, semi-labile organic carbon, bacteria
Citing the chapter:	von Jackowski A, Grosse J, Nöthig E-M, Engel A. 2020 Dynamics of organic matter and bacterial activity in the Fram Strait during summer and autumn. *Phil. Trans. R. Soc. A* 378: 20190366. DOI: 10.1098/rsta.2019.0366
Contribution to the chapter:	Anabel von Jackowski and Anja Engel designed the scientific study. Anabel von Jackowski and Julia Grosse performed the onboard sampling. Anabel von Jackowski analyzed the data. Anabel von Jackowski and Anja Engel wrote the publication with contributions from the co-authors.

Abstract

The Arctic Ocean is considerably affected by the consequences of global warming, including more extreme seasonal fluctuations in the physical environment. So far, little is known about seasonality in Arctic marine ecosystems in particular microbial dynamics and cycling of organic matter. The limited characterization can be partially attributed to logistic difficulties of sampling in the Arctic Ocean beyond the summer season. Here, we investigated the distribution and composition of dissolved organic matter (DOM), gel particles and heterotrophic bacterial activity in the Fram Strait during summer and autumn. Our results revealed that phytoplankton biomass influenced the concentration and composition of semi-labile dissolved organic carbon (DOC), which strongly decreased from summer to autumn. The seasonal decrease in bioavailability of DOM appeared to be the dominant control on bacterial abundance and activity, while no temperature effect was determined. Additionally, there were clear differences in transparent exopolymer particles (TEP) and Coomassie stainable particles (CSP) dynamics. The amount of TEP and CSP decreased from summer to autumn, but CSP was relatively enriched in both seasons. Our study therewith indicates clear seasonal differences in the microbial cycling of organic matter in the Fram Strait. Our data may help to establish baseline knowledge about seasonal changes in microbial ecosystem dynamics to better assess the impact of environmental change in the warming Arctic Ocean.

This article is part of the theme issue 'The changing Arctic Ocean: consequences for biological communities, biogeochemical processes and ecosystem functioning'.

Introduction

Anthropogenic climate change is warming the Arctic Ocean about two to three times faster than the global average (Masson-Delmotte et al., 2018). A sensitive indicator of the degree of warming is the loss of sea ice. The year 2018 marked the sixth-lowest sea ice minimum in the nearly 40-year satellite record (National Snow Snow Ice Data Center, 2018). Warming of the Arctic results in seasonal, thin and fragile sea ice, thereby completely changing the landscape of icy ecosystems (Comiso, 2012; Kashiwase et al., 2017; Maslanik et al., 2011; Nghiem et al., 2006). These environmental changes are already influencing phytoplankton dynamics since ice-retreat was responsible for the 30% increase of net primary production between 1998 and 2012 (Arrigo & van Dijken, 2015). The change in phytoplankton dynamics

could impact bacterial dynamics in the near future since phytoplankton release organic matter that is remineralized by bacteria. This remineralization drives the respiratory flux of CO_2 from the ocean to the atmosphere. Despite the important role of bacteria in the global carbon cycle, the control on heterotrophic bacterial activity in the Arctic is not well-understood.

Recent studies have identified the lability of dissolved organic carbon (DOC) as a major factor controlling bacterial activity in polar environments (Ducklow et al., 2012; Kirchman, Morán, et al., 2009; Piontek et al., 2014). The lability of DOC can be classified as a continuum from very labile to ultra-refractory DOC: labile components are used within hours to days, while refractory components have a residence time of centuries to millennia. Semi-labile DOC has a turnover of weeks to months, which allows it to accumulate in the upper water column during the productive season (Hansell et al., 2009). Dominant biochemical components within the semi-labile fraction include dissolved combined carbohydrates (dCCHO) and dissolved hydrolysable amino acids (dHAA; Goldberg et al., 2009, 2011; Skoog & Benner, 1997). Furthermore, the semi-labile fraction can partition into gel particles, constituting a dynamic continuum from dissolved precursors to single colloids (approx. 1 nm) and macro gels (greater than 1 mm; Engel et al., 2012; Meng & Liu, 2016; Verdugo et al., 2004). Polysaccharide- containing micro gels, referred to as transparent exopolymer particles (TEP), are among the best-described micro gels in the ocean. The amount of TEP released into the ocean increases during the senescent bloom phase when phytoplankton growth approaches nutrient depletion (Engel, 2009; Engel et al., 2002; Logan et al., 1994; Mari & Kiørboe, 1996; Passow, 2002). Another type of micro gel are Coomassie Blue stainable particles (CSP). CSP are presumably formed by extracellular proteins, but few endeavours have explored their production (Long & Azam, 1996; Thornton, 2018). The organic content that has aggregated as TEP and CSP can serve as substrates for particle-attached bacteria and also provide an important vector for export to the deep sea (Bar-Zeev et al., 2012; Verdugo, 2012).

The degree to which microbial cycling of organic matter is subject to change under the pressure of global warming is difficult to predict. Satellite-based models have the advantage of using annual data and accounting for seasonal dynamics (Arrigo & van Dijken, 2015; Vernet et al., 2019), but ecosystem or nutrient models rely on in situ data, like Forest et al. (2011). However, most in situ data in the Arctic are collected during the summer. This seasonal data bias is owing to the logistical difficulties of sampling in the Arctic during the dark and colder seasons. The predictions are further implicated by a regional

bias since the majority of data for heterotrophic microbial processes are collected in the Beaufort Sea and Chukchi Sea (Maranger et al., 2015). Our study aimed at filling seasonal gaps by investigating DOM dynamics and bacterial activity in the Fram Strait during summer and autumn. The objective of this study was to assess (i) the seasonal shifts in DOC availability and in BP and (ii) to evaluate seasonal changes in DOM-microbe interactions for carbon-cycling within the pelagic Arctic ecosystem.

Methods

Study Site

Samples were collected in the Fram Strait with the RV Polarstern cruise PS114 from 16 to 23 July 2018 during summer and with the RV Maria S. Merian cruise MSM77 from 16 September to 4 October 2018 during autumn (Fig. 2.1; Table S 3.1). The sampling campaigns were part of yearly measurements in proximity to the Long-Term Ecological Research (LTER) observatory HAUSGARTEN situated in the eastern Fram Strait. The Fram Strait is the only deep gateway to the central Arctic Ocean and is characterized by two distinct hydrographic regimes. In the east, the northward-flowing West Spitsbergen Current (WSC) transports warm saline Atlantic water (AW; >2°C; >34.9 PSU) into the Arctic basin. On the opposite side of the 450 km wide Strait, the southward-flowing East Greenland Current (EGC) transports cold polar water (PW; <0°C; <34.7 PSU) along the Greenland shelf. Here, water masses that were not distinctly characterized as AW or PW were defined as intermediate water (IW).

Discrete sampling parameters

Sampling procedures were identical during both cruises. Seawater samples were collected at five depths (surface; above, in, and below the deep chlorophyll maximum (DCM); 100 m) using a SEA-BIRD CTD rosette sampling system equipped with 24 Niskin bottles. The chlorophyll maximum was identified by running a fluorescence probe on the downward cast of the CTD.

Samples for chlorophyll-*a* were collected on 25mm GF/F (Whatman, GE Healthcare Life Sciences, UK) and subsequently frozen (−20°C) until extraction using 90% acetone for photometric analyses (Turner Designs, USA), slightly modified after Evans et al. (1987). Chlorophyll-*a* was used as a proxy for phytoplankton biomass. Duplicate samples for dissolved organic

carbon (DOC) and total dissolved nitrogen (TDN) were filtered through 0.45 µm GMF GD/X filters (Whatman, GE Healthcare Life Sciences, UK) and collected in combusted glass ampoules (8h, 450°C). DOC/TDN was acidified and stored at 4◦C until simultaneous analysis after Engel & Galgani (2016) with a detection limit (DL) of 1 µmol l^{-1}. Duplicate samples for total dissolved phosphorus (TDP) were filtered through 0.45 µm Acrodisk filters (GHP membrane, Pall Corporation, USA) and frozen (− 20°C) until analysis. TDP and dissolved inorganic phosphorus (DIP) were analysed after (Murphy & Riley, 1962) with a DL of 2 µmol l^{-1}. DIP was subtracted from TDP to obtain dissolved organic phosphorus (DOP). Duplicate samples for high-molecular-weight (greater than 1 kDa) dissolved combined carbohydrates (dCCHO) were filtered through 0.45 µm Acrodisk filters, collected in combusted glass vials (8 h, 450°C) and frozen (− 20°C) until analysis after Engel & Händel (2011) with a DL of 10 nmol l^{-1}. The analysis classified 11 monomers: arabinose, fucose, galactose, galactosamine, galacturonic acid, glucosamine, glucose, glucuronic acid, rhamnose, co-elute mannose and xylose. Duplicate samples for dissolved hydrolysable amino acids (dHAA) were filtered through 0.45 µm Acrodisk filters, collected in combusted glass vials (8 h, 450°C) and frozen (− 20°C) until analysis. dHAA were measured with ortho- phthaldialdehyde derivatization by high-performance liquid chromatography (HPLC; Dittmar et al., 2009; Lindroth & Mopper, 1979). The HPLC (Agilent Technologies, USA) was equipped with a C18 column (Phenomenex, USA) with a precision of less than 5% and DL of 2 nmol l^{-1}. The analysis classified 13 monomers: alanine, arginine, aspartic acid, isoleucine, glutamic acid, glycine, leucine, phenylalanine, serine, threonine, tyrosine, valine; and γ-aminobutyric acid (GABA).

Duplicate samples for gel particle analysis were filtered onto 25 mm 0.4 µm-pore sized Nucleopore track-etched polycarbonate filters (Whatman, GE Healthcare Life Sciences, UK). Filters for transparent exopolymer particle (TEP) analysis were stained using Alcian Blue (Alldredge et al., 1993) for 5 s, whereas those for Coomassie Blue stainable particles (CSP) were stained with Coomassie Blue (Long & Azam, 1996) for 30 s. Filters were subsequently placed on CytoClear slides (Poretics Inc., USA) and then frozen (− 20°C) until analysis. Slides were imaged using an Axioscope A.1 with an attached Axio-Cam MRC (Zeiss, Germany) at 20× magnification and processed with ImageJ (Engel, 2009). The image processing allowed the determination of particle abundance as well as particle size (area). Particle abundance is of interest for aggregation and degradation processes (Ling & Alldredge, 2003), whereas the size is a measure for estimating the carbon and nitrogen content of the individual gels (Mari, 1999; Mari & Burd, 1998).

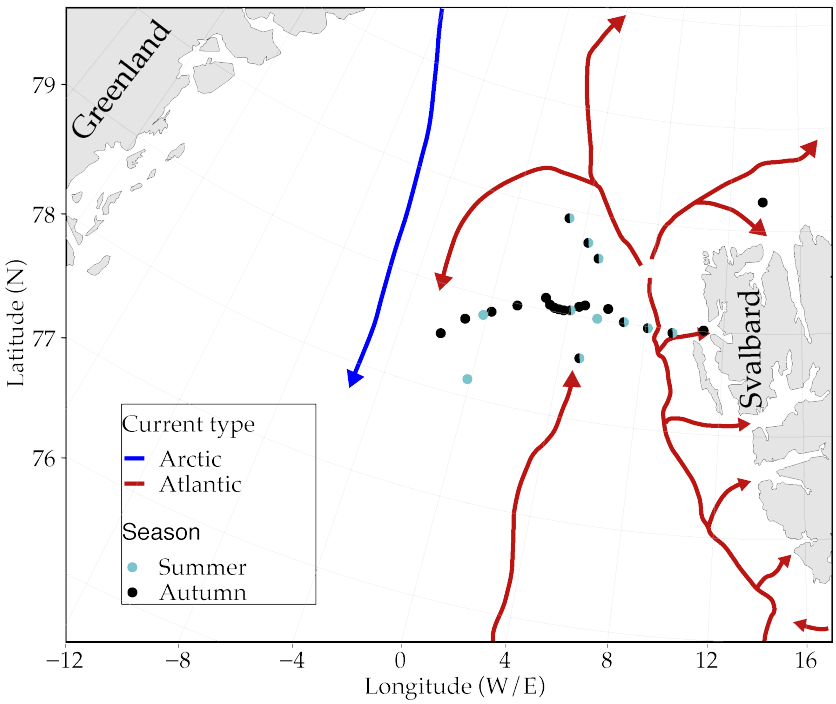

Figure 3.1 | Map of stations within the Fram Strait in the proximity of the LTER observatory HAUSGARTEN. The samples during summer were collected with the RV Polarstern on board cruise PS114 from 16 July to 23 July 2018 and during autumn with the RV Maria S. Merian on board MSM77 from 16 September to 4 October 2018. Warm-water with Atlantic-origin (red arrows/northward) enters via the West Spitsbergen Current (WSC) in the eastern Fram Strait and cold polar water of Arctic-origin (blue arrows/southward) exits via East Greenland Current (EGC) in the west of the Fram Strait.

Samples for cell abundance were fixed with glutardialdehyde (GDA, 25%), and subsequently frozen (− 80°C) until further analysis. Prior to analysis, the flow cytometer (FACSCalibur, Becton Dickinson, USA) was calibrated and standardized with TruCount beads (Becton Dickinson, USA). The cells were stained using SybrGreen I (Thermo Fisher Scientific, USA) and subsequently counted by flow cytometry using the Cell Quest 3.3 software with a DL of 2000 events per second. Additionally, subpopulations of low nucleic acid content (LNA) and high nucleic acid content (HNA) bacteria were derived by distinguishing between differences in fluorescence intensity (Bouvier et al., 2007; Robertson & Button, 1989; E. Sherr et al., 2006).

Bacterial production (BP) was measured onboard the research vessels using the microcentrifuge method (Smith & Azam, 1992). Duplicate samples and one killed control (1.5 ml each) were labelled using ^{3}H-leucine (BioTrend, USA) at a final concentration of 20 nmol l^{-1}. ^{3}H-leucine had a specific activity of 100Ci $mmol^{-1}$. The samples were incubated for 6 h in the dark at 4°C and terminated using trichloroacetic acid (TCA) at a final concentration of 5%.

Leucine incorporation was converted into BP by applying a factor of 1.5 kg C mol leucine^{-1} assuming no intracellular isotope dilution (Kirchman et al., 2005; Simon & Azam, 1989).

Calculations and statistical analysis

In the text and tables, n refers to the number of observations and nst to the number of integrated stations. Stations were integrated over the upper 100m using trapezoidal integration. The calculations for the carbon and nitrogen content of dCCHO and dHAA were based on carbon and nitrogen atoms contained in the identified monomers. Carbon content of dCCHO and dHAA was normalized to DOC as % DOC. The incorporation of semi-labile DOC into BP per day (% SL-DOC d^{-1}) was calculated by BP (mmol C m^{-2} d^{-1}) ÷ semi-labile DOC (mmol m^{-2}) × 100.

Statistical analyses were conducted using the software R (v3.5.1) in RStudio (v1.1.414; Ihaka & Gentleman, 1996). Variables were fed into a statistical mixed model (Laird & Ware, 1982; Verbeke & Molenberghs, 2000) including season (‘Summer’, ‘Autumn’) and either depth (‘surface’, ‘above DCM’, ‘DCM’, ‘below DCM’, ‘100 m’) or water mass (‘AW’, ‘IW’, ‘PW’) as well as their interaction term as fixed factors. The station was regarded as a random factor and the residuals were assumed to be normally distributed and to be homo/heteroscedastic with respect to the different levels. Based on this model, a pseudo-r^2 (Nakagawa & Schielzeth, 2013) and an analysis of variances (ANOVA) was conducted, followed by multiple contrast tests (MCT) in order to compare the several levels of the influence factors, respectively. Statistical results are reported in the Table S 3.2.

Packages used in the scope of this study included PlotSvalbard (v0.7.11; Vihtakari, n.d.), ggplot2 (v3.2.0; Wickham, 2016), nlme (v.3.1-139; Pinheiro et al., 2020), piecewiseSEM (v2.0.2; Lefcheck, 2016), multcomp (v1.4-10; Hothorn et al., 2008), lsmeans (v2.30-0; Lenth, 2016), car(v3.0-2; Fox & Weisberg, 2019), FactorMineR (v1.41; Husson et al., n.d.) and corrgram (v1.13; Wright, 2018).

Results

The study area was predominantly ice-free during both summer and autumn. Ice floes were observed north of 79.5°N and west of 0°W/E in summer and north of 79.5°N and further west at 2°W in autumn. Single ice floes were encountered at ‘N4’ in summer and ‘D4’ in autumn (Table S 3.1). Water

temperature ranged from 0.75°C to 6.2°C in summer (n=53) and from 0.52°C to 7.1°C in autumn (n=110; Table 3.1), therefore only characterizing as AT and IW. During both cruises, a fluorescence peak was observed between 20 and 40m water depth indicating a DCM. However, the fluorescence peak was of lower intensity and occasionally below the detection limit at some stations in autumn. Chlorophyll- a ranged from 21 to 209 mg m^{-2} in summer (n_{st}=11) and from 15 to 41mg m^{-2} in autumn (n_{st}=22) and thus was three times higher in summer compared to autumn (Fig 3.2; Table 3.1). Chlorophyll-a concentrations were significantly different in the AW between the summer and autumn (ANOVA $F_{1,136}$=39.4, p<0.0001; MCT p<0.001; Appendix, Table S 3.2), while concentrations did not significantly change in IW.

Composition of organic matter

DOC ranged from 6029 to 8171 mmol m^{-2} in summer (n_{st}=11) and from 5953 to 8103 mmol m^{-2} in autumn (n_{st}=22). DOC concentrations (Table 3.1) showed no significant seasonal difference (Mann-Whitney-test, p=0.8; Table S 3.2). Semi-labile DOC made up 8.4 ± 4.7% of total DOC (% DOC) in summer (n=53) and 3.5 ± 0.8% DOC in autumn (n=110; Fig. 3.2 and 3.4). Semi-labile DOC, and components thereof, significantly correlated with chlorophyll-*a* concentrations (Fig. 3.3). Furthermore, semi-labile DOC was significantly different between AW and IW in summer, but not autumn (ANOVA $F_{1,130}$=6.1, p<0.05; MCT p<0.001; Table S 3.2). TDN ranged from 819 to 1287 mmol m^{-2} in summer (n_{st}=11) and from 780 to 1597 mmol m^{-2} in autumn (n_{st}=22). TDP ranged from 31 to 49 mmol m^{-2} in summer (n_{st}=11) and from 38 to 121mmol m^{-2} in autumn (n_{st}=22). DOP ranged from 5 to 21 mmol m^{-2} in summer (n_{st}=11) and from 2 to 11 mmol m^{-2} in autumn (n_{st}=9).

dCCHO ranged from 43 to 107 mmol m^{-2} in summer (n_{st}=11) and from 24 to 42 mmol m^{-2} in autumn (n_{st}=22). The molecular composition shows that dCCHO was dominated by glucose (14–66 mol%) and co-elute mannose/xylose (14–55 mol%) during both seasons. To investigate a potential change in dCCHO composition along with the quantitative decrease from summer to autumn, we applied principal component analysis (PCA). The first principal component (PC1) explained 51.9% and was primarily influenced by the season (Fig. S 3.1). The second principal component (PC2) explained 17.7% and was primarily influenced by the depth (Fig. S 3.1). dCCHO was significantly different between summer and autumn (Mann-Whitney-test, p<0.0001) in all depths (ANOVA F4,130=17.4, p<0.0001; MCT p<0.01; Table S 3.2). dCCHO contributed 6.3 ± 3.6% DOC to semi-labile DOC in summer (n=53) and 2.6 ± 0.7% DOC in autumn (n=110; Table 3.1).

dHAA ranged from 22 to 62 mmol m^{-2} in summer (n_{st}=11) and from 13 to 20 mmol m^{-2} in autumn (n_{st}=19). The molecular composition showed that dHAA was dominated by glycine in summer (13–35 mol%; 23.6 ± 4.8 mol%; n=53) and autumn (23–38 mol%; 30.8 ± 2.8 mol%; n=104). The second most abundant dHAA was glutamic acid, which was higher in summer (8–24 mol%; 15.1 ± 3.7 mol%; n=53) than in autumn (7–17 mol%; 10.5 ± 1.7 mol%; n=104). Again, we applied PCA using the relative composition to determine a change in quality and degradation state (K. Kaiser & Benner, 2009). PC1 explained 40.1% and was primarily influenced by the depth (Fig. S 3.2). PC2 explained 12.3% and was primarily influenced by the season (Fig. S 3.2).

Table 3.1 | Arithmetic means and one standard deviation of variables determined in the Fram Strait during summer and autumn. The '*n*' refers to the number of observations.

		summer	*n*	autumn	*n*
temperature	°C	4.50±1.49	53	4.59±1.52	110
salinity	PSU	34.84±0.40	53	34.82±0.29	110
chlorophyll-*a*	µg l^{-1}	1.11±1.02	53	0.36±0.29	110
DOC	µmol l^{-1}	73.65±9.04	53	72.46±5.64	110
semi-labile DOC	µmol l^{-1}	6.24±3.49	53	2.52±0.60	104
semi-labile DOC	%DOC	8.4±4.7	53	3.5±0.8	104
dCCHO	µmol C l^{-1}	4.65±2.68	53	1.87±0.47	110
dCCHO	%DOC	6.3±3.6	53	2.6±0.7	110
dHAA	µmol C l^{-1}	1.59±0.93	53	0.66±0.20	104
dHAA	%DOC	2.1±1.2	53	1.0±0.3	104
semi-labile C:N	ratio	10.7±2.0	53	9.3±1.5	104
TEP particles	x10^6 l-1	11.58±8.17	53	7.01±4.80	95
TEP area	cm^2 l-1	1.08±0.71	53	0.42±0.29	95
TEP	µg C l-1	21.4±14.5	53	7.1±5.2	95
CSP particles	x10^6 l-1	14.64±9.38	53	11.69±7.92	95
CSP area	cm^2 l-1	1.43±1.16	53	1.06±0.74	95
bacterial abundance	x10^5 ml-1	9.35±4.36	53	6.41±2.65	110
HNA	%	60.2±7.8	53	50.7±5.5	110
BP	µg C l^{-1} d^{-1}	0.65±0.47	52	0.14±0.11	110
BP_{cell}	fg C $cell^{-1}$ d^{-1}	0.71±0.43	52	0.21±0.11	110

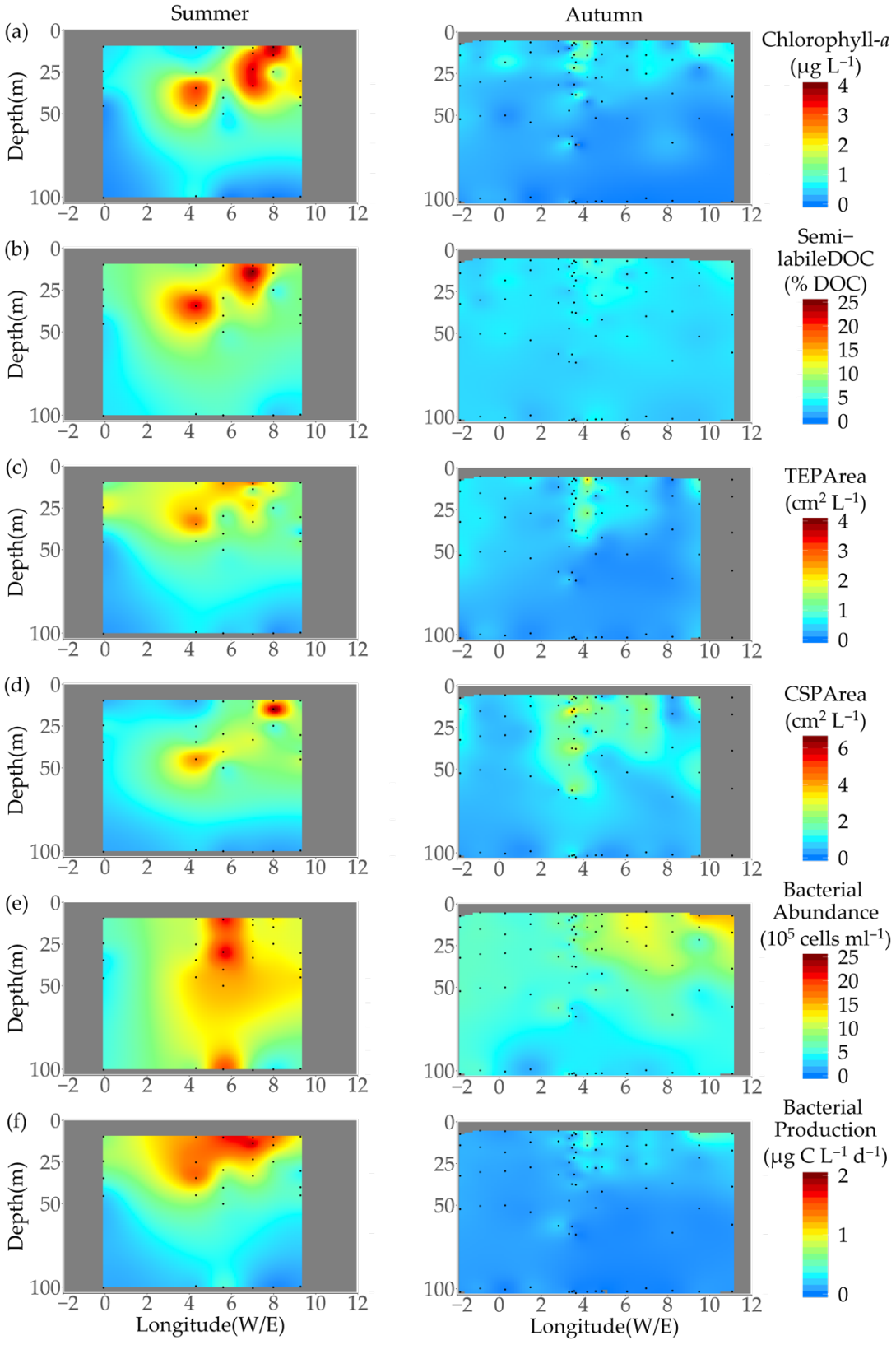

Figure 3.2 | Spatial variability along the approximately 79°N latitude in the Fram Strait during the summer (left) and autumn (right) of 2018. The parameters shown include (a) chlorophyll-*a*, (b) semi-labile carbon, area of (c) TEP and (d) CSP, (e) bacterial abundance and (f) bacterial production (BP). No data are available for the grey shaded region; stations not shown include: N3-N5, NSB1, S3, R1 (electronic supplementary material, Table S 3.1).

There was a significant difference between summer and autumn (Mann-Whitney-test, $p<0.0001$) by depth and water masses (Table S 3.2). dHAA contributed 3.1 ± 1.2% DOC in summer (n=53) and 1.0 ± 0.3% DOC in autumn (n=104; Table 3.1).

TEP abundance ranged from 365 to 1936 × 10^6 m^{-2} in summer (n_{st}=11) and from 220 to 1398 × 10^6 m^{-2} in autumn (n_{st}=18). The total area of TEP ranged from 45 to 295 × 10^6 cm^2 m^{-2} in summer (n_{st}=11) and from 4 to 12 × 10^4 cm^2 m^{-2} in autumn (n_{st}=19). The area of TEP was significantly different between summer and autumn (Mann-Whitney-test; $p<0.0001$; Table S 3.2) with the strongest differences in the surface to below DCM (ANOVA $F_{4,118}$=16.0, $p<0.0001$; MCT $p<0.0001$; Table S 3.2). Concentration of carbon in TEP (TEP-C) ranged from 82 to 255 mmol m^{-2} in summer (n_{st}=11) and to 19 to 115 mmol m^{-2} in autumn (n_{st}=19). TEP-C relative to the DOC pool was 2.1 ± 0.9% DOC (n_{st}=11) in summer and 0.7 ± 0.3% DOC in autumn (n_{st}=19; Fig. 3.4). CSP abundance ranged from 672 to 1801 × 10^6 m^{-2} in summer (n_{st}=11) and from 284 to 2344 ×10^6 m^{-2} in autumn (n_{st}=19). The total area of CSP ranged from 63 to 377 × 10^6 cm^2 m^{-2} in summer (n_{st}=11) and from 3 to 25 × 10^4 cm^2 m^{-2} in autumn (n_{st}=19). The [TEP]:[CSP] ratio (area:area) was 1:1.6 in summer and 1:3.0 in autumn, reflecting the relative increase of CSP in autumn.

Bacterial distribution and production

Bacterial abundance ranged from 3 to 22 × 10^5 cells ml^{-1} in summer (n=53) and from 2 to 15 × 10^5 cells ml^{-1} in autumn (n=110; Fig. 3.2). Bacterial abundance was significantly different in AW, but not IW between summer and autumn showing that bacteria behave differently in the two water masses (ANOVA $F_{1,136}$=10.6 $p<0.001$; MCT; Table S 3.2). Bacterial abundances in AW decreased from 10.34 ± 4.32 × 10^5 cells ml^{-1} in summer (n=41) to 6.02 ± 2.53 × 10^5 cells ml^{-1} in autumn (n=59), compared to the IW where it increased from 5.97 ± 2.40 × 10^5 cells ml^{-1} in summer (n=11) to 6.87 ± 2.73 × 10^5 cells ml^{-1} in autumn (n=51). Yet, the significant correlations with chlorophyll-*a* (r^2=0.47, $p<0.001$) and semi-labile DOC (r^2=0.48, $p<0.001$; Fig. 3.3), indicate that semi-labile DOC controlled bacterial abundances in all water masses. In addition, we differentiated between LNA and HNA. Abundance of LNA ranged from 1 to 9 × 10^5 cells ml^{-1} in summer (n=53) and 1 to 8 × 10^5 cells ml^{-1} in autumn (n=110). The abundance of HNA ranged from 2 to 13 × 10^5 cells ml^{-1} in summer (n=53) and 1 to 9 × 10^5 cells ml^{-1} in autumn (n=110). Therefore, the fraction of HNA decreased from summer to autumn (Fig. 3.4; Table 3.1). The ratio of [HNA]:[LNA]

(abundance:abundance) was 1.6:1 in summer (n=53) and 1.1:1 in autumn (n=110).

BP was measured at 4°C for all samples and ranged from 15 to 75 mg C m^{-2} d^{-1} in summer (n_{st}=11) and from 3 to 15 mg C m^{-2} d^{-1} in autumn (n_{st}=22). BP was more than four times higher in summer than in autumn (Table 3.1) and significantly changed in all depths (ANOVA $F_{4,129}$=16.9, p <0.001; Table S 3.2). Again, the significant correlation to chlorophyll-*a* as well as labile components (Fig. 3.3) suggests that the lability was responsible for the significant difference in BP between summer and autumn. Carbon incorporated into BP was 0.80 ± 0.37% SL-DOC d^{-1} in summer (n=11) and 0.45 ± 0.27% SL-DOC d^{-1} in autumn (n=22; Fig. 3.4).

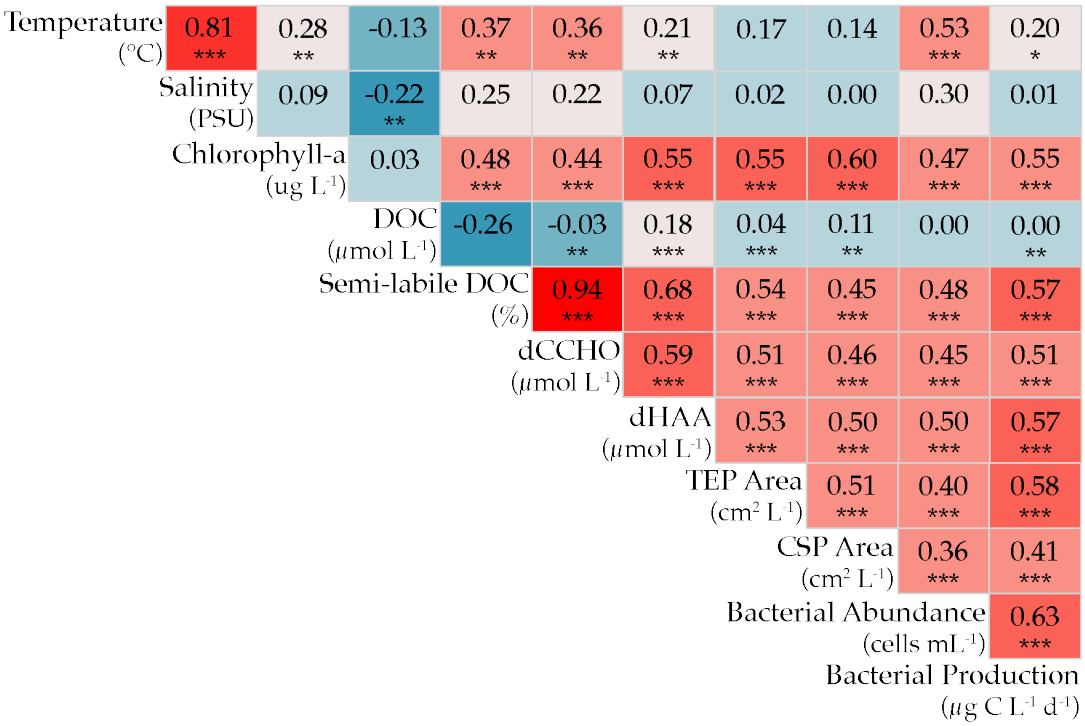

Figure 3.3 | Correlations of physical and biochemical parameters in the upper 100 m of the Fram Strait in 2018. Low correlations are shown in a blue shade, followed by teal, grey, salmon and red indicating a strong correlation. Significances are shown by asterisks as '***' <0.001,'**' <0.01,'*' <0.05 and ' ' >0.05.

Discussion

Our study focuses on potential changes in DOM composition and the dependency of microbial activity in the Fram Strait between summer and autumn. Conditions during the field sampling in summer reflected the late-bloom phase of the main annual phytoplankton bloom development, which typically occurs in June/July (Piontek et al., 2014). Phytoplankton release an increased amount of bioavailable DOM towards the end of the bloom (Engel & Händel, 2011; Ittekkot et al., 1981), which can explain the observed twofold higher concentration of dCCHO and dHAA in summer compared to autumn. The observed concentrations of 0.80 ± 0.46 µmol dCCHO l^{-1} in the Fram Strait are close to the 0.90 ± 0.32 µmol dCCHO l^{-1} reported for the Beaufort Sea during summer (Panagiotopoulos et al., 2014). Accordingly, the average contribution of dCCHO to the DOC pool (% DOC) of 6.3 ± 3.6% DOC is lower than the 8 ± 3% DOC in Beaufort Basin (Panagiotopoulos et al., 2014). In addition to the spatial variations, carbohydrates displayed a temporal variation. To the best of our knowledge, this is the first study showing a twofold decline of dCCHO between summer and autumn for the Arctic. The observed change is similar to the decline from approximately 4% DOC in summer to approximately 2% DOC in winter shown for the euphotic zone of the Sargasso Sea (Goldberg et al., 2009). Furthermore, the decrease by 3.7% DOC until autumn resembles the trend between the upper 80 m and the deep Beaufort basin in summer (3% DOC; Panagiotopoulos et al., 2014).

This indicates that the seasonal production of bioavailable DOM within the Fram Strait was almost degraded until autumn. The remaining carbohydrates in the water column exhibited a more refractory state but could be a potential substrate for bacteria during the winter. Although carbohydrates are an important carbon and energy source for bacteria, amino acids also serve as a nitrogen source and directly support biomass production (Amon et al., 2001; Davis & Benner, 2005, 2007; Meon & Amon, 2004; Rich et al., 1997; Shen et al., 2012, 2018). The seasonal trajectory of dHAA appears to increase from 1.5% DOC in spring (Davis & Benner, 2005) to 2.1–2.3% DOC in summer (Davis & Benner (2007), this study) and subsequently decreases to 1.0 ± 0.3% DOC until autumn. In particular, the drawdown of dHAA below the 1.1% DOC, a threshold set for the least reactive fraction of semi-labile DOM using bioassay experiments (Davis & Benner, 2007) indicates that the labile dHAA reservoir is likely to be exhausted in autumn. Changes in the seasonal dHAA reservoir are furthermore apparent in the amino acid composition (Fig. S 3.2). For example, the molar fraction of glutamic acid increased by 4.7 mol% between spring and summer (Davis & Benner, 2005), whereas it

decreased by 4.6 mol% between summer and autumn in this study. In contrast, glycine decreased between spring and summer by 2.3 mol% (Davis & Benner, 2005), while it increased between summer and autumn by 7.5 mol% in this study. Consequently, the amino acid reservoir appears to be highly dynamic throughout the year with an increase of semi-labile components toward summer and a rapid utilization until autumn.

BP persists in different magnitudes throughout all seasons in the Arctic, albeit with a strong decrease from the productive to the unproductive season (Garneau et al., 2008; Iversen & Seuthe, 2011; Nguyen et al., 2012; Sherr & Sherr, 2003; Sherr et al., 2003; Vaqué et al., 2008). Measured BP rates determined for summer during this study are representative for the Fram Strait, i.e. surface BP 1.12 ± 0.4 µg C l^{-1} d^{-1} is very close to 1.14 ± 0.4 µg C l^{-1} d^{-1} observed between 0.8–9.5°E in 2011 (Piontek et al., 2014). The fourfold decline observed from summer to autumn is similar to the decreases previously reported for coastal regions such as Franklin Bay, Canada (Garneau et al., 2008; Nguyen et al., 2012) and Kongsfjorden, Svalbard (Iversen & Seuthe, 2011). In addition to BP, the bacterial abundance and the proportion of HNA declined from summer to autumn. HNA are considered to represent the more metabolically active subpopulation that also appears to be substrate-driven (Cuevas et al., 2011; Piontek et al., 2014). Consequently, as semi-labile DOC components declined so did BP and the proportion of HNA, which suggests that bacteria are primarily controlled by the availability of semi-labile DOC in summer and autumn (Fig. 3.4). However, semi-labile DOC can be equally as important as temperature in controlling bacterial activity (Kirchman et al., 2005; Kirchman, Hill, et al., 2009; Piontek et al., 2014; Sala et al., 2008). Our study does not directly support this since temperatures remained unchanged and BP still declined from summer to autumn, but synergistic combined effects could arise during other seasons or in the future due to warming. Synergistic effects have been observed if the demand for labile organic matter is met (Piontek et al., 2014). When future scenarios of climate warming are taken into account, an elevated release of semi-labile DOC in summer could lead to an increase of BP under warmer temperatures. The synergistic effects may be less pronounced in autumn and winter when bacteria consume organic matter with a more refractory state. Alternatively, a rise in temperature might also allow microbial degradation of refractory compounds (Lønborg et al., 2018), indicating that the reactivity of DOC could be less controlling for BP in the future. At the time of our study, the bioavailability of DOM has been the dominant control on bacterial activity during the productive and unproductive season. This, however, does not rule out the possibility of synergistic effects in the future.

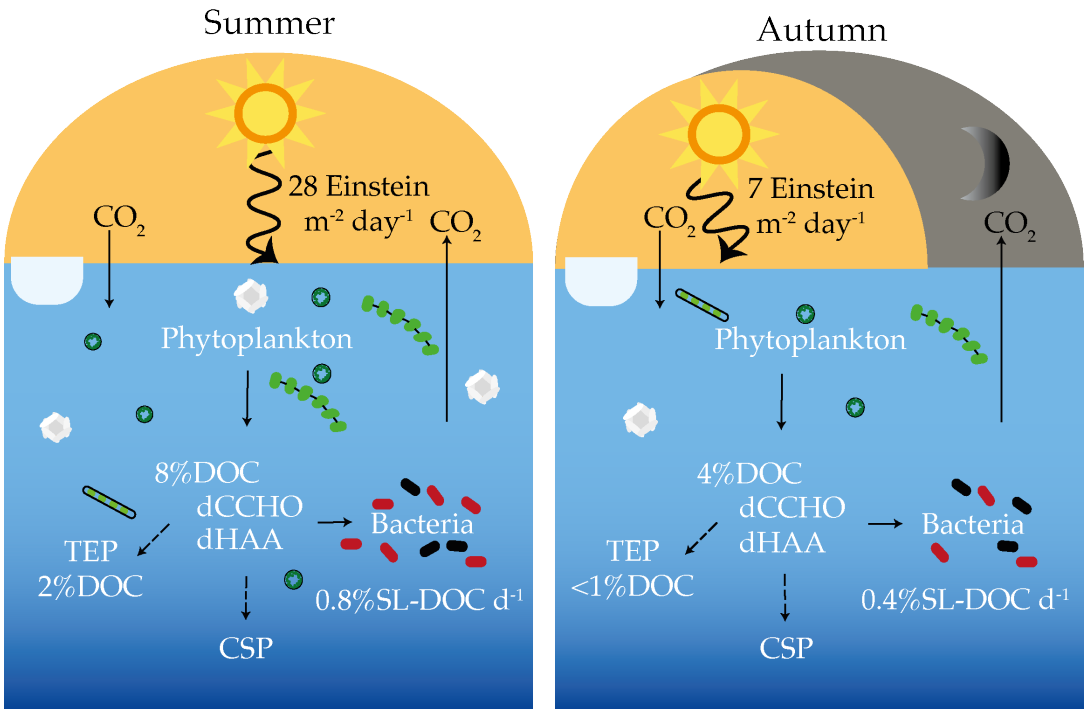

Figure 3.4 | Partitioning of organic carbon between the dissolved and microbial pools for integrated water column of the Fram Strait during summer (left) and autumn (right). Phytoplankton release semi-labile DOM components like dCCHO and dHAA that can further partition into TEP and CSP. The decline in semi-labile DOC triggers a decrease in bacterial incorporation of semi-labile DOC (%SL-DOC d− 1) and the bacterial community composition from summer to autumn. HNA bacteria are coloured in red and LNA bacteria in black. PAR data are a monthly estimate from MODIS-Aqua satellite of a 4-km spatial resolution between 1-31 July 2018 for summer and 1-30 September 2018 within 78-80°N and -2°W-13°E from https://giovanni.gsfc.nasa.gov.

Bacteria might further supplement their demand for labile components by accessing the dynamic continuum of gel particles. Precursors of gel particles like TEP are released by phytoplankton during the senescent bloom phase (Engel, Piontek, et al., 2017; Ortega-Retuerta et al., 2018; Passow, 2002). In particular, the inter-annual variability of TEP in the Fram Strait has been related to the abundance of the prymnesiophyte *Phaeocystis pouchetii* (Engel, Piontek, et al., 2017). The twofold higher phytoplankton biomass and amounts of TEP in our study compared to previous observations by Busch et al. (2017) suggests that the phytoplankton community release different concentrations of TEP into the water column during summer. To the best of our knowledge, our study is the first to show that TEP abundance, area and carbon content decreased more than twofold from summer to autumn (Fig. 3.2 and 3.4). The decrease in abundance and carbon content of TEP indicates that the particle content attributed to P. *pouchettii* diminishes quickly over time (Reigstad & Wassmann, 2007). Within a given season, TEP could have been subject to microbial remineralization by extracellular enzymes

(Berman-Frank et al., 2016; Ortega-Retuerta et al., 2018), coagulation processes and sinking into the deeper water column (Busch et al., 2017). In contrast to TEP, CSP abundance and area declined by a factor less than one between the two seasons (Fig. 3.2; Table 3.1). The production of CSP has been related to the picocyanobacterium Synechococcus spp. (Cisternas-Novoa et al., 2015), which is highly abundant in the Arctic gateway throughout the year (Paulsen et al., 2016). Again, amounts of CSP in summer and autumn were twice as high compared to 2015 (Busch et al., 2017), suggesting that formation by phytoplankton precursors, cell breakage and lysis (Verdugo, 2012) was higher during our study. Therefore, our results imply that cell deaths from the diatom-dominated summer bloom and the production by Synechococcus continue to release CSP until autumn. The continued amounts of CSP provide protein-rich micro gels for bacterial degradation after the dissolved pool of dHAA has been used. Our results show the loss of TEP and relative enrichment of CSP from summer to autumn thereby suggesting that gel particles could provide different temporal functions to the microbial food web. Future investigations of gel particle composition and the associated community composition might resolve whether the two types of particles provide different micro-niches for particle-attached bacteria at different times of the year (Carrias et al., 2002; Fadeev et al., 2018; Zäncker et al., 2019).

Microbial dynamics within the Arctic ecosystem are seasonally and regionally variable, which makes an assessment of future changes challenging. Climate change associated alterations, such as rising temperatures and decreasing nutrient budgets, hold the potential to support phytoplankton release of semi-labile DOC that could support higher BP rates in summer and the beginning of autumn. Unfortunately, the lack of data for autumn 2018 did not allow us to discuss nutrients in the scope of this study. In the future, an increase in the amount of bioavailable DOM could stimulate the competition for mineral nutrients between phytoplankton and bacteria (Thingstad et al., 2008), releasing more CO_2 during bacterial respiration. Therefore, future changes to BP might reduce the net community production in the microbial food web and weaken CO_2 sequestration in the Arctic (Vernet et al., 2019). As such, parameters characterizing microbial food web dynamics, including components within semi-labile DOM, are of importance if we aim to assess future carbon cycling in the changing Arctic ecosystem.

Conclusion

Our observations demonstrate the importance of studying the effect of seasonal DOM dynamics on the microbial food web. Sampling in summer and

autumn has allowed us to evaluate part of the seasonal shifts in microbial cycling of organic matter within the Fram Strait. Elevated concentrations of semi-labile DOC indicate an accumulation of recently produced DOM in summer. In autumn, the decrease in semi-labile DOC coincided with a decline in bacterial abundances and BP. Furthermore, we observed clear differences in the seasonal progression of gel particles with a twofold decrease in TEP and relative enrichment in CSP between summer and autumn. Our study highlighted that the availability of DOM shifts from summer to autumn and controls DOM-microbe interactions in the Fram Strait. Understanding the seasonal shifts in microbial cycling is of great importance in vulnerable environments like the Arctic, since seasonality may change in the future and potentially weaken the CO_2 sequestration in the Arctic Ocean.

Data accessibility. Data are available on PANGAEA Database (von Jackowski et al., 2020a; von Jackowski & Engel, 2019).

Authors' contributions. A.v.J. and A.E. conceived the study, analysed and interpreted the data. A.v.J. and J.G. collected the samples and conducted the BP measurements. E.-M.N. provided chlorophyll data. All authors contributed to writing the manuscript.

Competing interests. We declare we have no competing interests.

Funding. The funding was provided by the Helmholtz Association and by the MicroARC project (grant no. 03F0802A) within the Changing Arctic Ocean program, jointly funded by the UKRI Natural Environment Research Council (NERC) and the German Federal Ministry of Education and Research (BMBF).

Acknowledgements. We thank the crew of the RV Polarstern and RV Maria S. Merian for their helpful support in obtaining the samples. A special thank you to Tania Klüver, Sandra Golde, Jon Roa, Sandra Murawski and Nadine Knüppel in helping with sampling on board or with analysis in the laboratory.

Chapter 4

Variations of microbial communities and substrate regimes in the eastern Fram Strait between summer and fall

Declaration on the contribution of the doctoral researcher to the chapter

Title of the thesis:	Seasonal Dynamics of Organic Matter Turnover in the Arctic Ocean
Title of the chapter:	**Contrasting microbial communities and substrate regimes in the eastern Fram Strait between summer and fall**
Chapter is in review with:	*Environmental Microbiology*
Authors of the chapter:	Anabel von Jackowski, Kevin W. Becker, Matthias Wietz, Christina Bienhold, Birthe Zäncker, Eva-Maria Nöthig and Anja Engel
Keywords of the chapter:	Arctic Ocean, seasonality, microbial community, 16S rRNA
Contribution to the chapter:	Anabel von Jackowski and Anja Engel designed the scientific study. Anabel von Jackowski and colleagues performed the onboard sampling. Anabel von Jackowski and Matthias Wietz analyzed the data. Anabel von Jackowski and Kevin Becker wrote the publication with contributions from the co-authors.

Abstract

Seasonal variations in day length and temperature, in combination with dynamic factors such as advection from the North Atlantic, influence primary production and the microbial loop in the Fram Strait. Here, we investigated the seasonal variability of phytoplankton-derived biopolymers, heterotrophic microbial abundance, and heterotrophic microbial composition within the upper 100 m during summer and fall. Our flow cytometry results revealed a shift in the autotrophic community from picoeukaryotes dominating in summer to a 34-fold increase of Synechococcus abundances by fall. Furthermore, a significant decline in the concentrations of biopolymers covaried with increasing microbial diversity based on 16S rRNA gene sequencing along with a community shift towards fewer polymer-degrading genera in fall. The seasonal succession in the biopolymer pool and microbes indicates distinct metabolic regimes, with a higher relative abundance of polysaccharide-degrading genera in summer and a higher relative abundance of generalists in fall. The parallel analysis of DOM and microbial diversity provides an important baseline for microbe-substrate relationships over the seasonal cycle in the Arctic.

Introduction

Phytoplankton-derived biopolymers are major components in living and detrital organic matter in the ocean (Biersmith & Benner, 1998; Hedges et al., 2002; Mabeau & Kloareg, 1987). Organic matter is constantly produced and degraded, allowing it to be classified into either particulate organic matter (POM; >0.7 µm) or dissolved organic matter (DOM; <0.7 µm; Benner et al., 1992). Particularly DOM, as the largest carbon reservoir, can further be partitioned by reactivity into the low-molecular-weight fraction (<1 kDa) or high-molecular-weight fraction (>1 kDa; Hansell et al., 2009). The variable reactivity of low-molecular-weight DOM includes monomers such as free carbohydrates and amino acids, whereas high-molecular-weight DOM includes biopolymers such as dissolved combined carbohydrates (DCCHO) and dissolved hydrolyzable amino acids (DHAA).

Biopolymers like DCCHO and DHAA serve as substrates for bacteria and archaea. For instance, *Flavobacteriaceae* are specialized in polysaccharide degradation, suggesting a possible link to their prevalence during the annual phytoplankton bloom in temperate and polar habitats (Cardozo Mino et al., 2021; Fadeev et al., 2018; Kirchman et al., 2010; Wilson et al., 2017). *Gammaproteobacteria* such as *Porticoccaceae* can be abundant in response

to algal decay as the release of high-molecular-weight DOM is particularly prominent during and towards the end of a phytoplankton bloom (Engel et al., 2011; Teeling et al., 2012).

Seasonal microbial observations are scarce in oligotrophic polar regions owed to the logistical difficulties of sampling during the dark and colder seasons (Maranger et al., 2015). Particularly, the Arctic Ocean has been rapidly changing with accelerated rates of sea ice loss, glacial runoff, and permafrost melt in the past decades (IPCC, 2019). The ongoing environmental changes coupled with pre-existing seasonal cycles, e.g., light, regulate the productivity of the pelagic realm. We know that the duration of daylight is closely coupled to phytoplankton biomass under elevated nutrient concentrations in the Fram Strait during spring (Randelhoff et al., 2018). As the productive season progresses, phytoplankton biomass drives biopolymers that promote turnover of organic matter and growth of heterotrophic communities (von Jackowski et al., 2020b; Piontek et al., 2014).

This study builds on strong seasonal changes in biopolymer concentrations and the microbial community in the Fram Strait (von Jackowski et al., 2020b; Wietz et al., 2021). We hypothesized that the pronounced seasonal change in labile biopolymers would considerably shift the relative abundances of biopolymer-degrading microbes between summer and fall. Furthermore, given the unique overlap of biochemical and microbial diversity datasets, we wanted to investigate whether individual DCCHO and DHAA components could be linked to specific taxa. Assessing the microbial community in the context of the biopolymer pool is an important step for a holistic understanding during DOM production and recycling. The approach establishes a baseline of microbial substrate regimes in the Fram Strait between summer and fall.

Methods

Sampling

Samples for biochemical and microbial analyses were collected in the upper 100 m of the water column using a rosette sampler equipped with 24 Niskin bottles. The rosette sampler was coupled to a CTD (SBE 911plus, Sea-bird, USA) equipped with two temperature probes, two conductivity probes, a Digiquartz pressure sensor, a WET Labs ECO-AFL/FL fluorometer, a WET Labs C-Star transmissometer, and an altimeter. The sampling depths were chosen based on the output of the WET Labs ECO-AFL/FL fluorometer that was used to estimate phytoplankton biomass and identify the deep

chlorophyll maximum (DCM). Specifically, four depths were of particular interest: surface (5 or 10 m), the DCM, below the DCM (BDCM), and 100 m. In summer, surface water was consistently sampled at 10 m, DCM at 20-43 m, and BDCM at 30-52 m. In fall, the surface water was sampled at 5 m, DCM at 20-34 m, and BDCM at 40-50 m. The CTD data are archived in the PANGAEA World Data Center (W.-J. von Appen et al., 2019; von Jackowski & Engel, 2019).

Particulate and Dissolved Organic Matter

Samples for particulate organic carbon (POC) were collected by filtering 1 to 4 L of seawater onto 0.7 µm pore-sized pre-combusted GF/F filters (500°C, 4h) and stored at –20°C. Back in the laboratory, the thawed filters were soaked in 0.1M HCl to remove inorganic carbon, dried at 60°C for 12 h, and measured using a EURO EA CHNS-O Elemental Analyzer (HEKAtech GmbH, Germany; Sharp, 1974).

Data for corresponding samples of dissolved organic carbon (DOC), dissolved combined carbohydrates (DCCHO), dissolved hydrolyzable amino acids (DHAA) were incorporated from von Jackowski *et al.* (2020). In brief, DOC was analyzed by the high-temperature catalytic oxidation method (TOC-VCSH, Shimadzu, Japan; Qian & Mopper, 1996; Sugimura & Suzuki, 1988). DCCHO analysis was conducted by high-performance anion-exchange chromatography coupled with pulsed amperometric detection (HPAEC-PAD, ICS 3000, Dionex, USA) that classified 11 sugars: arabinose, fucose, galactose, galactosamine, galacturonic acid, glucose, glucosamine, glucuronic acid, rhamnose, and co-elute mannose and xylose (Engel & Händel, 2011). DHAA analysis was performed using ortho-phthaldialdehyde derivatization by high-performance liquid chromatography (HPLC, Agilent, USA) that classified 13 monomers: alanine, arginine, aspartic acid, gamma-aminobutyric acid (GABA), glutamic acid, glycine, isoleucine, leucine, phenylalanine, serine, threonine, tyrosine, and valine (Dittmar et al., 2009; Lindroth & Mopper, 1979).

Microbial Production

Rates of primary production (PP) were measured *in situ* using the ^{14}C method, modified based on Engel et al. (2013). The seawater from the surface and DCM was incubated in duplicates with an additional dark control for a duration of 24 h (Table S 4.1). To account for the changing light field in the ocean, the surface samples were incubated at 100 µEinstein and the

DCM samples were incubated at 45 µEintein. To also account for the changing diurnal cycle, the samples were incubated under constant light during summer, while the hours of light roughly matched the given day in fall. For example, incubation times decreased from 14 h (e.g., on 16.09.2018) at the beginning of the MSM77 expedition to 9.5 h (e.g., 04.10.2018) at the end of the MSM77 expedition.

Each incubation was fractionated and terminated in three subsamples: total PP (PP-TOC), particulate PP (PP-POC), and dissolved PP (PP-DOC). The PP-TOC fraction was taken directly from the incubation flask, the PP-POC fraction was filtered onto a filtered onto a 25 mm 0.4 µm-pore sized Nucleopore track-etched polycarbonate filter (Whatman, GE Healthcare Life Sciences, UK), and the PP-DOC fraction was subsampled from the filtrate. To convert the activities into a rate, we assumed a DIC concentration of 2100 µmol kg^{-1} for both cruises. Data for the corresponding bacterial production (BP) based on the ^{3}H-microcentrifuge method (Smith & Azam, 1992) was incorporated from von Jackowski *et al.* (2020).

Cell Abundance

Samples for cell abundance were fixed on board with glutardialdehyde at 2% final concentration and stored frozen (−80°C) until analysis by flow cytometry (FACSCalibur, Becton Dickinson, USA). The flow cytometer was calibrated and standardized with TruCount beads (Becton Dickinson, USA). Due to a detection limit of 50 µm, samples were filtered through a mesh before counting using the Cell Quest 3.3 software with a DL of 2000 events s^{-1}. Orange autofluorescence was used to detect the phycoerythrin of cyanobacteria (*Synechococcus*) and cryptophytes, whereas red fluorescence was used to detect and distinguish picoeukaryotes (<2 µm) from nanoeukaryotes (~ 2-20 µm; Read et al., 2014). Samples for heterotrophic cell analysis were filtered and stained with SybrGreenI (Invitrogen, USA), with data from the corresponding samples incorporated from von Jackowski *et al.* (2020).

Microbial Community Analysis

Seawater samples (1-4 L) were filtered through 0.22-µm Sterivex cartridges (Merck-Millipore, USA) using a peristaltic pump within 1.5−2 h after retrieval of the CTD rosette and stored frozen (–80°C) until extraction. Filters were transferred from cartridges into kit-supplied tubes, and genomic DNA was isolated using a combined mechanical and chemical procedure using the

PowerWater® DNA Isolation Kit (QIAGEN, Germany). Amplicon libraries were prepared according to the 16S Metagenomic Sequencing Library protocol (Illumina, USA) using universal 16S rRNA gene primers 515F 5′-GTGYCAGCMGCCGCGGTAA-3′ and 926R 5′-CCGYCAATTYMTTTRAG TTT-3′ (Parada et al., 2016) covering the V4-V5 hypervariable region. Sequences were acquired using a 2x300 bp paired-end run on a MiSeq platform (Illumina, USA) at CeBiTec (Bielefeld, Germany). Sequence data have been deposited in the European Nucleotide Archive (ENA) at EMBL-EBI under accession number PRJEB43926, using the data brokerage service of the German Federation for Biological Data (GFBio; Diepenbroek *et al.*, 2014) in compliance with MIxS standards (Yilmaz et al., 2011).

Sequence adaptors and primers were clipped using cutadapt, allowing a mismatch proportion error of 0.16 (M. Martin, 2011). Further processing was conducted in a server-based R installation (v3.6.0) to filter and merge reads into amplicon sequence variants (ASVs) using 'dada2' (v1.10.1; Callahan *et al.*, 2016). ASVs were taxonomically classified using the SILVA SSU Reference dataset (release 132, 2018). ASVs matching chloroplast or mitochondrial sequences were removed, and only ASV with >3 counts in more than 3% of samples was considered. We used 'phyloseq' (v1.30.0; McMurdie and Holmes, 2013) to manage sample data matrices. The 'iNEXT' package (v2.0.20; Hsieh *et al.*, 2016) was used to calculate rarefaction curves, sample coverage, and alpha-diversity indices.

Statistical Analyses

Parameters that showed significant differences between the BDCM and 100 m were subsequently grouped into surface-to-BCDM ("surface", "DCM", and "BDCM") and 100 m. Detailed results of statistical analyses are documented in Table S 4.2 and scripts are publically available at https://github.com/anabelvonjackowski.

Statistical analyses applied to the biogeochemical data included a Wilcoxon-Mann-Whitney-Test, analysis of variances (ANOVA), and a mixed model. If the interactive terms of the ANOVA were significant, they were fed into multiple contrast tests (Laird & Ware, 1982; Verbeke & Molenberghs, 2000) that included season ("summer", "fall") and depth ("surface", "DCM", "BDCM", and "100 m") with the station as the random factor.

Statistical analyses applied to the amplicon data included ANOVAs, NMDS, and log_2fold-change (log_2FC). PERMANOVAs with 999 permutations were

based on season and depth using Bray-Curtis distances in the 'vegan' package (v2.5.7, 'adonis function; Oksanen *et al.*, 2019). NMDS was based on Bray-Curtis dissimilarities using the packages 'phyloseq' (v1.30.0 'ordinate' function; McMurdie and Holmes, 2013) and 'vegan' ('vegdist' function; Oksanen *et al.*, 2019). Hierarchical cluster analysis of heatmaps was based on the 'complete' agglomeration method ('vegan' package 'hclust' function; Oksanen *et al.*, 2019). log_2FC calculated the enriched families and genera between seasons using an adjusted p-value of 0.05 using 'DESeq2' (v1.25.0; Love *et al.*, 2014).

Microbial abundances and biopolymer concentrations were contextualized using Spearman rank correlation analysis using 'microbiomeSeq' package (v0.1, 'tax_env_cor' function; Ssekagiri and Ijaz, 2020). Additionally, variables were scaled ('vegan' package 'rda' function, scaled=TRUE) and selected ('vegan' package 'ordistep' function) during a forward selection by which the p-value was adjusted for multiple testing by Holm-Bonferroni.

Results and Discussion

The Study Area

This study focused on eight stations within the Long-Term Ecological Research (LTER) observatory HAUSGARTEN in the Fram Strait (Soltwedel et al., 2016). Samples were collected during the expeditions PS114 with *RV Polarstern* from July 16th to 23rd, 2018 (herein referred to as summer) and MSM77 with *RV Maria S. Merian* from September 16th to October 4th, 2018 (herein referred to as fall; Fig. 4.1 A; Table S 4.1).

The summer and fall expedition showed differing conditions in the day length while maintaining the typical characteristics associated with the WSC. Daylight was continuous in summer and decreased from 14 h to 9.5 h at the beginning towards the end of the fall expedition. In contrast, temperatures rose from 4.53 ± 1.45 °C in summer (n=32) to 5.35 ± 0.94 °C in fall (n=30; Fig. S 4.1). The salinity of 34.83 ± 0.48 PSU in summer (n=32) and 34.90 ± 0.26 PSU in fall (n=30) was also characteristic of the WSC.

Seasonal Variability in POC and Autotrophic Microbes

POC decreased threefold in the upper 100 m from 18.07 ± 10.05 µmol L^{-1} in summer (n=32) to 5.25 ± 3.78 µmol L^{-1} in fall (n=32, Wilcoxon Rank Sum Test p<0.001; Fig. 4.1 B). The spatial variability of POC within the upper 100 m

showed a significant twofold decrease below the deep chlorophyll maximum (BDCM; 30-52 m) and 100 m in summer, while no difference was observed during fall (ANOVA Season:Depth $F_{3,56}$=5.39, p<0.01; Multiple Contrast Test p<0.05; Table S 4.2). The seasonal change in POC concentration was clearly related to phytoplankton biomass with a corresponding decline in chlorophyll-*a* (von Jackowski et al., 2020b) and total biovolume (Lampe et al., 2021) from summer to fall. An alternative explanation could be that POC concentrations declined due to rising temperatures, which have been suggested to enhance the partitioning from particulate to dissolved pools (Kim et al., 2011; Vernet et al., 2017; Wohlers et al., 2009). Although partitioning cannot be ruled out entirely, the simultaneous decline in POC and DOC concentrations indicate that the DOC pool was diminished largely by biopolymers.

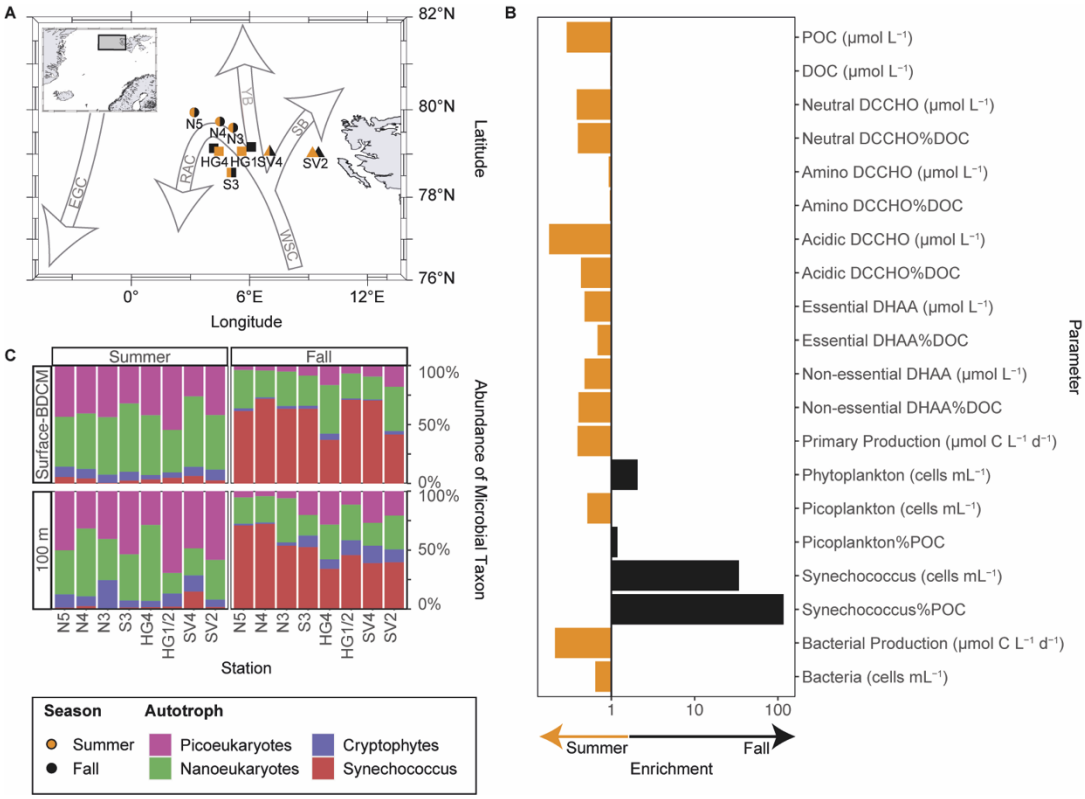

Figure 4.1 | Sampling sites, enrichment, and relative abundance of phytoplankton in the upper 100 m during summer and fall. (A) Samples were taken onboard the RV Polarstern from July 16th to July 23rd, 2018 (orange) and the RV *Maria S. Merian* from September 16th to October 4th, 2018 (black). The stations (shape) are marked as follows: the northern stations (circles), the central HAUSGARTEN stations (squares), and the Svalbard stations (triangles). Arrows illustrate the main currents in the Fram Strait. (B) Enrichments in the upper 100 m towards summer (left) and fall (right). (C) Relative abundance of autotrophs measured using flow cytometry in the surface (5 or 10 m) to BDCM (<50 m) and 100 m. **Abbreviations:** EGC, East Greenland Current; RAC, Return Atlantic Current; SB, Svalbard Branch; WSC, West Spitsbergen Current; YB, Yermark Branch; Biogeochemical and ecological data from corresponding samples of von Jackowski *et al.* (2020).

PP decreased more than twofold in the PP-DOC and showed a significant three-fold decrease in the PP-POC from summer to fall (Wilcoxon Rank Sum Test $p<0.05$; Fig. 4.1 B). PP-DOC declined from 1.2 ± 0.1 µmol C L^{-1} d^{-1} in summer (n=6) to 0.6 ± 0.2 µmol C L^{-1} d^{-1} in fall (n=10). PP-POC declined from 0.9 ± 0.1 µmol C L^{-1} d^{-1} in summer (n=6) to 0.3 ± 0.02 µmol C L^{-1} d^{-1} in the fall (n=10). Appropriately, the cell abundances of autotrophic microbes like cryptophytes and picoeukaryotes significantly decreased between summer and fall (Wilcoxon Rank Sum Test $p<0.001$; Table S 4.2). Cryptophyte abundances declined from 0.7 ± 0.4 cells L^{-1} in summer (n=32) to 0.2 ± 0.2 cells L^{-1} in fall (n=32). We observed cryptophyte abundances decrease significantly between the BDCM and 100 m in summer and fall (ANOVA Season:Depth $p<0.05$, Multiple Contrast Test $p<0.05$ and $p<0.01$, respectively; Table S 4.2). Similarly, picoeukaryote abundances declined from 4.5 ± 3.8 × 10^6 cells L^{-1} in summer (n=32) to 2.3 ± 3.9 × 10^6 cells L^{-1} in fall (n=32). Converting picoeukaryote abundances into carbon, by assuming a carbon biomass conversion factor of 530 fg C L^{-1} (Worden et al., 2004), showed that picoeukaryotes contributed 2.4 ± 2.0 µg C L^{-1} or 1.1% POC to the carbon pool in summer (n=32) and 1.2 ± 2.1 µg C L^{-1} or 1.3%POC in fall (n=32; Fig. 4.1 B). Nanoeukaryotic abundance showed the least seasonal change and decreased from 5.1 ± 4.1 × 10^6 cells L^{-1} in summer (n=32) to 4.9 ± 5.2 × 10^6 cells L^{-1} during fall (n=32). It is indeed likely that the PP-DOC fraction decreased as a result of declining cryptophyte, picoeukaryote, and nanoeukaryote cell numbers. In particular, picoeukaryotes might be less influenced by temperature and salinity but instead driven by the seasonal light intensity and duration within the WSC (Paulsen et al., 2016). All in all, our data support the observed decline in relative biovolume from summer to fall in the eastern Fram Strait (Lampe et al., 2021).

In contrast to the autotrophic microbes, absolute and relative abundances of *Synechococcus* significantly increased from summer to fall in the flow cytometry and 16S rRNA dataset (Wilcoxon Rank Sum Test $p<0.001$; Table S 4.2). *Synechococcus* abundances increased 34-fold from 0.4 ± 0.5 × 10^6 cells L^{-1} in summer (n=32) to 14.6 ± 22.5 × 10^6 cells L^{-1} in fall (n=32; Fig. 4.1 B-C). Converting the *Synechococcus* abundances into carbon, by assuming a biomass conversion factor of 109.5 fg C L^{-1} (Kana & Glibert, 1987), showed that *Synechococcus* contributed 0.05 ± 0.05 µg C L^{-1} or 0.02%POC to the carbon pool in summer (n=32) and subsequently increased 117-fold to 1.6 ± 2.5 µg C L^{-1} or 2.2%POC in fall (n=32; Fig. 4.1 B-C). The seasonal shift in *Synechococcus* abundances might be as follows in the upper 100 m of the Fram Strait: 0.43 ± 0.45 × 10^6 cells L^{-1} in

July (this study), 3.02 ± 3.79 x 10^6 cells L^{-1} in August (Paulsen et al., 2016), 14.60 ± 22.54 × 10^6 cells L^{-1} in September/October (this study), and 0.48 ± 0.08 × 10^6 cells L^{-1} in November (Paulsen et al., 2016); assuming no inter-annual variation. If a four-fold inter-annual variability does occur, this could have far-reaching implications for the Arctic epipelagic carbon pool and the biopolymer pool. Cyanobacteria have the lowest carbon-to-nitrogen ratios among most autotrophic microbes (Finkel et al., 2016) and likely compete for bioavailable DOM with heterotrophic microbes due to their osmotrophy strategy (Yelton et al., 2016). Overall, there is a need for more continuous measurements through stationary or drift expeditions to verify the seasonal variability of *Synechococcus* entering the Arctic Ocean through the Fram Strait.

Quality of biopolymer pool

To assess the carbohydrate content of the biopolymer pool, we differentiated DCCHO into neutral sugars, acidic sugars, and amino sugars. Neutral and acidic sugars showed significantly different concentrations between summer and fall (Wilcoxon Rank Sum Test $p<0.001$), particularly between the BDCM (30-52 m) and 100 m during summer (ANOVA Season:Depth $p<0.01$; Multiple Contrast Test $p<0.05$; Table S 4.2). Neutral sugars accounted for the largest biopolymer proportion to the dissolved organic carbon pool (DCCHO%DOC) and molecular composition of DCCHO pool (mol%DCCHO; Table 4.1). The dominance of hydrolyzed glucose and mannose/xylose in summer (29 ± 11 mol% and 31 ± 9 mol%, respectively) and fall (31 ± 8 and 37 ± 5, respectively) confirms that the North Atlantic transports relatively degraded DOC into the Arctic Ocean where DOC further loses bioavailability (Amon & Benner, 2003; Piontek et al., 2020; Rich et al., 1997). Furthermore, this study is among few others to report on the hydrolyzable acidic and amino sugar compositions in the North Atlantic (Engel et al., 2012; Grosse et al., 2021). Acidic sugars decreased in the concentration, DCCHO%DOC and mol%DCCHO (Table 4.1), again supporting the strong decline in freshly excreted DOC throughout the upper 100 m from summer to fall (Borchard & Engel, 2015). In contrast to acidic sugars, amino sugars showed minimal changes in their concentration and DCCHO%DOC but showed a two-fold increase of mol%DCCHO throughout the upper 100 m (Table 4.1). The relative increase in amino sugars contribution to DCCHO might be explained by the presence of galacturonic acid and glucuronic acid in bacteria-derived DOC (Benner & Kaiser, 2003). As bacterial numbers decline towards fall, cell depth or viral lysis releases cellular-derived amino sugars into the surrounding water. The low decay coefficients of amino sugars make them

resistant to decomposition and increase their residence time, which results in a two-fold increase of mol%DCCHO until fall (Kawasaki & Benner, 2006).

To assess the protein content of the biopolymer pool, we differentiated DHAA into essential amino acids (EAA) and non-essential amino acids (NEAA). Concentrations of EAA and NEAA decreased significantly between summer and fall (Table 4.2; Wilcoxon Rank Sum Test $p<0.001$), particularly between the BDCM (30-52 m) and 100 m during summer (ANOVA Season:Depth $p<0.001$; Multiple Contrast Test $p<0.05$; Table S 4.2). The significant reduction in the amino acid reservoir is indicative of rapid utilization of nitrogen-rich compounds from summer to fall. Furthermore, the measured EAA and NEAA concentrations determined during fall appear to be representative for post-bloom conditions; i.e., EAA: 89.7 nmol L^{-1}, 0.5 DHAA%DOC, and 50.4 mol%DHAA; NEAA: 90.6 nmol L^{-1}, 0.5 DHAA%DOC, and 49.6 mol%DHAA in upper 100 m of the eastern Fram Strait in 2017 (Grosse et al., 2021).

Microbial community composition in context of biopolymer pool

Amplicon sequencing of the 16S rRNA V4-V5 hypervariable region resulted in 4,872,711 sequences assigned to 2960 amplicon sequence variants (ASVs). Alpha diversity analyses covered more than 80% of the sequence richness (Fig. S 4.2). Microbial species richness and evenness (Shannon-Wiener index, inverse Simpson index) along with NMDS highlighted the significant differences by season and depth (Fig. 4.2, Wilcoxon Rank Sum Test $p<0.001$, ANOVA $p<0.01$; Table S 4.2).

Around 81% ASVs were shared between summer and fall, suggesting a retention generalist taxa that cope with the shift of the biopolymer pool (Fig. S 4.3). Generalist taxa were defined as ASVs with at >3 counts and 3% sequence abundance in the entire dataset. Further significant differences were observed between the surface-to-BCDM and 100 m during summer and fall (ANOSIM $p<0.01$; Table S 4.2; Fig. S 4.3 B). Within the surface-to-BCDM, generalists including *Planktomarina* and SAR11 clades significantly correlated with hydrolyzed acidic sugars (+, summer), serine (+, fall), and glycine (-) during both seasons (Fig. 4.3, 4.4 A-B). At 100 m, generalists showed significant correlations with isoleucine (positive, both seasons) and glucose (negative, both seasons; Fig. 4.4 C-D).

Table 4.1 | Concentration and relative composition of dissolved combined carbohydrates (DCCHO) in the water column. DCCHO were differentiated into neutral sugars, acidic sugars, and amino sugars. The contribution of DOC is given in %DOC, the relative composition in mol%, and " n" refers the number of samples.

Season	Layer	nmol L^{-1}	DCCHO %DOC	mol% DCCHO	nmol L^{-1}	DCCHO %DOC	mol% DCCHO	nmol L^{-1}	DCCHO %DOC	mol% DCCHO	
Summer	Surface-100 m	749.1	5.9	92.9	24.6	1.5	2.7	31.4	0.3	4.4	32
	Surface-BDCM	887.5	6.8	92.7	31.0	1.8	3.2	35.4	0.3	4.1	24
	100 m	333.6	3.0	93.3	5.2	0.6	1.3	19.5	0.2	5.4	8
Fall	Surface-100 m	287.6	2.3	89.5	4.4	0.7	1.2	29.2	0.2	9.3	32
	Surface-BDCM	301.4	2.4	89.0	5.1	0.7	1.3	32.1	0.3	9.8	24
	100 m	246.1	2.1	91.2	2.3	0.4	0.8	20.8	0.2	8.0	8

Table 4.2 | Concentration and relative composition of dissolved hydrolyzable amino acids (DHAA) in the water column. DHAA were differentiated into essential amino acids and non-essential amino acids The contribution of DOC is given in %DOC, the relative composition in mol%, and " n" refers the number of samples. The contribution of DOC is given in %DOC, the relative

		Essential Amino Acids			Non-Essential Amino Acids			*n*
Season	Layer	nmol L^{-1}	DCCHO%DOC	mol%DCCHO	nmol L^{-1}	DCCHO%DOC	mol%DCCHO	
Summer	Surface-100 m	189.9	1.0	47.9	219.6	1.2	52.1	32
	Surface-BDCM	219.8	1.2	46.4	261.9	1.4	53.6	24
	100 m	100.3	0.6	52.4	92.9	0.5	47.6	8
Fall	Surface-100 m	90.6	0.4	50.8	89.2	0.5	49.2	31
	Surface-BDCM	95.3	0.4	50.3	95.5	0.5	49.7	23
	100 m	77.1	0.4	52.1	71.4	0.4	47.9	8

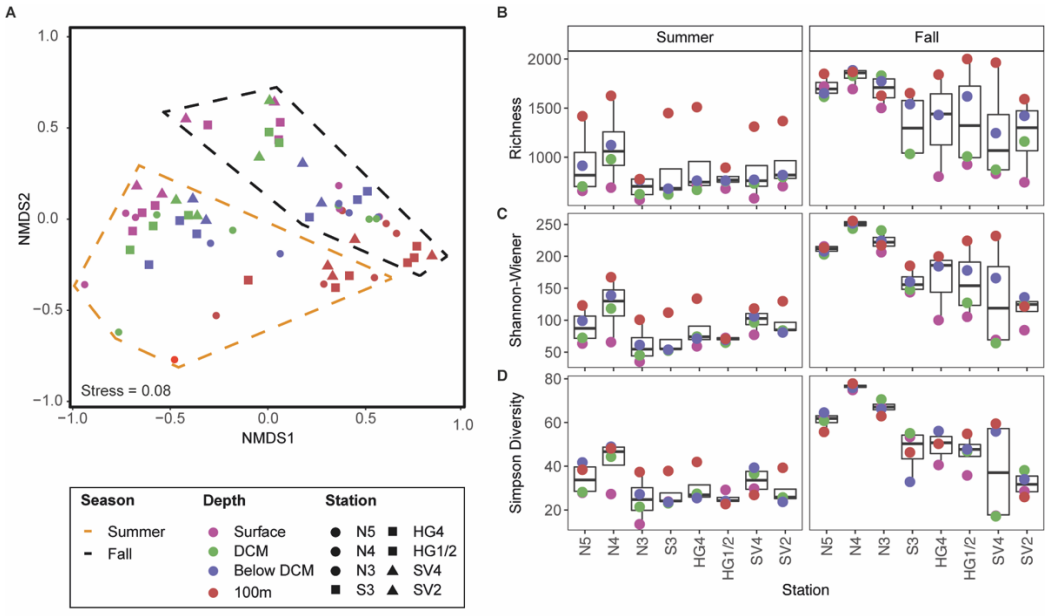

Figure 4.2 | Ordination and diversity of microbial community during summer and fall. (A) NMDS plot based on Bray-Curtis dissimilarities of ASV counts, i.e., highest taxonomic resolution, with depth (surface, 5-10 m; DCM, 20-40 m; BDCM, ~50 m; 100 m) and station illustrated by colors and shapes respectively (stress: 0.08). (B) Box plot indicating species richness. (C) Box plot indicating Shannon-Wiener diversity index (SDI). (D) Box plot indicating the inverse Simpson diversity index. DCM, deep chlorophyll maximum; BDCM, below deep chlorophyll maximum.

Labile biopolymers selected for a narrow microbial diversity and 3% unique ASVs during summer. Biopolymers including fucose (forward-selection, F=3.6, q<0.05) and rhamnose (forward-selection, F=4.5, q<0.01) significantly constrained the samples and ASVs in the ordination space of the RDA (Fig. 4.5). ASVs of significantly enriched taxa included *SAR92 clade*, *OM43* clade, and unclassified groups among the top 30 (log_2FC q<0.05; Fig. 4.3; Table S 4.2). Especially, *SAR92 clade* was significantly enriched in the surface-to-BDCM (log_2FC=3.7 q<0.01). *SAR92 clade* has previously been associated with *Phaeocystis* colonies (Bertrand et al., 2015; Delmont et al., 2014, 2015), which tend to be an abundant prymnesiophyte in the Fram Strait during summer (Lampe et al., 2021; Wietz et al., 2021). Alongside the *SAR92 clade*, we observed representatives of *Flavobacteriaceae* like *Aurantivirga*, *Formosa*, *Polaribacter*, and *Ulvibacter* that are known for their abilities for polysaccharide degradation (Fig. 4.3 A; Buchan et al., 2014; Cottrell & Kirchman, 2000; Reintjes et al., 2019). Also, we observed the presence of Verrucomicrobiae like *Luteolibacter* and *Lentimonas* in the Fram Strait (Fig. 4.3 A; Cardman et al., 2014; Jain et al., 2020; Rapp et al., 2018). These taxa displayed significant positive correlations with fucose, amino sugars, threonine, and γ-aminobutyric acid (GABA; Fig. 4.4 A).

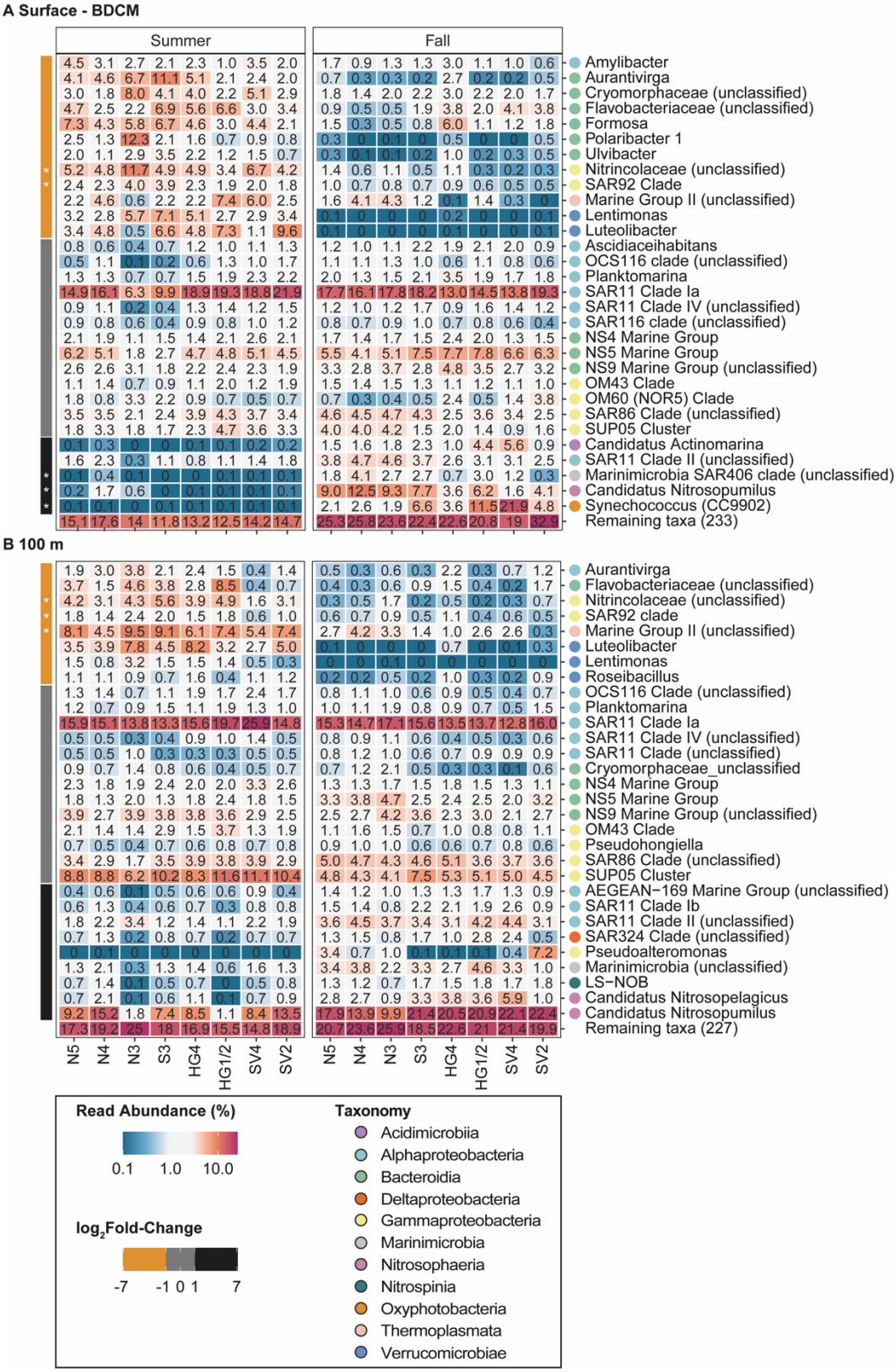

Figure 4.3 | Relative abundance with enrichments in the upper 100 m during summer and fall. (A) Relative abundance of top 30 genera in the surface – BDCM (5-50 m) were averaged due to the lack of significant differences between these depths (see text). (B) Relative abundance of top 30 genera in 100 m. The enrichments (colored bars) between the seasons were calculated using log_2Fold-Change (orange = summer, black = fall, grey = no seasonal enrichment) with significant differences marked by an asterisk (p adj<0.05). Abbreviations: BDCM, below deep chlorophyll maximum.

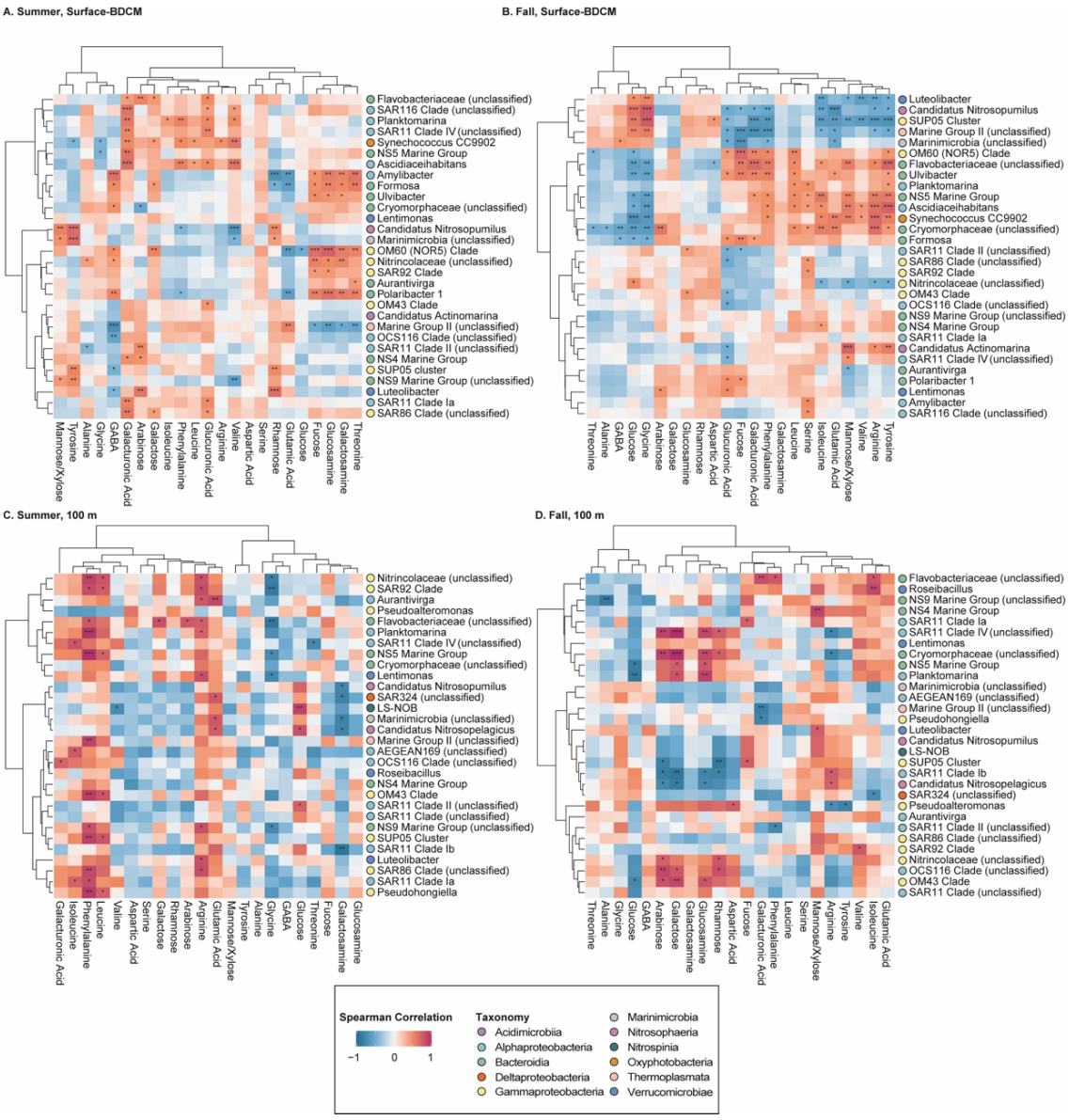

Figure 4.4 | Spearman rank correlation matrix of genera and biopolymers in the upper 100 m during summer and fall. (A) Correlations of top 30 genera in surface to BDCM (10-50 m) due to lack of significant differences between these depths during summer. (B) Correlations of top 30 genera in surface to BDCM (5-50 m) due to lack of significant differences between these depths during fall. **C** Correlations of top 30 genera in 100 m during summer. **D** Correlations of top 30 genera in 100 m during fall. The clusters was performed using "complete" clusters analysis and the spearman correlation (blue to red) was performed and associated with adjusted p-values for multiple testing. Abbreviations: BDCM, below deep chlorophyll maximum. Corresponding biopolymer data retrieved from von Jackowski *et al.* (2020). Significance codes are shown by asterisks: '***' <0.001,'**' <0.01,'*' <0.05 and ' '> 0.05.

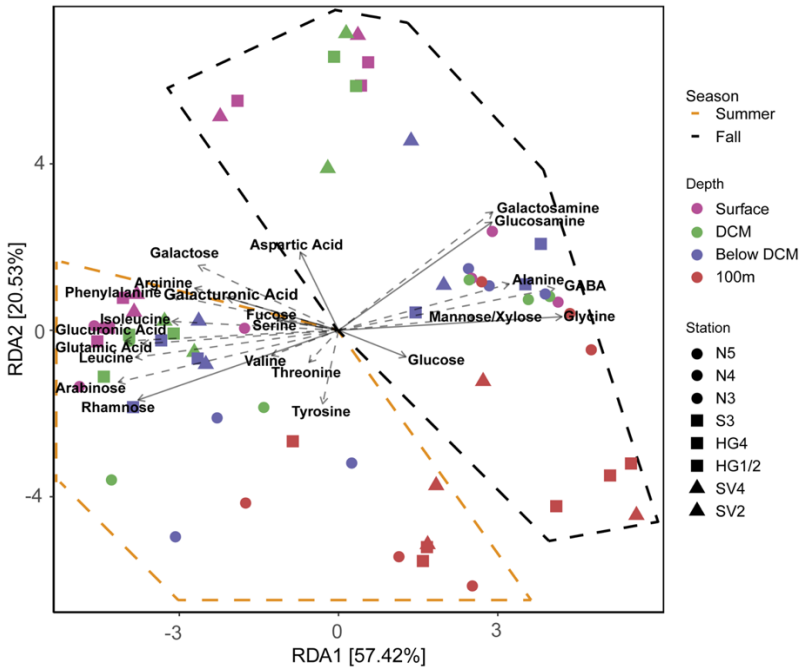

Figure 4.5 | RDA based on Hellinger transformed samples. The continuous arrows correspond to the significant forward-selected variables, while the dashed arrows correspond to the remaining parameters included in this study. The samples are marked by depth (color) and station (shape), while the boxes were manually added to the figure to add the seasonal separation. Abbreviations: GABA, gamma-aminobutyric acid. Data for dissolved parameters and gel particle data from corresponding samples by von Jackowski et al. (2020).

Particularly, the correlations to GABA can serve as an indicator for microbial activity. Measuring GABA concentrations could possibly portray amino acid turnover more accurately than the ^{3}H-leucine bacterial production, which can at times substantially underestimates bacterial growth (Popendorf et al., 2020). At 100 m, we observed a significant increase of Candidatus *Nitrosopumilus*, *LS-NOB*, and unclassified groups like Marine Group II (all log_2FC, q<0.01; Fig. 4.3; Table S 4.2). The increase in taxa like Candidatus *Nitrosopumilus* in 100 m closely resembles the community in fall rather than the photic zone above, which suggests that the community in 100 m is already specialized in refractory biopolymer assimilation (Fig. 4.4 C).

In fall, the wider microbial diversity showed significant enrichments in *Synechococcus* and unclassified *Marinimicrobia* (SAR406 clade) in the upper 100 m (log_2FC q<0.05; Fig. 4.3; Table S 4.2). Biopolymers that significantly constrained the samples and ASVs in the ordination space of the RDA included aspartic acid, glucosamine, glucose, and glycine (Fig. 4.5). Yet, *Synechococcus* significantly negatively correlated with glucose and glycine (Fig. 4.4 B), which suggests that high-molecular-weight biopolymers cannot explain the substrate demand of the fall community. Nonetheless, rising relative abundances of microbes that scavenge for refractory substrates like

Candidatus *Nitrosopelagicus*, Candidatus *Nitrosopumilus*, and LS-NOB suggest ongoing nitrate replenishment in the fall (Fig. 4.4 C-D). This co-occurrence of ammonia and nitrite oxidizers illustrates the initial recycling phase at the start of the polar night.

Microbial communities are fundamentally linked with organic matter. Our in-depth assessment of microbial communities, in the context of the organic matter pool, identified seasonality autotrophic and heterotrophic communities that are associated with different components of the biopolymer pool. The observed seasonality of autotrophic microbes was closely related to a decline in POC, production rates, and cell abundances. The most notable seasonal shift was observed in *Synechococcus*, which can use their osmotrophy strategy to compete for biopolymers with heterotrophic microbes. Amongst the heterotrophic community, the lower alpha-diversity suggests that specialized groups target labile biopolymers in summer, while a higher alpha-diversity suggests that taxa, including ammonia and nitrite oxidizers, scavenge for refractory substrates in fall. This study highlights seasonally driven associations between substrate regimes and microbiome structure, providing a first step towards anticipating possible changes to the carbon source or sink capacities of the Arctic Ocean under climate change.

Data Availability. Data are archived in the PANGAEA World Data Center and the European Nucleotide Archive (ENA) at EMBL-EBI under accession number PRJEB43926.

Acknowledgments. We thank the RV Polarstern and RV Maria S. Merian crews for their support during sample acquisition. Special thanks to Jana Bäger, Jakob Barz, Nadine Knüppel, Sandra Murawski, Swantje Rogge, Tania Klüver, Jon Roa, and Sandra Golde for sampling onboard and laboratory analyses. We also give thanks to Julia Grosse, who sampled for primary production onboard RV Polarstern. Sampling for bacterial sequence analyses was carried out in the framework of the HGF infrastructure program FRAM (Frontiers in Arctic Marine Monitoring). We are very grateful for the comments from the two anonymous reviewers that greatly improved the manuscript.
The work was funded by the Helmholtz Association and by the MicroARC project (03F0802A) within the Changing Arctic Ocean program, jointly funded by the UKRI Natural Environment Research Council (NERC) and the German Federal Ministry of Education and Research (BMBF). Open Access funding enabled and organized by project MicroARC (03F0802A). RV Polarstern was funded under grant AWI_PS114_01.

Authors' contributions. AvJ and AE conceived the study. AvJ, MW, and CB coordinated the sampling. MW processed the sequence data. AvJ analyzed and interpreted the data. The manuscript was primarily written by AvJ and KB with contributions from all co-authors.

Conflict of interest. The authors declare that they have no conflict of interest.

Chapter 5

Summertime trends of semi-labile DOC across the Fram Strait

Declaration on the contribution of the doctoral candidate to the chapter

Title of the thesis:	Seasonal Dynamics of Organic Matter Turnover in the Arctic Ocean
Title of the chapter:	**Summertime trends of semi-labile DOC across the Fram Strait**
Chapter in preparation for:	*JGR Biogeosciences*
Authors of the chapter:	Anabel von Jackowski, Vanessa Lampe, Judith Piontek, Anja Engel
Keywords of the chapter:	Arctic Ocean, time series, semi-labile dissolved organic carbon, bacteria
Contribution to the chapter:	Anabel von Jackowski and Anja Engel designed the scientific study. Vanessa Lampe developed the remote sensing approach. Anabel von Jackowski synthesized and analyzed the biogeochemical and microbial data.

Chapter 6

General Conclusion and Perspectives

General Conclusion

The Arctic is characterized by extreme seasonal differences in daylight and temperature that influence phytoplankton. Seasonal daylight ranges from all day in summer to darkness in winter and is the limiting factor for primary production. Meanwhile, phytoplankton-derived organic matter and temperatures co-limit microbes (Kirchman, Morán, et al., 2009; Piontek et al., 2015). The multifactorial control on seasonal microbial dynamics is only beginning to be understood with a predominant focus on temperate and tropical waters (e.g., Gilbert et al., 2012; Cram et al., 2015; Lindh et al., 2015; Ward et al., 2017). Unfortunately, high-frequency seasonal observations are rare for the polar regions, although the Arctic is experiencing sea ice loss, Atlantification, and borealization. To close the gap in seasonal observations, the work presented in this thesis *(a)* quantified the DOC bioavailability and microbial turnover between summer and fall, *(b)* analyzed the microbe-substrate relationships between summer and fall, and *(c)* assessed the inter-annual variability of semi-labile DOC during the summers from 2009-2019.

In the first research manuscript (**Chapter 3**), we were able to extend summertime microbial observations to fall in the Fram Strait. We observed a two- to threefold decline in the concentrations of chlorophyll-*a*, DCCHO, and DHAA between summer and fall. The SLDOC reservoir was highly dynamic with an elevated content of labile components (i.e., galactosamine, glutamic acid, leucine) in summer that was followed by a rapid utilization and more refractory components (i.e., glycine, alanine, threonine) in fall. Consequently, the rapid turnover rate of semi-labile DOC likely contributed to the fourfold decrease in bacterial production between summer and fall. Additionally, microbes can access the dynamic continuum of microgels, where we observed an uncoupled seasonal variability between carbohydrate-rich TEP and protein-rich CSP. Particle volume and carbon content of TEP decreased twofold, while CSP only showed a minor seasonal decrease that resulted in a relative increase of CSP to total microgel volume between summer and fall. Our publication highlights the seasonal controls on microbial dynamics in the Fram Strait and contributes to the baseline dependencies needed for higher-resolution model applications.

In **Chapter 4**, we extended our observations of seasonal microbial dynamics (described in chapter 3) by further exploring possible substate preferences within the microbial community. The presented manuscript explores the seasonal associations in the autotrophic community (<50 µm) and heterotrophic community to the DOM pool. The autotrophic community shifted

from picoeukaryotes in summer to a dominance of *Synechococcus* in fall, and a simultaneous decrease in primary production. This suggests that *Synechococcus* plays a minor role in the carbon fixation and possibly engages in an osmotrophic strategy to compete for bioavailable DOM with microbes. To fully understand microbe-substrate preferences has been difficult given the cultivation limitations of microbes. Nonetheless, we were able to identify a generalist taxa and seasonally-associated taxa that can be linked to biopolymers. *SAR92 clade*, *OM43 clade*, and representatives of *Flavobacteriaceae* could be linked to labile biopolymers during summer. In contrast, microbes that scavenge for refractory substrates like *Candidatus Nitrosopelagicus*, *Candidatus Nitrosopumilus*, and *LS-NOB* suggest ongoing nitrate replenishment in fall. Our study emphasizes the fundamental connection between the microbial community and substrate regimes towards understanding the carbon source and sink capacities of the Arctic Ocean.

In the third research manuscript (**Chapter 5**), I used the gained knowledge (from chapters 3 and 4) to investigate the inter-annual dataset of semi-labile DOC across the Fram Strait from 2009 to 2019. To account for the spatial variability, I separated the dataset into the Atlantic and polar sectors. The sector-specific bloom dynamics were extremely useful to arrange the *in situ* biogeochemical and microbial data. My observations demonstrated that the terminating phytoplankton bloom releases DCCHO that rapidly stimulates bacterial abundances and production in the Atlantic sector. Simultaneously, the bacteria appear to have a high demand for nitrogen, with DHAA%DOC indicating a low DOM reactivity in the Atlantic sector. In the polar sector, the phytoplankton bloom peaks around May, which resulted in low concentrations DCCHO and DHAA. Still, DCCHO stimulated cellular abundances of HNA bacteria and bacterial production despite temperatures near the freezing point. Our study highlights the fast-paced changes and spatial controls of phytoplankton-SLDOC-microbe interactions across the Fram Strait during summer.

Perspectives

The work presented in this thesis provides new insights into the seasonal dynamics of organic matter turnover and microbial community composition in the Fram Strait. The combination of biogeochemistry and ecology has contributed to our understanding of the microbial processes in the Arctic Ocean. However, our research has raised further research questions and ideas that need to be addressed in future studies:

1. **Identify taxa-specific substrate exudation and acquisition.** Studies on the molecular and chemical composition of phytoplankton exudates are scarce and the necessary preliminary cataloging of organic biomarkers needs to be improved. Currently, the Redfield ratio of 106C:16N:1P is the key concept to link nutrient availability and macromolecular composition of phytoplankton (Falkowski, 2000; T. Weber & Deutsch, 2012; T. S. Weber & Deutsch, 2010). However, the concept of the Redfield ratio neglects species-specific deviations in C:N:P of phytoplankton and across environments (Finkel et al., 2016; Martiny et al., 2013; Quigg et al., 2003, 2011). Future studies could resolve the macromolecular diversity of organic biomarkers and provide a taxa-specific DOM composition to understand the mechanisms of substrate recycling of microbes. This could be achieved by using emerging techniques such as fluorescently labeled polysaccharide incubations (Reintjes et al., 2017), dual-isotope stable isotope probing (SIP; Wegener et al., 2012, 2016), and implementing 'omics' to further resolve spatial and temporal metabolic preferences towards either LMW or HMW hydrolysis products.

2. **Sources and fate of DOM in the meso- and bathypelagic zones.** This thesis predominately focused on organic matter cycling in the euphotic zone, although ocean basins are on average 1000 m deep. The meso- and bathypelagic zones are typically characterized by low temperatures and refractory DOC but an unexpected rise in apparent oxygen utilization that provides evidence for microbial carbon turnover. Nonetheless, despite the microbial genetic and metabolic diversity in the deep sea (e.g., Acinas et al., 2021), the microbial cycling of the DOC pool is largely unexplored. Microbes must be supported by the dissolution of sinking particles (Cherrier et al., 1999; Hansman et al., 2009) and/or fixation of inorganic carbon through energy sources like ammonium and hydrogen sulfide (Hansman et al., 2009; Ingalls et al., 2006). Future studies could measure carbon assimilation using dark ^{14}C fixation in combination with

N^1-guanyl-1,7-diaminoheptane (GC7) to discriminate between archaeal and bacterial carbon fixation (Jansson et al., 2000).

3. **Expanding the FRAM Ocean Observing System.** Researchers at the Alfred Wegener Institute Helmholtz Centre for Polar and Marine Research, Bremerhaven, Germany have collected seawater samples for chlorophyll-*a* and POC in the Arctic Ocean since 1991 (Nöthig et al., 2020). These efforts were used to establish the PEBCAO group that built a microbial observatory that ranges from biogeochemical parameters to microscopical methods and is one-of-a-kind for the Arctic. The data collection of PEBCAO occurs on an annual frequency, which is comparable to many time series stations around the world (Buttigieg et al., 2018).

   Simultaneous to the *in situ* sampling efforts, the AWI has maintained the mooring array *Hybrid Arctic/Antarctic Float Observing System* (HAFOS) at LTER observatory HAUSGARTEN since 1997. The HAFOS moorings were expanded as part of the *FRontiers in Arctic marine Monitoring* (FRAM) Ocean Observing System in 2014 (Soltwedel et al., 2013). The HAFOS and FRAM moorings include classical tools (e.g., sediment traps) and cutting-edge technologies (e.g., Remote Access water Samplers) that allow for year-round microscopic and molecular-based observations of the plankton and microbial community (e.g., Wietz et al., 2021).

   Currently, the majority of HAUSGARTEN microbial parameters are solely collected on the annual expeditions to the Fram Strait. In the future, the PEBCAO microbial observatory could be expanded in the framework of FRAM. Merging PEBCAO and FRAM will allow for annual data collection and contextualizing current data snapshots that instantaneously serve as a quality control. Ecological and biogeochemical parameters that could be integrated onto mooring arrays include microbial cell abundances, DOC, and CDOM optical sensors. Innovative solutions will continually improve our understanding of seasonal microbial dynamics in the Arctic Ocean and on a global scale.

4. **Microbial turnover of DOM in the "new" Arctic Ocean.** Around 300 years ago, the Arctic probably had a sea ice cover and frozen permafrost to the edges of the polar circle. Today, industrialization has triggered climate change that is rapidly melting the sea ice, promoting Atlantification, and accelerating permafrost thaw. Particularly permafrost

thaw is unlocking terrestrial DOM and induces a “browning” of the coastal waters. The changing pelagic conditions come with many uncertainties with regard to the light attenuation in the water column, DOM bioavailability, and microbial activity (Cavicchioli et al., 2019; Sipler et al., 2017; Wauthy et al., 2018). To assess whether an influx of terrestrial DOM has an effect and the extent to which it affects microbial dynamics, it is once again critical to determine a baseline. Future studies could focus on the DOM composition, degradation state, and bioavailability from the shelf regions to the oligotrophic central Arctic Ocean. Furthermore, the *in situ* measurements can be complemented by incubation experiments that simulate climate-driven effects of the future Arctic.

Supplementary Information

Supplementary Figures and Tables for Chapter 3

Dynamics of organic matter and bacterial activity in the Fram Strait during summer and autumn

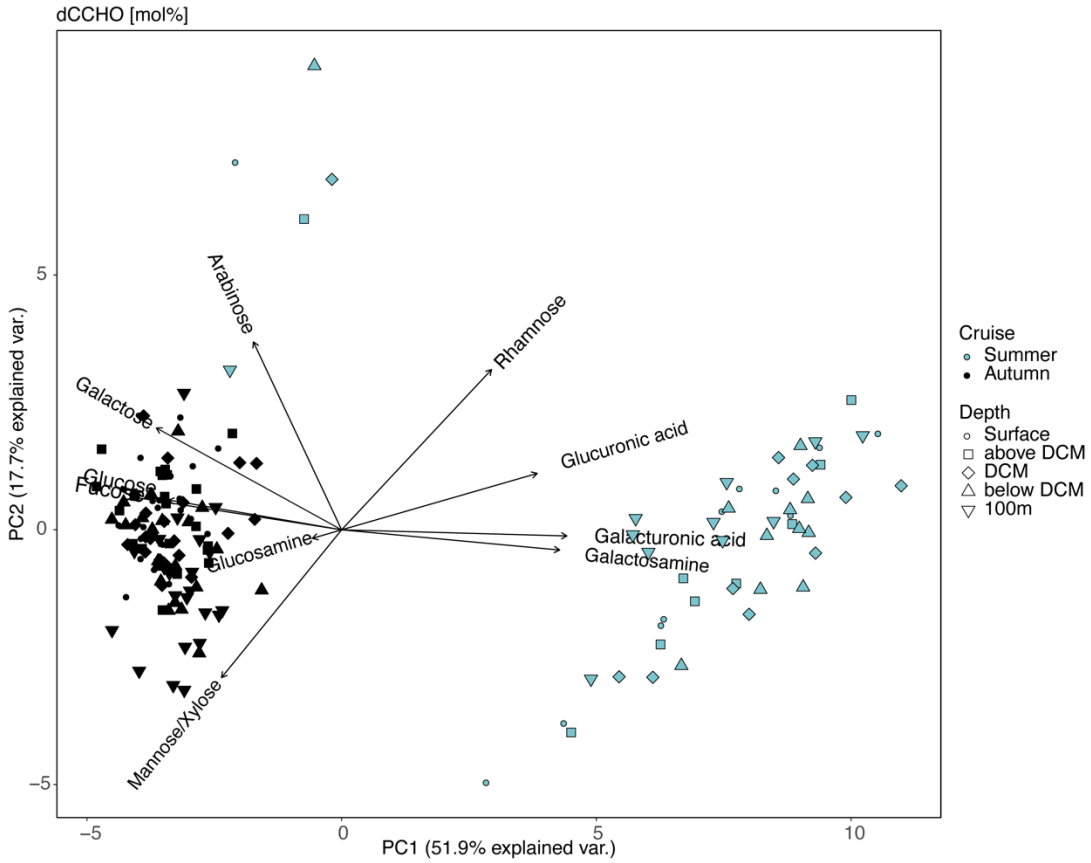

Figure S 3.1 | Relative composition (mol%) of dissolved combined carbohydrates (dCCHO) to determine a change in quality within the upper 100 m of the Fram Strait between summer and autumn. The summer samples were collected from July 16th to July 23rd, 2018 and autumn samples from September 16th to October 4th, 2018. The colour shows the two seasons: summer in blue and autumn in black. The shapes show the five depths: Surface (circle), above DCM (square), DCM (rhombus), below DCM (triangle faced up) and 100m (triangle faced down).

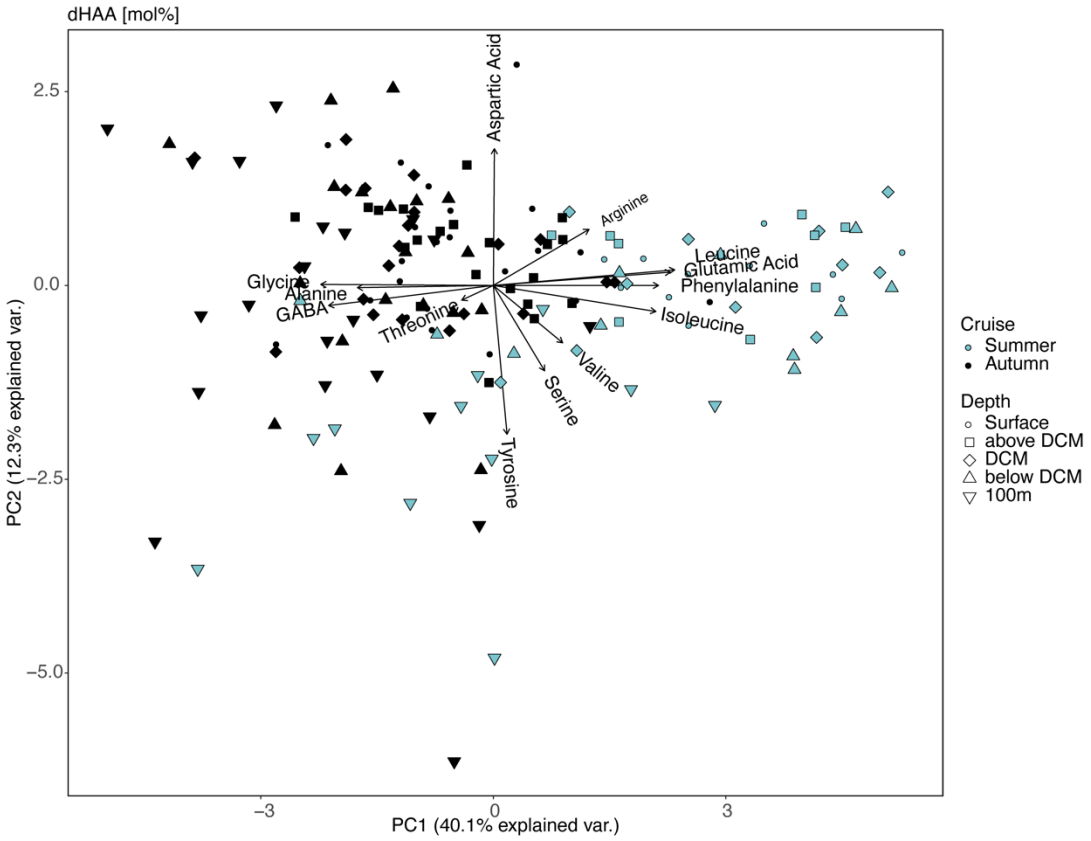

Figure S 3.2 | Relative composition (mol%) of dissolved hydrolysable amino acids (dHAA) to determine a change in quality within the upper 100 m of the Fram Strait between summer and autumn. The summer samples were collected from July 16th to July 23rd, 2018 and autumn samples from September 16th to October 4th, 2018. The colour shows the two seasons: summer in blue and autumn in black. The shapes show the five depths: Surface (circle), above DCM (square), DCM (rhombus), below DCM (triangle faced up) and 100m (triangle faced down).

Table S 3.1 | Stations within LTER HAUSGARTEN observatory and the associated CTD cast sampled in the upper 100m of the Fram Strait in the summer and autumn. The summer samples were collected with the RV Polarstern (PS114) from July 16th to July 23rd, 2018 and autumn samples with the RV Maria S. Merian (MSM77) from September 16th to October 4th, 2018. CTD dataset is available doi.pangaea.de/10.1594/PANGAEA.907467 and discrete samples are available: doi.org/10.1594/PANGAEA.915751

Season	Station	Sampling Date (dd.mm.yyyy)	CTD ID	Latitude (degrees)	Longitude (degrees)
Summer	HG1/2	19.07.2018	PS114_20-1	79.0244	5.6254
	HG4	16.07.2018	PS114_4-1	79.0237	4.3322
	N3	23.07.2018	PS114_33-1	79.5986	5.1662
	N4	22.07.2018	PS114_32-2	79.7410	4.5226
	N5	22.07.2018	PS114_31-1	79.9451	3.2006
	R1	19.07.2018	PS114_23-1	78.1874	-0.0080
	R2	20.07.2018	PS114_25-2	78.8313	-0.0545
	S3	17.07.2018	PS114_9-1	78.6165	5.0680
	SV2	19.07.2018	PS114_16-1	78.9803	9.2990
	SV3	18.07.2018	PS114_13-2	79.0190	8.0078
	SV4	18.07.2018	PS114_12-1	79.0118	7.0351
Autumn	D1	30.09.2018	MSM77_44-1	78.9997	1.5012
	D2	02.10.2018	MSM77_48-1	78.8825	0.3007
	D3	02.10.2018	MSM77_47-1	78.7498	-0.8832
	D4_2	01.10.2018	MSM77_46-4	78.5492	-1.8368
	HG1	20.09.2018	MSM77_13-1	79.1330	6.0942
	HG2	20.09.2018	MSM77_12-1	79.1302	4.9025
	HG3	19.09.2018	MSM77_8-1	79.1080	4.6005
	HG4	17.09.2018	MSM77_4-3	79.0592	4.2002
	HG5	28.09.2018	MSM77_36-1	79.0632	3.6595
	HG6	18.09.2018	MSM77_6-1	79.0600	3.5825
	HG7	28.09.2018	MSM77_37-1	79.0602	3.4772
	HG8	29.09.2018	MSM77_40-1	79.0643	3.3373
	HG9	29.09.2018	MSM77_41-1	79.1337	2.8372
	N3	04.10.2018	MSM77_54-1	79.6035	5.1730
	N4	04.10.2018	MSM77_53-3	79.7363	4.4850
	N5	03.10.2018	MSM77_52-1	79.9380	3.1948
	NSB_1	24.09.2018	MSM77_29-1	80.3000	13.9990
	S3	16.09.2018	MSM77_3-1	78.616	5.0675
	SV1	23.09.2018	MSM77_24-1	79.0283	11.086
	SV2	23.09.2018	MSM77_22-1	78.9800	9.5140
	SV3	22.09.2018	MSM77_19-1	78.9998	8.2500
	SV4	21.09.2018	MSM77_17-1	79.0298	6.9945

Table S 3.2 | Statistical analysis run for the study on all discrete parameters for the Fram Strait between summer and autumn. The summer samples were collected from July 16th to July 23rd, 2018 and autumn samples from September 16th to October 4th, 2018. The tests include: t-test, a statistical mixed model, an analysis of variances (ANOVA) and multiple contrast tests (MCT). MCT we only conducted if the ANOVA was significant. For details, please refer to Methods section. Abbreviations for the parameters are: Standard error (Std. Error); dissolved organic carbon (DOC); dissolved combined carbohydrates (dCCHO); dissolved hydrolysable amino acid (dHAA), particle area of transparent exopolymer particle (TEP Area); particle area of Coomassie stainable particles (CSP Area); bacterial abundance (BA); low nucleic acid bacteria (LNA); high nucleic acid bacteria (HNA) and bacterial production (BP). "AT" refers to Atlantic water and "IW" to intermediate water based on temperature-salinity characteristics.

Test	Variables	W-Statistic	p-value
Wilcoxon-Mann-Whitney	Season:Temperature	3000	0.78
	Season:Salinity	2600	**0.020**
	Season:DOC	3000	0.85
	Season:SLDOC	4900	**2.0×10^{-15}**
	Season:dCCHO	5200	**1.5×10^{-15}**
	Season:dHAA	4700	**1.7×10^{-12}**
	Season:TEP Area	4000	**1.3×10^{-9}**
	Season: CSP Area	2800	0.13
	Season: BA	4200	**5.1×10^{-6}**

(Table S 3.2. continued)

Test	Variables	W-Statistic	p-value	
Wilcoxon-Mann-Whitney	Season: HNA	4600	**2.7×10^{-9}**	
	Season: LNA	3400	0.090	
	Season: BP	6000	**3.8×10^{-15}**	
Test	**Variables**	**F-value**	**p-value**	**Further test?**
Mixed Model ANOVA	Temperature ~ Season	14	**0.00030**	
	Temperature ~Depth	3.3	**0.010**	
	Temperature ~Season*Depth	2.3	0.10	No MCT
	Temperature ~ Season	13	**0.00050**	
	Temperature ~ Watermass	15	**0.00020**	
	Temperature ~ Season*Watermass	0.70	0.40	No MCT
	Salinity ~ Season	6.9	**0.010**	
	Salinity ~ Depth	10	**<0.00010**	
	Salinity ~ Season*Depth	0.80	0.50	No MCT
	Salinity ~ Season	5.0	**0.030**	
	Salinity ~ Watermass	7.0	**<0.00010**	
	Salinity ~ Season*Watermass	4.0	0.051	No MCT
	Chl-*a* ~ Season	15	**0.00020**	
	Chl-*a* ~ Depth	33	**<0.00010**	
	Chl-*a* ~ Season*epth	4.9	**0.0010**	MCT
	Chl-*a* ~ Season	11	**0.0015**	
	Chl-*a* ~ Watermass	5.9	**0.017**	
	Chl-*a* ~ Season*Watermass	39	**<0.00010**	MCT

(Table S 3.2. continued)

Test	Variables	W-Statistic	p-value	Further Test?
Mixed Model ANOVA	DOC ~ Season	3.3	0.10	
	DOC ~ Depth	9.6	**<0.00010**	
	DOC ~ Season*Depth	3.7	**0.010**	MCT
	DOC ~ Season	2.2	0.14	
	DOC ~ Watermass	13	**0.00050**	
	DOC ~ Season*Watermass	0.63	0.43	No MCT
	SLDOC ~ Season	25	**<0.00010**	
	SLDOC ~ Depth	27	**<0.00010**	
	SLDOC ~ Season*Depth	17	**<0.00010**	MCT
	SLDOC ~Season	84	**<0.00010**	
	SLDOC ~Watermass	8.4	**0.0045**	
	SLDOC ~Season*Watermass	6.1	**0.015**	MCT
	dCCHO ~ Season	20	**<0.00010**	
	dCCHO ~ Depth	18	**<0.00010**	
	dCCHO ~ Season*Depth	17	**<0.00010**	MCT
	dCCHO ~ Season	85	**<0.00010**	
	dCCHO ~ Watermass	6.1	**0.015**	
	dCCHO ~ Season*Watermass	3.6	0.059	No MCT
	dHAA ~ Season	31	**<0.00010**	
	dHAA ~ Depth	25	**<0.00010**	
	dHAA ~ Season*Depth	9.8	**<0.00010**	MCT

Test	Variables	W-Statistic	p-value	Further Test?
Mixed Model ANOVA	dHAA ~ Season	60	**<0.00010**	
	dHAA ~ Watermass	11	**0.0015**	
	dHAA ~ Season*Watermass	13	**0.00040**	MCT
	TEP Area ~ Season	20	**<0.00010**	
	TEP Area ~ Depth	29	**<0.00010**	
	TEP Area ~ Season*Depth	16	**<0.00010**	MCT
	TEP Area ~ Season	65	**<0.00010**	
	TEP Area ~ Watermass	18	**0.00010**	
	TEP Area ~ Season*Watermass	1.3	0.26	No MCT
	CSP Area ~Season	30	**<0.00010**	
	CSP Area ~Depth	34	**<0.00010**	
	CSP Area ~Season*Depth	3.0	**0.021**	MCT
	CSP Area ~ Season	4.0	**0.048**	
	CSP Area ~ Watermass	2.1	0.15	
	CSP Area ~ Season*Watermass	30	**<0.00010**	MCT
	BA ~ Season	54	**<0.00010**	
	BA ~ Depth	15	**<0.00010**	
	BA ~ Season*Depth	1.5	0.20	No MCT
	BA ~ Season	40.3	**<0.00010**	
	BA ~ Watermass	1.4	0.24	
	BA ~ Season*Watermass	10.6	**0.00010**	MCT

(Table S 3.2. continued)

Test	Variables	F-value	p-value	Further test?
Mixed Model ANOVA	HNA ~ Season	89	**<0.00010**	
	HNA~ Depth	20	**<0.00010**	
	HNA~ Season*Depth	0.60	0.66	No MCT
	HNA ~ Season	64	**<0.00010**	
	HNA ~ Watermass	5.1	**0.026**	
	HNA ~ Season*Watermass	6.6	**0.012**	MCT
	LNA ~ Season	16	**<0.00010**	
	LNA ~ Depth	8.4	**<0.00010**	
	LNA ~ Season*Depth	3.6	**0.0081**	MCT
	LNA ~ Season	13	**0.00040**	
	LNA ~ Watermass	0.090	0.77	
	LNA ~ Season*Watermass	15	**0.00020**	MCT
	BP ~ Season	52	**<0.00010**	
	BP ~ Depth	37	**<0.00010**	
	BP ~ Season*Depth	17	**<0.00010**	MCT
	BP ~ Season	17	**<0.00010**	
	BP ~ Watermass	67	**<0.00010**	
	BP ~ Season*Watermass	22	**<0.00010**	MCT

Test	Variables	Estimate	Std. Error	p-value
Mixed Contrast Test (MCT)	Chl-a ~ Season*Depth			
	• Summer - Autumn, Surface	0.52	0.32	0.43
	• Summer - Autumn, ab.DCM	0.79	0.28	**0.030**
	• Summer - Autumn, DCM	1.2	0.36	**0.010**
	• Summer - Autumn, bel.DCM	1.1	0.30	**0.0010**
	• Summer - Autumn, 100 m	0.15	0.090	0.44
	Chla ~ Season*Watermass			
	• Summer, AW-IW	0.91	0.17	**1.1×10^{-6}**
	• Autumn, AW-IW	-0.23	0.050	**9.1×10^{-5}**
	• AW, Summer-Autumn	1.1	0.17	**6.5×10^{-9}**
	• IW, Summer-Autumn	-0.080	0.070	0.45
	DOC~ Season*Depth			
	• Summer - Autumn, Surface	4.8	2.2	0.14
	• Summer - Autumn, ab.DCM	6.3	2.3	**0.040**
	• Summer - Autumn, DCM	3.5	2.2	0.42
	• Summer - Autumn, bel.DCM	0.4	2.2	1.0
	• Summer - Autumn, 100 m	-4.1	2.2	0.27
	SLDOC~ Season*Depth			
	• Summer - Autumn, Surface	5.0	0.76	**1.0×10^{-5}**
	• Summer - Autumn, ab.DCM	5.6	1.2	**3.3×10^{-5}**
	• Summer - Autumn, DCM	4.9	1.1	**0.00010**
	• Summer - Autumn, bel.DCM	3.1	0.66	**3.1×10^{-5}**
	• Summer - Autumn, 100 m	0.65	0.18	**0.0023**

(Table S 3.2. continued)

Test	Variables	Estimate	Std. Error	p-value
Mixed Contrast Test (MCT)	SLDOC ~ Season*Watermass			
	• Summer, AW-IW	1.4	0.72	0.11
	• Autumn, AW-IW	-0.4	0.13	**0.0026**
	• AW, Summer-Autumn	4.2	0.58	**1.0×10^{-10}**
	• IW, Summer-Autumn	2.4	0.44	**4.7×10^{-7}**
	• dCCHO ~ Season*Depth			
	Summer - Autumn, Surface	660	110	**1.0×10^{-5}**
	• Summer - Autumn, ab.DCM	740	160	**0.0001**
	• Summer - Autumn, DCM	640	140	**2.6×10^{-5}**
	• Summer - Autumn, bel.DCM	370	73	**1.0×10^{-5}**
	• Summer - Autumn, 100 m	74	24	**0.013**
	dHAA ~ Season*Depth			
	• Summer - Autumn, Surface	272	44	**0.00010**
	• Summer - Autumn, ab.DCM	320	89	**0.0023**
	• Summer - Autumn, DCM	270	72	**0.0010**
	• Summer - Autumn, bel.DCM	230	63	**0.0018**
	• Summer - Autumn, 100 m	48	19	0.060
	dHAA ~ Season*Watermass			
	• Summer, AW-IW	130	45	**0.0095**
	• Autumn, AW-IW	-40	10	**0.00020**
	• AW, Summer-Autumn	270	38	**1.8×10^{-10}**
	• IW, Summer-Autumn	98	27	**0.00090**

Test	Variables	Estimate	Std. Error	p-value
Mixed Contrast Test (MCT)	TEP Area ~ Season*Depth			
	• Summer - Autumn, Surface	120	19	**1.0×10^{-5}**
	• Summer - Autumn, ab.DCM	84	14	**1.0×10^{-5}**
	• Summer - Autumn, DCM	83	20	**0.00030**
	• Summer - Autumn, bel.DCM	67	13	**1.0×10^{-5}**
	• Summer - Autumn, 100 m	10	6.0	0.37
	CSP Area ~ Season*Depth			
	• Summer - Autumn, Surface	15	30	0.99
	• Summer - Autumn, ab.DCM	34	18	0.27
	• Summer - Autumn, DCM	63	29	0.15
	• Summer - Autumn, bel.DCM	108	25	**0.00020**
	• Summer - Autumn, 100 m	17	14	0.74
	CSP Area ~ Season*Watermass			
	• Summer, AW-IW	81	17	**1.2×10^{-5}**
	• Autumn, AW-IW	-54	18	**0.0057**
	BA ~ Season*Watermass			
	• Summer, AW-IW	4.2	0.58	**1.0×10^{-10}**
	• Autumn, AW-IW	0.39	1.0	0.91
	• HNA ~ Season*Watermass			
	• Summer, AW-IW	54000	57000	0.57
	• Autumn, AW-IW	-120000	37000	**0.0024**
	• AW, Summer-Autumn	290000	34000	**1.0×10^{-10}**
	• IW, Summer-Autumn	110000	60000	0.12

(Table S 3.2. continued)

Test	Variables	Estimate	Std. Error	p-value
Mixed Contrast Test (MCT)	LNA ~ Season*Depth			
	• Summer - Autumn, Surface	19000	40000	0.99
	• Summer - Autumn, ab.DCM	30000	43000	0.97
	• Summer - Autumn, DCM	50000	40000	0.69
	• Summer - Autumn, bel.DCM	150000	40000	**0.0011**
	• Summer - Autumn, 100 m	180000	40000	**0.00010**
	LNA ~ Season*Watermass			
	• Summer, AW-IW	130000	26000	**4.8×10^{-6}**
	• Autumn, AW-IW	-73000	47000	0.22
	TEP Area ~ Season*Depth			
	Summer - Autumn, Surface	0.91	0.12	**1.0×10^{-5}**
	Summer - Autumn, ab.DCM	0.65	0.15	**0.00010**
	Summer - Autumn, DCM	0.53	0.12	**0.00010**
	Summer - Autumn, bel.DCM	0.40	0.08	**1.0×10^{-5}**
	Summer - Autumn, 100 m	0.11	0.03	**0.0031**

Supplementary Figures and Tables for Chapter 4

Contrasting microbial communities and substrate regimes in the eastern Fram Strait between summer and fall

Figure S 4.1 | Environmental conditions during summer and fall in the Fram Strait. A The temperature by latitude and longitude during summer. B The temperature by latitude and longitude during fall. C The fluorescence, temperature and salinity were measured using the CTD at “ HG4” during summer and fall. The fluorescence was measured using a WET Labs ECO-AFL/FL fluorometer, the temperature was measured using a SEA-BIRD temperature probe, and salinity was measured using a SEA-BIRD conductivity probe. The horizontal lines indicate the sampling depths of the surface, DCM, BDCM, and 100 m. Abbreviation: DCM, deep chlorophyll maximum; BDCM, below deep chlorophyll maximum.

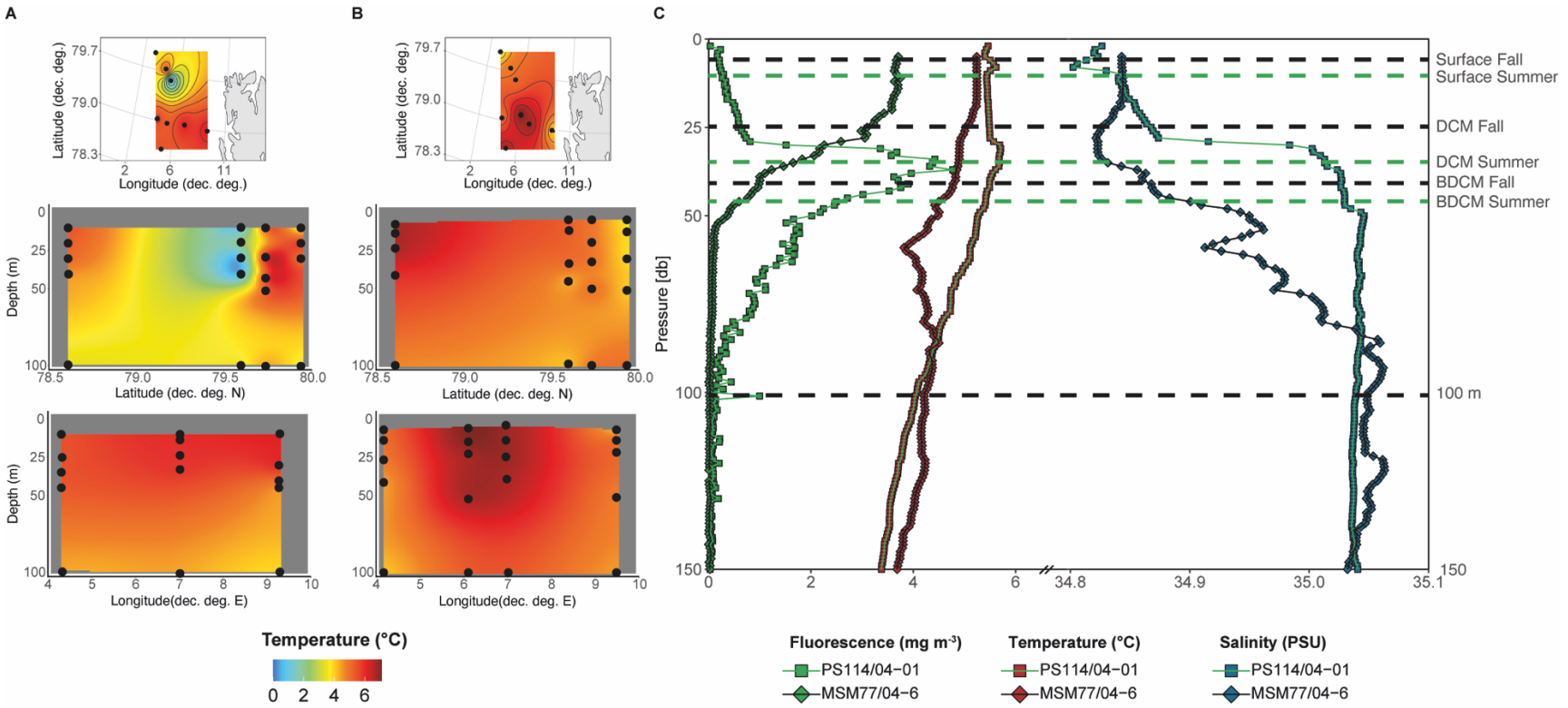

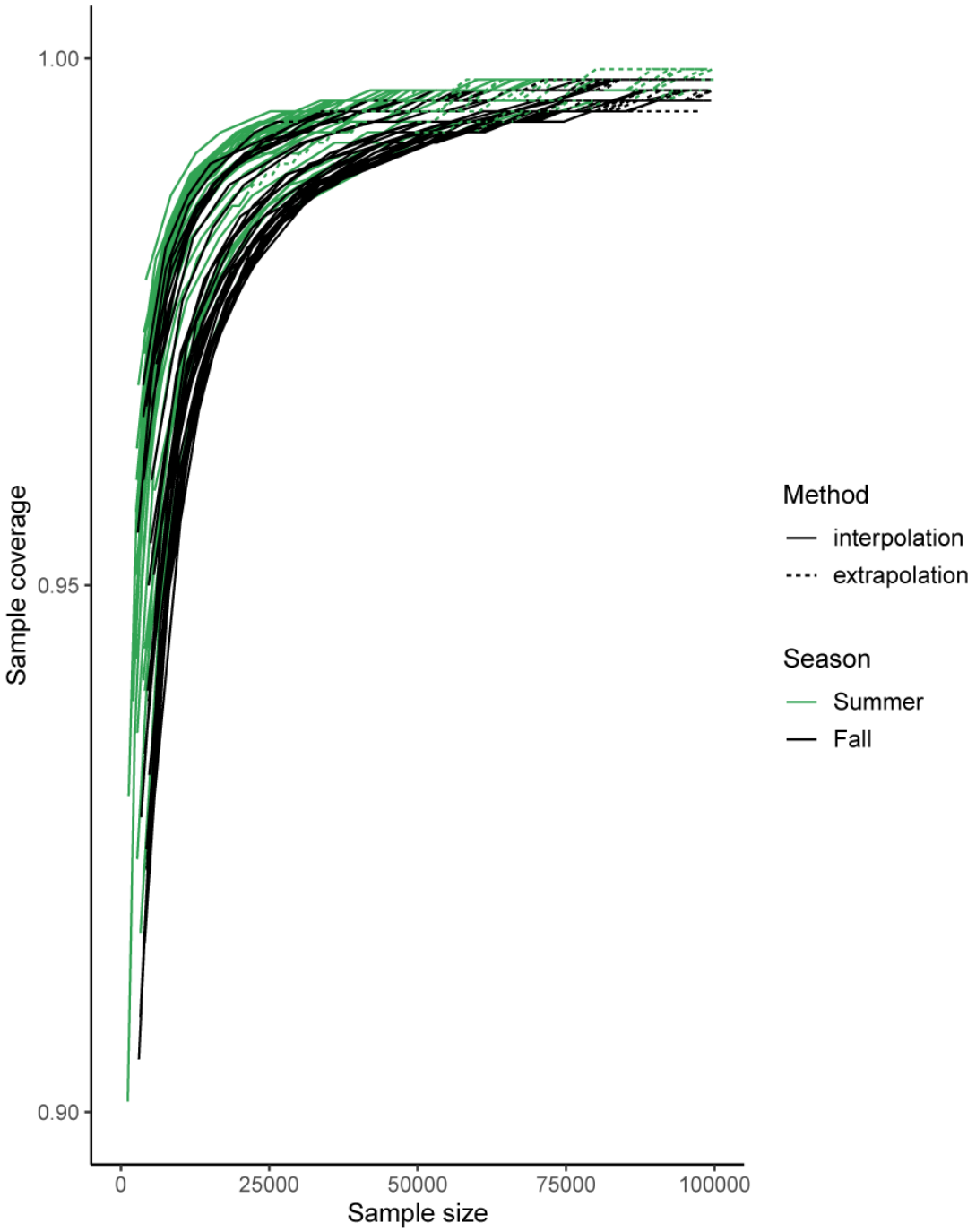

Figure S 4.2| Rarefaction curves of samples between summer and fall in the Fram Strait. The colors represent the season.

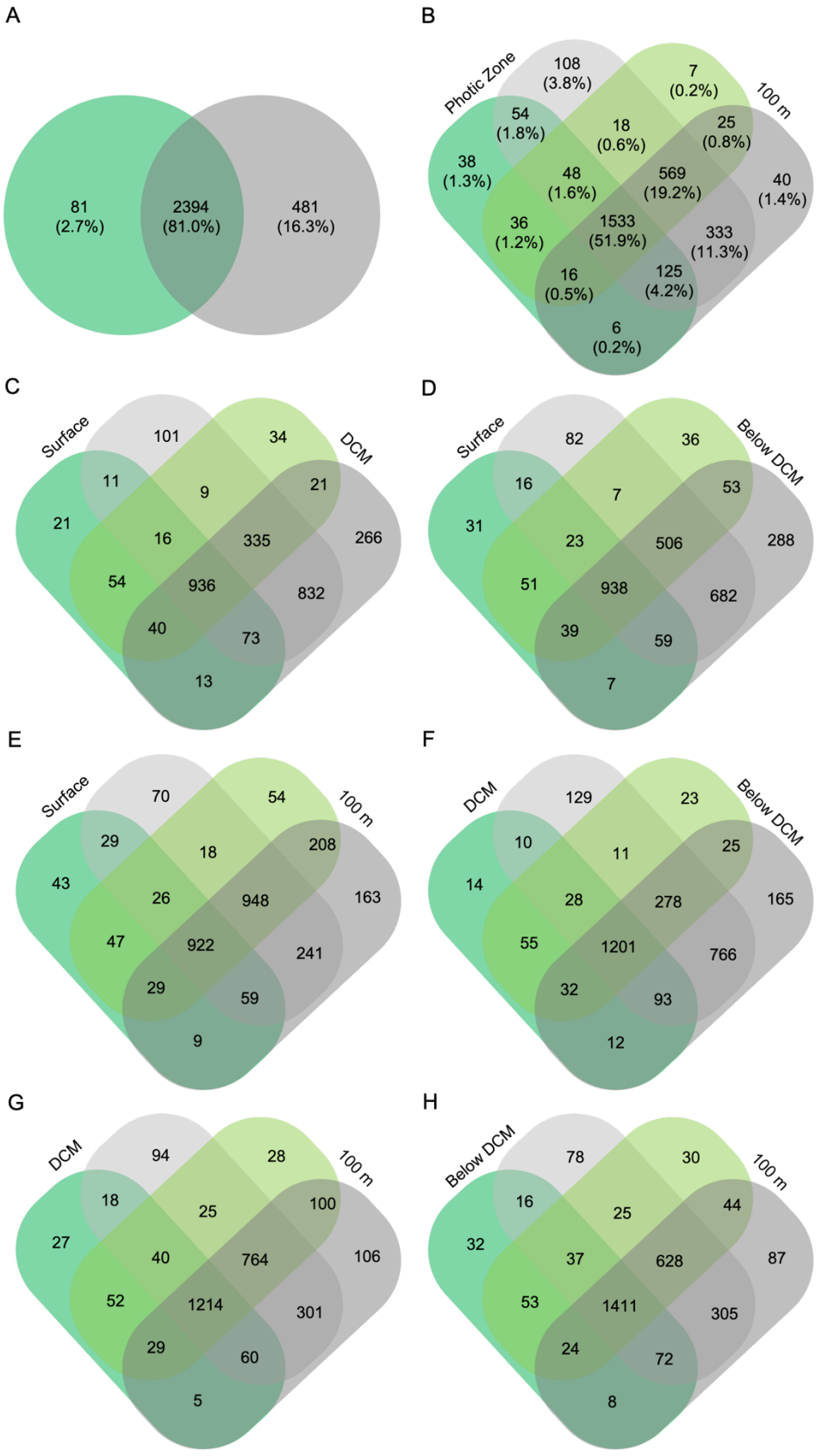

Figure S 4.3 | Venn diagrams of shared ASVs between the microbial community. A Summer compared to fall. B-H All the depths sampled in the upper 100 m.

Table S 4.1 | List of stations and parameters sampled during RV Polarstern expedition PS114 and RV Maria S. Merian expedition MSM77. Abbreviations: Particulate organic carbon (POC, µmol L^{-1}); dissolved organic carbon (DOC, µmol L^{-1}); dissolved combined carbohydrates (DCCHO, µmol L^{-1}); dissolved hydrolyzable amino acids (DHAA, µmol L^{-1}); primary production (PP; µmol C L^{-1} d^{-1}); phytoplankton abundances (PA, cells mL^{-1}); bacterial production (BP, µmol C L^{-1} d^{-1}); bacterial abundances (BA, cells mL^{-1}).

	General Information						Number of Samples per Parameter								
Season	Station	Sampling Date (dd.mm.yyyy)	PANGAEA Station ID	Latitude (degrees)	Longitude (degrees)	Depths (m)	POC	DOC	DCCHO	DHAA	PP	PA	BP	BA	16S rRNA
Summer	HG1/2	19.07.18	PS114_20-1	79.0244	5.6254	10,40,50,100	4	4	4	4	0	4	4	4	4
	HG4	16.07.18	PS114_4-1	79.0237	4.3322	10,35,45,100	4	4	4	4	2	4	4	4	4
	N3	23.07.18	PS114_33-1	79.5986	5.1662	10,20,30,100	4	4	4	4	0	4	4	4	4
	N4	22.07.18	PS114_32-2	79.7410	4.5226	10,43,53,100	4	4	4	4	0	4	4	4	4
	N5	22.07.18	PS114_31-1	79.9452	3.2006	10,20,30,100	4	4	4	4	2	4	4	4	4
	S3	17.07.18	PS114_9-1	78.6165	5.0680	10,30,40,100	4	4	4	4	0	4	4	4	4
	SV2	19.07.18	PS114_16-1	78.9803	9.2990	10,40,45,100	4	4	4	4	0	4	4	4	4
	SV4	18.07.18	PS114_12-1	79.0118	7.0351	10,23,33,100	4	4	4	4	2	4	4	4	4

(Table S 4.1 continued)

	General Information						Number of Samples per Parameter								
Season	Station	Sampling Date (dd.mm.yyyy)	PANGAEA Station ID	Latitude (degrees)	Longitude (degrees)	Depths (m)	POC	DOC	DCCHO	DHAA	PP	PA	BP	BA	16S rRNA
Fall	HG1	20.09.18	MSM77_13-1	79.1330	6.0942	5,21,50,100	4	4	4	4	0	4	4	4	3
	HG4	17.09.18	MSM77_4-3	79.0591	4.2002	5,25,40,100	4	4	4	3	2	4	4	4	4
	N3	04.10.18	MSM77_54-1	79.6035	5.1730	5,34,46,100	4	4	4	4	1	4	4	4	4
	N4	04.10.18	MSM77_53-3	79.7363	4.4850	5,20,50,100	4	4	4	4	0	4	4	4	4
	N5	03.10.18	MSM77_52-1	79.9380	3.1948	5,13,50,100	4	4	4	4	1	4	4	4	4
	S3	16.09.18	MSM77_3-1	78.6162	5.0675	5,22,40,100	4	4	4	4	2	4	4	4	4
	SV2	23.09.18	MSM77_22-1	78.9800	9.5140	5,20,50,100	4	4	4	4	0	4	4	4	4
	SV4	21.09.18	MSM77_17-1	79.0299	9.5140	5,25,40,100	4	4	4	4	2	4	4	4	4

Table S 4.2 | Summary of statistical tests with significant p-values in bold. Abbreviations: Analysis of Similarities (ANOSIM); Analysis of Variance (ANOVA); Degree of Freedom (DOF); Log_2 Fold Change (Log_2FC); Permutational Analysis of Variance (PERMANOVA); Observed Richness (Richness).

Test	Variables	Distribution	W-Value	p-value
Wilcoxon-Mann-Whitney	Cruise ~ Temp (°C)	Heterogeneous	350	0.09
	- Season ~ PP TOC (umol/L/d)	Heterogeneous	45	0.11
	- Season ~ PP POC (umol/L/d)	Heterogeneous	50	**0.031**
	- Season ~ PP DOC (umol/L/d)	Heterogeneous	36	0.56
	- Season ~ POC (umol/L)	Heterogeneous	950	**$4.2x10^{-11}$**
	- Season ~ Neutral Sugars (umol/L)	Heterogeneous	950	**$4.2x10^{-11}$**
	- Season ~ Acidic Sugars (umol/L)	Heterogeneous	860	**$1.9x10^{-6}$**
	- Season ~ Amino Sugars (umol/L)	Heterogeneous	590	0.28
	- Season ~ Essential Amino Acid (umol/L)	Heterogeneous	870	**$3.3x10^{-8}$**
	- Season ~ Non-Essential Amino Acid (umol/L)	Heterogeneous	850	**$1.7x10^{-7}$**
	- Season ~ Synnechoccus (cell/mL)	Heterogeneous	120	**$2.6x10^{-7}$**
	- Season ~ Cryptopytes (cell/mL)	Heterogeneous	870	**$1.6x10^{-6}$**
	- Season ~ Picoeukaryotes (cell/mL)	Heterogeneous	810	**$8.6x10^{-5}$**
	- Season ~ Nanoeukaryotes (cell/mL)	Heterogeneous	580	0.4
	- Season ~ Richness	Heterogeneous	100	**$6.3x10^{-8}$**
	- Season ~ Shannon-Wiener Index	Heterogeneous	95	**$1.6x10^{-9}$**
	- Season ~ Inverse Simpson Index	Heterogeneous	150	**$3.3x10^{-7}$**

Test	Variables	DOF	F-value	p-value
ANOVA	PP-POC (umol/L) ~ Season*Depth, random=~1|Station			
	• Season	1	7.5	0.025
	• Depth	1	5.1	0.055
	• Season:Depth	1	0.030	0.87
	POC (umol/L) ~ Season*Depth, random=~1|Station			
	• Season	1	75	**<0.0001**
	• Depth	3	11	**<0.0001**
	• Season:Depth	3	5.4	**0.0028**
	Neutral DCCHO (umol/L) ~ Season*Depth, rand.=~1|Station			
	• Season	1	66	**<0.00010**
	• Depth	3	9.1	**0.00010**
	• Season:Depth	3	6.0	**0.002**
	Acidic DCCHO (umol/L) ~ Season*Depth, rand.=~1|Station			
	• Season	1	76	**<0.00010**
	• Depth	3	24	**<0.00010**
	• Season:Depth	3	22	**<0.00010**
	Essential DHAA (umol/L) ~ Season*Depth, rand.=~1|Station			
	• Season	1	37	**<0.00010**
	• Depth	3	13	**<0.00010**
	• Season:Depth	3	10	**0.00010**

(Table S 4.2 continued)

Test	Variables	DOF	F-value	p-value
ANOVA	Non-Essential DHAA (umol/L) ~ Season*Depth, rand.=~1|Station			
	• Season	1	23	**0.00010**
	• Depth	3	9.5	**0.00010**
	• Season:Depth	3	9.1	**<0.00010**
	Synnechoccus (cell/mL) ~ Season*Depth,random =~1|Station			
	• Season	1	12	**0.0010**
	• Depth	3	12	**<0.00010**
	• Season:Depth	3	4.1	**0.011**
	Cryptophytes (cell/mL) ~ Season*Depth, random=~1|Station			
	• Season	1	39	**<0.00010**
	• Depth	3	19	**<0.00010**
	• Season:Depth	3	3.4	**0.025**
	Picoeukaryotes (cell/mL) ~ Season*Depth, random=~1|Station			
	• Season	1	55	**<0.00010**
	• Depth	3	21	**<0.00010**
	• Season:Depth	3	1.5	0.22
	Nanoeukaryotes (cell/mL) ~ Season*Depth, random=~1|Station			
	• Season	1	0.51	0.48
	• Depth	3	21	**<0.00010**
	• Season:Depth	3	1.3	0.28

Test	Variables	DOF	F-value	p-value
ANOVA	Heterotrophs (cell/mL) ~ Season*Depth, random=~1|Station			
	• Season	1	55	**<0.00010**
	• Depth	3	9.6	**<0.00010**
	• Season:Depth	3	1.5	0.23
	PP (umol/L/d) ~ Season, random=~1|Station			
	• Season	1	8.0	**0.030**
	• Depth	1	6.1	**0.049**
	• Season:Depth	1	0.010	0.95
	BP (umol/L/d) ~ Season, random=~1|Station			
	• Season	1	42	**<0.00010**
	• Depth	3	19	**<0.00010**
	• Season:Depth	3	12	**<0.00010**

Test	Variables	ANOSIM statistic	p-value
ANOSIM	ASV Matrix ~ Summer - Fall	0.69	**0.0010**
	ASV Matrix ~ Summer, Surface-DCM	0.14	0.051
	ASV Matrix ~ Summer, DCM-Below DCM	-0.075	0.80
	ASV Matrix ~ Summer, Below DCM-100m	0.45	**0.0010**
	ASV Matrix ~ Summer, Photic Zone-100m	0.59	**0.0010**
	ASV Matrix ~ Fall, Surface-DCM	-0.077	0.80
	ASV Matrix ~ Fall, DCM-Below DCM	0.11	0.099
	ASV Matrix ~ Fall, Below DCM-100m	0.42	**0.0030**
	ASV Matrix ~ Fall, Photic Zone-100m	0.26	**0.026**

(Table S 4.2. continued)

Test	**Variables**	**DOF**	**F-value**	**p-value**
PERMANOVA	Observed Richness ~ Season*Depth			
	Season	1	52	**1.8×10^{-9}**
	Depth	3	10	**2.0×10^{-5}**
	Season:Depth	3	1.4	0.25
	Residuals	55		
	Shannon-Wiener Diversity ~ Season*Depth			
	Season	1	55	**7.5×10^{-10}**
	Depth	3	3.0	**0.039**
	Season:Depth	3	0.50	0.69
	Residuals	55		
	Simpson Diversity ~ Season*Depth			
	Season	1	34	**3.1×10^{-7}**
	Depth	3	0.77	0.51
	Season:Depth	3	0.26	0.85
	Residuals	55		
Test	Variables	**Lower**	**Upper**	**p-value**
Tukey Test	Richness Summer, Photic - 100 m	-720.04	-300	**2.2×10^{-5}**
	Richness Summer, Surface – DCM	-297.25	400	0.98
	Richness Summer, DCM - below DCM	-438.75	260	0.90
	Richness Summer, below DCM - 100 m	-819.63	-120	**0.0053**
	Shannon-Wiener Summer, Photic - 100 m	-63.74	-17	**0.0013**
	Shannon-Wiener Summer, Surface - DCM	-39.04	39	**1.0**
	Shannon-Wiener Summer, DCM - below DCM	-48.25	30	0.92

Test	Variables	Lower	Upper	p-value
Tukey Test	Shannon-Wiener Summer, below DCM - 100 m	-74	4.8	0.10
	Richness Fall, Photic - 100 m	-72	24	0.31
	Richness Fall, Surface – DCM	-650	290	0.72
	Richness Fall, DCM - below DCM	-700	230	0.52
	Richness Fall, below DCM - 100 m	-580	320	0.85
	Shannon-Wiener Fall, Photic - 100 m	-640	-51	**0.023**
	Shannon-Wiener Fall, Surface – DCM	-98	62	0.93
	Shannon-Wiener Fall, DCM - below DCM	-100	56	0.84
	Shannon-Wiener Fall, below DCM - 100 m	-80	75	1.0
Test	**Variables**	**Estimate**	**t-value**	**p-**
Multiple Contrast Test (MCT)	POC (umol/L) Summer, Surface – DCM	4.0	0.78	0.98
	POC (umol/L) Summer, DCM- Below DCM	-4.3	-0.84	0.97
	POC (umol/L) Summer, Below DCM- 100m	-11	-3.33	**0.015**
	POC (umol/L) Fall, Surface – DCM	-2.3	-1.10	0.88
	POC (umol/L) Fall, DCM- Below DCM	-2.7	-2.6	0.098
	POC (umol/L) Fall, Below DCM- 100m	-0.64	-1.6	0.58
	DCCHO (umol/L) Summer, Surface – DCM	0.050	0.23	1.0
	DCCHO (umol/L) Summer, DCM- Below DCM	-0.30	-1.6	0.57
	DCCHO (umol/L) Summer, Below DCM- 100m	-0.41	-5.1	**< 0.0010**
	DCCHO (umol/L) Fall, Surface – DCM	-0.030	-0.80	0.97
	DCCHO (umol/L) Fall, DCM- Below DCM	-0.030	-1.5	0.62
	DCCHO (umol/L) Fall, Below DCM- 100m	-0.040	-2.5	0.11

(Table S 4.2. continued)

Test	Variables	Estimate	t-value	p-value
Multiple Contrast Test (MCT)	DHAA (umol/L) Summer, Surface – DCM	0.030	0.27	1.0
	DHAA (umol/L) Summer, DCM- Below DCM	-0.060	-0.50	1.0
	DHAA (umol/L) Summer, Below DCM- 100m	-0.26	-3.3	**0.019**
	DHAA (umol/L) Fall, Surface – DCM	-0.030	-0.80	0.97
	DHAA (umol/L) Fall, DCM- Below DCM	-0.030	-1.4	0.70
	DHAA (umol/L) Fall, Below DCM- 100m	-0.020	-1.4	0.71
	TEP (cm^2/L) Summer, Surface – DCM	-0.42	-1.3	0.79
	TEP (cm^2/L) Summer, DCM- Below DCM	-0.30	-1.08	0.89
	TEP (cm^2/L) Summer, Below DCM- 100m	-0.70	-4.6	**< 0.0010**
	TEP (cm^2/L) Fall, Surface – DCM	-0.14	-0.73	0.98
	TEP (cm^2/L) Fall, DCM- Below DCM	-0.19	-2.0	0.32
	TEP (cm2/L) Fall, Below DCM- 100m	-0.07	-1.3	0.80
	CSP (cm^2/L) Summer, Surface – DCM	0.78	2.1	0.30
	CSP (cm^2/L) Summer, DCM- Below DCM	0.08	0.16	1.00
	CSP (cm^2/L) Summer, Below DCM- 100m	-1.5	-3.5	**0.0085**
	CSP (cm^2/L) Fall, Surface – DCM	-0.27	-0.85	0.97
	CSP (cm^2/L) Fall, DCM- Below DCM	-0.18	-0.76	0.98
	CSP (cm^2/L) Fall, Below DCM- 100m	-0.37	-2.7	0.078
	Synnechoccus (cell/mL) Summer, Surface – DCM	-260	-1.1	0.87
	Synnechoccus (cell/mL) Summer, DCM- Below DCM	-120	-0.76	0.98
	Synnechoccus (cell/mL) Summer, Below DCM- 100m	-312	-2.8	0.057
	Synnechoccus (cell/mL) Fall, Surface – DCM	-9100	-0.64	0.99
	Synnechoccus (cell/mL) Fall, DCM- Below DCM	-16000	-1.9	0.37
	Synnechoccus (cell/mL) Fall, Below DCM- 100m	-3500	-1.7	0.53

(Table S 4.2. continued)

Test	Variables	Estimate	t-value	p-value
Multiple Contrast Test (MCT)	Cryptopytes (cell/mL) Summer, Surface – DCM	-220	-1.0	0.91
	Cryptopytes (cell/mL) Summer, DCM- Below DCM	-93	-0.54	1.00
	Cryptopytes (cell/mL) Summer, Below DCM- 100m	-400	-3.1	**0.033**
	Cryptopytes (cell/mL) Fall, Surface – DCM	-78	-0.7	0.98
	Cryptopytes (cell/mL) Fall, DCM- Below DCM	-160	-2.2	0.23
	Cryptopytes (cell/mL) Fall, Below DCM- 100m	-96	-3.5	**0.0092**
	Picoeukaryote (cell/mL) Summer, Surface – DCM	-4800	-3.1	**0.025**
	Picoeukaryote (cell/mL) Summer, DCM- Below DCM	-1100	-0.92	0.94
	Picoeukaryote (cell/mL) Summer, Below DCM- 100m	-1900	-2.4	0.14
	Picoeukaryote (cell/mL) Fall, Surface – DCM	-2800	-1.2	0.82
	Picoeukaryote (cell/mL) Fall, DCM- Below DCM	-2400	-2.1	0.25
	Picoeukaryote (cell/mL) Fall, Below DCM- 100m	-330	-1.5	0.64
	Nanoeukaryote (cell/mL) Summer, Surface – DCM	-930	-0.47	1.0
	Nanoeukaryote (cell/mL) Summer, DCM- Below DCM	-970	-0.46	1.0
	Nanoeukaryote (cell/mL) Summer, Below DCM- 100m	-4200	-2.8	0.063
	Nanoeukaryote (cell/mL) Fall, Surface – DCM	-1900	-0.69	0.99
	Nanoeukaryote (cell/mL) Fall, DCM- Below DCM	-4900	-2.3	0.21
	Nanoeukaryote (cell/mL) Fall, Below DCM- 100m	-1500	-2.0	0.33
	Heterotrophs (cell/mL) Summer, Surface – DCM	-92000	-1.0	0.93
	Heterotrophs (cell/mL) Summer, DCM- Below DCM	-7700	-0.050	1.0
	Heterotrophs (cell/mL) Summer, Below DCM- 100m	-	-1.1	0.91
	Heterotrophs (cell/mL) Fall, Surface – DCM	-	-1.5	0.70
	Heterotrophs (cell/mL) Fall, DCM- Below DCM	-	-2.4	0.17
	Heterotrophs (cell/mL) Fall, Below DCM- 100m	-	-1.6	0.63

(Table S 4.2. continued)

Test	Variables	Estimate	t-value	p-value
Multiple Contrast Test (MCT)	PP (umol/L/d) Summer, Surface – DCM	-0.40	-0.68	0.76
	PP (umol/L/d) Fall, Surface - DCM	-0.45	-2.4	0.10
	BP (umol/L/d) Summer, Surface – DCM	-0.043	-2.7	0.082
	BP (umol/L/d) Summer, DCM- Below	-0.017	-1.2	0.83
	BP (umol/L/d) Summer, Below DCM-	-0.024	-2.7	0.084
	BP (umol/L/d) Fall, Surface – DCM	-0.007	-1.3	0.80
	BP (umol/L/d) Fall, DCM- Below DCM	-0.008	-3.9	**0.0033**
	BP (umol/L/d) Fall, Below DCM- 100m	-0.002	-1.9	0.40

Test	Variables	Genus Level	Log_2FC	q-value
log_2Fold-Change	Photic Zone, Summer (-)~ Fall (+)	*AEGEAN-169 marine group*	2.9	**0.028**
alpha = 0.05		*Candidatus Nitrosopelagicus*	3.1	**0.028**
		Candidatus Nitrosopumilus	2.8	**0.031**
		LS-NOB	3.0	**0.028**
		Marinimicrobia unclassified	4.0	**0.0021**
		Synechococcus CC9902	4.4	**0.0026**
		Nitrincolaceae unclassified	-4.2	**0.0049**
		Proteobacteria unclassified	-4.2	**0.0040**
		Rickettsiales	-3.5	**0.013**
		SAR92 clade	-3.8	**0.0056**
	100 m, Summer (-)~ Fall (+)	*Arctic97B-4 marine group*	2.8	**0.043**
		Marinimicrobia unclassified	3.1	**0.018**
		Marine Group II unclassified	-2.8	**0.027**

(Table S 4.2. continued)

Test	Variables	Genus Level	Log_2FC	q-value
log_2Fold-Change	100 m, Summer (-)~ Fall (+)	Proteobacteria unclassified	-2.9	**0.027**
alpha = 0.05		*Rickettsiales*	-2.7	**0.029**
	Summer, Photic (+)~ 100 m (-)	*Candidatus Puniceispirillum*	3.8	**0.0047**
		Cryomorphaceae	3.9	**0.0019**
		Flavobacteriacea	4.3	**0.0019**
		NS5 marine group	2.8	**0.023**
	Summer, Photic (+)~ 100 m (-)	Proteobacteria unclassified	4.4	**0.0019**
		SAR116 clade	3.1	**0.013**
		SAR92 clade	3.7	**0.0047**
		Synechococcus CC9902	3.0	**0.027**
		AEGEAN-169 marine group	-2.4	**0.040**
		Candidatus Nitrosopelagicus	-4.4	**$6.3x10^{-4}$**
		Candidatus Nitrosopumilus	-4.5	**$6.4x10^{-4}$**
		LS-NOB	-4.3	**$6.4x10^{-4}$**
		Marine Group II unclassified	-3.2	**0.0079**
		Marinimicrobia unclassified	-4.6	**$2.5x10^{-4}$**
		Nitrospina	-3.2	**0.0079**
		OM27 clade	-3.8	**0.0016**
		SAR11 Clade Ib	-3.6	**0.0024**
		SAR202 clade	-3.6	**0.0025**
		SAR324 clade	-3.3	**0.0079**
		Sva0996 marine group	-2.5	**0.040**

(Table S 4.2. continued)

Test	Variables	Genus Level	Log_2FC	q-value
log_2Fold-Change Alpha = 0.05	Fall, Photic (+)~ 100 m (-)	*Candidatus Puniceispirillum*	3.31	**0.024**
		Cryomorphaceae	3.28	**0.020**
		Flavobacteriacea	3.11	**0.024**
		NS5 marine group	2.87	**0.028**
		Synechococcus CC9902	7.54	**$8.6x10^{-5}$**
		Arctic97B-4 marine group	-3.18	**0.020**
		AT-s3-44	-2.69	**0.047**
		Candidatus Nitrosopelagicus	-4.41	**$8.4x10^{-4}$**
		Candidatus Nitrosopumilus	-2.82	**0.027**
		Marinimicrobia unclassified	-3.84	**$8.8x10^{-4}$**
		Nitrospina	-3.03	**0.019**
		OM190	-3.45	**0.0093**
		PB19	-4.23	**$8.8x10^{-4}$**
		SAR11 Clade Ib	-5.52	**$1.5x10^{-5}$**
		SAR202 clade	-4.99	**$2.0x10^{-4}$**
Test	**Variables**	**AIC**	**F-value**	**q-value**
Forward- Selection ASV with >3 counts in >3% of Samples~ Biopolymers	Alanine	496.59	0.57	0.97
	Arabinose	495.54	1.47	0.09
	Arginine	496.00	1.07	0.38
	Aspartic Acid	497.02	3.32	**0.025**
	CSP Area	499.68	5.79	**0.005**
	Fucose	497.50	3.76	**0.010**
	GABA	496.10	0.99	0.47

(Table S 4.2. continued)

Test	Variables	AIC	F-value	q-value
Forward- Selection	Galactosamine	496.00	1.07	0.36
ASV with >3 counts in	Galactose	496.40	0.73	0.81
>3% of Samples~	Galacturonic Acid	496.04	1.04	0.38
Biopolymers	Glucosamine	498.42	4.60	**0.020**
	Glucose	497.22	3.50	**0.020**
	Glucuronic Acid	495.35	1.63	0.070
	Glutamic Acid	496.51	0.63	0.91
	Glycine	496.84	3.16	**0.035**
	Isoleucine	495.77	1.27	0.18
	Leucine	496.34	0.78	0.69
	Mannose/Xylose	495.55	1.46	0.15
	Phenylalanine	496.07	1.01	0.36
	Rhamnose	499.10	5.25	**0.0050**
	Serine	495.24	1.73	0.065
	TEP Area	501.53	7.58	**0.0050**
	Threonine	495.99	1.08	0.36
	Tyrosine	495.13	1.82	0.065
	Valine	496.08	1.00	0.43

Supplementary Figures and Tables for Chapter 5

Summertime trends of semi-labile DOC across the Fram Strait

Table S 5.1 | Dates and coordinates of sample collections. SST cluster denotes whether the sample was categorized into the Atlantic or Polar sector.

Expedition	HAUSGARTEN Station	Date (DD.MM.YYYY)	Lat (DD)	Long (DD)	SST Sector
ARK24/2	HG4	10.07.2009	79.0700	4.2000	Atlantic
ARK24/2	HG6	11.07.2009	79.0700	3.5800	Atlantic
ARK24/2	HG7	13.07.2009	79.0600	3.4900	Polar
ARK24/2	N4	14.07.2009	79.7400	4.4900	Atlantic
ARK24/2	N1	15.07.2009	79.2900	4.3400	Atlantic
ARK24/2	S1	16.07.2009	78.9200	5.0000	Atlantic
ARK24/2	S2	17.07.2009	78.7900	5.3400	Atlantic
ARK25/2	HG1	06.07.2010	79.1300	6.1000	Atlantic
ARK25/2	SV2	06.07.2010	78.9800	9.5200	Atlantic
ARK25/2	HG2	07.07.2010	79.1300	4.9000	Atlantic
ARK25/2	#166-1	11.07.2010	78.8300	4.0000	Atlantic
ARK25/2	HG9	12.07.2010	79.1400	2.7600	Polar
ARK25/2	HG4	12.07.2010	79.0000	4.3000	Atlantic
ARK25/2	HG4	12.07.2010	79.0000	4.3000	Atlantic
ARK25/2	HG5	12.07.2010	79.0500	3.7400	Atlantic
ARK25/2	HG6	12.07.2010	79.0500	3.5900	Atlantic
ARK25/2	HG7	13.07.2010	79.0600	3.4800	Atlantic
ARK25/2	HG8	13.07.2010	79.0600	3.3100	Atlantic
ARK25/2	N4	14.07.2010	79.7400	4.4800	Atlantic
ARK25/2	N4	14.07.2010	79.7400	4.4800	Atlantic
ARK25/2	N3	15.07.2010	79.5900	5.2100	Atlantic
ARK25/2	N2	15.07.2010	79.4300	4.7500	Atlantic
ARK25/2	N1	16.07.2010	79.2800	4.3300	Atlantic
ARK25/2	S2	04.07.2010	78.7800	5.3300	Atlantic
ARK25/2	S1	05.07.2010	78.9200	5.0000	Atlantic
ARK25/2	#194-1	17.07.2010	78.8300	0.3900	Polar
ARK25/2	#210-2	20.07.2010	78.8300	-2.1200	Polar
ARK25/2	#220-1	21.07.2010	78.8300	-3.9000	Polar
ARK26/2	HG2	15.07.2011	79.1411	4.8939	Atlantic
ARK26/2	HG3	20.07.2011	79.1139	4.6092	Polar
ARK26/2	HG4	29.07.2011	79.0067	4.3375	Polar
ARK26/2	HG6	21.07.2011	79.0547	3.6025	Polar
ARK26/2	HG6	21.07.2011	79.0547	3.6025	Polar
ARK26/2	HG7	21.07.2011	79.0611	3.4703	Polar
ARK26/2	HG8	21.07.2011	79.0703	3.3261	Polar
ARK26/2	HG9	17.07.2011	79.1189	2.7647	Polar
ARK26/2	HG9	17.07.2011	79.1189	2.7647	Polar
ARK26/2	N5	26.07.2011	79.9501	3.1411	Polar
ARK26/2	N4	23.07.2011	79.7294	4.4669	Polar
ARK26/2	N3	27.07.2011	79.6056	5.2394	Polar
ARK26/2	S3	27.07.2011	78.6001	5.0514	Atlantic

ARK26/2	S2	29.07.2011	78.7894	5.3283	Atlantic
ARK26/2	S1	29.07.2011	78.9197	5.0033	Atlantic
ARK26/2	SV4	20.07.2011	79.0522	7.0161	Atlantic
PS80	HG1	17.07.2012	79.1352	6.1052	Atlantic
PS80	HG1	17.07.2012	79.1352	6.1052	Atlantic
PS80	HG2	17.07.2012	79.1302	4.9373	Atlantic
PS80	HG3	16.07.2012	79.1080	4.6020	Atlantic
PS80	HG4	16.07.2012	79.0077	4.3315	Atlantic
PS80	HG5	21.07.2012	79.0637	3.6457	Atlantic
PS80	HG6	22.07.2012	79.0608	3.5798	Atlantic
PS80	HG7	22.07.2012	79.0603	3.4762	Atlantic
PS80	HG8	22.07.2012	79.0643	3.3328	Atlantic
PS80	HG9	22.07.2012	79.1338	2.8410	Atlantic
PS80	S1	21.07.2012	78.9168	5.0023	Atlantic
PS80	S2	19.07.2012	78.7802	5.3308	Atlantic
PS80	S3	20.07.2012	78.6102	5.0680	Atlantic
PS80	N1	26.07.2012	79.2832	4.3280	Atlantic
PS80	N2	25.07.2012	79.4098	4.6978	Atlantic
PS80	N3	24.07.2012	79.6037	5.1713	Atlantic
PS80	N4	23.07.2012	79.7403	4.5037	Atlantic
PS80	N5	24.07.2012	79.9332	3.1797	Atlantic
PS80	SV4	18.07.2012	79.0295	6.9978	Atlantic
PS80	SV1	18.07.2012	79.0280	11.0757	Atlantic
PS85	HG1	24.06.2014	79.1350	6.0895	Atlantic
PS85	HG2	24.06.2014	79.1305	4.8952	Atlantic
PS85	HG4	22.06.2014	79.0650	4.1788	Atlantic
PS85	HG9	23.06.2014	79.1487	2.7908	Polar
PS85	N4	25.06.2014	79.7588	4.2762	Polar
PS85	F9	26.06.2014	78.8347	-0.9150	Polar
PS85	411	14.06.2014	77.7177	-15.4782	Polar
PS85	424	15.06.2014	77.9940	-14.2767	Polar
PS85	426	16.06.2014	78.8052	-9.9307	Polar
PS85	429	16.06.2014	78.8313	-8.5648	Polar
PS85	437	17.06.2014	78.8328	-5.4975	Polar
PS85	437	17.06.2014	78.8328	-5.4975	Polar
PS85	444	18.06.2014	78.8312	-3.9803	Polar
PS85	444	18.06.2014	78.8312	-3.9803	Polar
PS85	455	21.06.2014	78.4533	-2.8328	Polar
PS85	455	21.06.2014	78.4533	-2.8328	Polar
PS93	HG1	10.08.2015	79.1330	6.1010	Atlantic
PS93	HG1	10.08.2015	79.1330	6.1010	Atlantic
PS93	HG2	09.08.2015	79.1303	4.9043	Atlantic
PS93	HG3	08.08.2015	79.1083	4.6000	Atlantic
PS93	HG4	26.07.2015	79.0652	4.1790	Atlantic

PS93	HG5	28.07.2015	79.0630	3.6600	Atlantic
PS93	HG5	28.07.2015	79.0630	3.6600	Atlantic
PS93	HG6	28.07.2015	79.0600	3.5830	Atlantic
PS93	HG6	28.07.2015	79.0600	3.5830	Atlantic
PS93	HG8	29.07.2015	79.0642	3.3363	Atlantic
PS93	HG9	12.08.2015	79.1337	2.8423	Atlantic
PS93	EG4	30.07.2015	78.8615	-2.7093	Polar
PS93	EG4	30.07.2015	78.8615	-2.7093	Polar
PS93	N5	02.08.2015	79.9383	3.1912	Atlantic
PS93	N4	04.08.2015	79.8217	4.2537	Atlantic
PS93	N3	11.08.2015	79.6040	5.1712	Atlantic
PS93	S3	24.07.2015	78.5990	5.0683	Atlantic
PS93	SV1	06.08.2015	79.0285	11.0878	Atlantic
PS93	SV3	07.08.2015	79.0007	8.2502	Atlantic
PS93	SV4	08.08.2015	79.0297	6.9990	Atlantic
PS99	HG1	09.07.2016	79.1392	6.0885	Atlantic
PS99	HG2	06.07.2016	79.1300	4.9067	Atlantic
PS99	HG3	10.07.2016	79.1077	4.5967	Polar
PS99	HG4	27.06.2016	79.0652	4.1728	Polar
PS99	HG5	28.06.2016	79.0672	3.6653	Polar
PS99	HG6	28.06.2016	79.0600	3.5702	Polar
PS99	HG8	29.06.2016	79.0722	3.3448	Polar
PS99	HG9	06.07.2016	79.1348	2.8458	Polar
PS99	EG4	30.06.2016	78.8160	-2.7288	Polar
PS99	EG3	01.07.2016	78.8622	-3.9733	Polar
PS99	EG2	01.07.2016	78.9367	-4.6503	Polar
PS99	EG1	02.07.2016	78.9908	-5.4093	Polar
PS99	S3	25.06.2016	78.6078	5.0468	Polar
PS99	N4	05.07.2016	79.7415	4.5035	Polar
PS99	N3	04.07.2016	79.5867	5.1700	Atlantic
PS99	SV1	09.07.2016	79.0263	11.0925	Atlantic
PS99	SV2	09.07.2016	78.9810	9.5125	Atlantic
PS99	SV3	09.07.2016	79.0027	8.3628	Atlantic
PS99	SV4	08.07.2016	79.0348	6.9740	Atlantic
PS107	HG1	12.08.2017	79.1398	6.0896	Atlantic
PS107	HG2	11.08.2017	79.1308	4.9029	Polar
PS107	HG3	11.08.2017	79.1082	4.5994	Polar
PS107	HG4	28.07.2017	79.0644	4.1811	Polar
PS107	HG5	28.07.2017	79.0533	3.7497	Polar
PS107	HG6	29.07.2017	79.0465	3.6059	Polar
PS107	HG6	29.07.2017	79.0465	3.6059	Polar
PS107	HG7	31.07.2017	79.0593	3.4820	Polar
PS107	HG9	01.08.2017	79.1234	2.8189	Polar
PS107	EG4	02.08.2017	78.8167	-2.8007	Polar

PS107	EG3	03.08.2017	78.8558	-3.9416	Polar
PS107	EG2	05.08.2017	78.9336	-4.6348	Polar
PS107	EG1	05.08.2017	78.9949	-5.4735	Polar
PS107	S3	25.07.2017	78.6084	5.0566	Atlantic
PS107	N5	09.08.2017	80.0003	2.9402	Polar
PS107	N4	08.08.2017	79.7272	4.5029	Polar
PS107	N3	10.08.2017	79.5881	5.1740	Polar
PS107	SV1	14.08.2017	79.0293	11.1017	Atlantic
PS107	SV2	14.08.2017	78.9829	9.5081	Atlantic
PS107	SV3	14.08.2017	79.0045	8.3636	Atlantic
PS107	SV4	13.08.2017	79.0341	7.0019	Atlantic
PS107	Station 0	02.08.2017	78.9643	0.0038	Polar
PS107	Transect 1	06.08.2017	79.3015	-1.9963	Polar
PS107	Transect 2	07.08.2017	79.4339	0.0027	Polar
PS114	HG4	16.07.2018	79.0237	4.3322	Atlantic
PS114	S3	17.07.2018	79.0241	4.3341	Atlantic
PS114	SV4	18.07.2018	79.0118	7.0351	Atlantic
PS114	SV3	18.07.2018	79.0190	8.0078	Atlantic
PS114	SV2	19.07.2018	78.9803	9.2990	Atlantic
PS114	HG1_2	19.07.2018	79.0244	5.6254	Atlantic
PS114	R1	19.07.2018	78.1874	-0.0080	Atlantic
PS114	R2	20.07.2018	78.8313	-0.0545	Atlantic
PS114	N5	22.07.2018	79.9452	3.2006	Polar
PS114	N4	22.07.2018	79.7410	4.5226	Polar
PS114	N3	23.07.2018	79.5986	5.1662	Polar
PS114	R3	21.07.2018	79.4887	-0.1063	Polar
PS114	R5	24.07.2018	80.8527	-0.1307	Polar
PS114	R4	25.07.2018	80.1579	0.1534	Polar
PS114	EG4	26.07.2018	78.8180	-2.7687	Polar
PS114	EG1	27.07.2018	79.0123	-5.2879	Polar
PS114	EG1	27.07.2018	79.0123	-5.2879	Polar
PS114	79N8-1	28.07.2018	79.6154	-16.5252	Polar
PS121	S3	17.08.2019	78.6165	5.0680	Atlantic
PS121	HG1	17.08.2019	79.1348	6.0858	Atlantic
PS121	HG4	19.08.2019	79.0637	4.1867	Atlantic
PS121	HG3	21.08.2019	79.1072	4.6274	Atlantic
PS121	HG5	23.08.2019	79.0568	3.6731	Atlantic
PS121	HG2	23.08.2019	79.1269	4.9090	Atlantic
PS121	HG6	25.08.2019	79.0632	3.5872	Atlantic
PS121	HG7	25.08.2019	79.0614	3.4832	Atlantic
PS121	HG8	26.08.2019	79.0658	3.3284	Atlantic
PS121	HG9	27.08.2019	79.0658	3.3284	Atlantic
PS121	Transit 0	28.08.2019	78.9594	0.0384	Polar
PS121	EG4	29.08.2019	78.8344	-2.7984	Polar

PS121	EG3	31.08.2019	78.8356	-4.0103	Polar
PS121	EG2	01.09.2019	78.9341	-4.6786	Polar
PS121	EG1	01.09.2019	78.9814	-5.3665	Polar
PS121	SV1	02.09.2019	79.0306	10.7728	Atlantic
PS121	SV2	03.09.2019	78.9861	9.4223	Atlantic
PS121	SV3	03.09.2019	78.9999	8.2423	Atlantic
PS121	N4	06.09.2019	79.7326	4.4681	Polar
PS121	N5	06.09.2019	79.9581	3.0657	Polar
PS121	N3	07.09.2019	79.5973	5.2084	Atlantic
PS121	SV4	09.09.2019	79.0187	6.9684	Atlantic
PS121	F4	10.09.2019	79.0237	6.9979	Atlantic

Table S 5.2 | Summary of statistical tests with significant p-values in bold.

Test	Variables	Distribution	W-Value	p-value
Wilcoxon-Mann-Whitney	Atlantic Chlorophyll *a* ~ Polar Chlorophyll *a*	Heterogeneous	1549202	**0.0020**
	Euphotic Atlantic Temperature ~ Polar Temperature	Heterogeneous	185218	**$< 2.2 \times 10^{-16}$**
	Euphotic Atlantic DOC ~ Euphotic Polar DOC	Heterogeneous	66483	**$< 2.2 \times 10^{-16}$**
	Euphotic Atlantic SLDOC ~ Euphotic Polar SLDOC	Heterogeneous	92381	**9.8×10^{-6}**
	Euphotic Atlantic BB ~ Euphotic Polar BB	Heterogeneous	128894	**$< 2.2 \times 10^{-16}$**
	Euphotic Atlantic BP ~ Euphotic Polar BP	Heterogeneous	26029	**0.0010**
	Meso. Atlantic SLDOC ~ Meso. Polar SLDOC	Heterogeneous	267	**0.025**
	Atlantic Sector, DOC Bloom : DOC Post-Bloom	Heterogeneous	35616	**0.0050**
	Atlantic Sector, SLDOC Bloom : SLDOC Post-Bloom	Heterogeneous	23881	**1.3×10^{-10}**
	Polar Sector, SLDOC Bloom : SLDOC Post-Bloom	Heterogeneous	11353	**7.2×10^{-4}**
	Polar Sector, BB Bloom : BB Post-Bloom	Heterogeneous	12688	0.22

References

Acinas, S. G., Sánchez, P., Salazar, G., Cornejo-Castillo, F. M., Sebastián, M., Logares, R., et al. (2021). Deep ocean metagenomes provide insight into the metabolic architecture of bathypelagic microbial communities. *Communications Biology*, *4*(604). https://doi.org/10.1038/s42003-021-02112-2

Alldredge, A. L., Passow, U., & Logan, B. E. (1993). The abundance and significance of a class of large, transparent organic particles in the ocean. *Deep-Sea Research Part I*, *40*(6). https://doi.org/10.1016/0967-0637(93)90129-Q

Aluwihare, L. I., Repeta, D. J., & Chen, R. F. (1997). A major biopolymeric component to dissolved organic carbon in surface sea water. *Nature*, *387*. https://doi.org/10.1038/387166a0

Aminot, A., & Kérouel, R. (2004). Dissolved organic carbon, nitrogen and phosphorus in the N-E Atlantic and the N-W Mediterranean with particular reference to non-refractory fractions and degradation. *Deep-Sea Research Part I: Oceanographic Research Papers*, *51*(12). https://doi.org/10.1016/j.dsr.2004.07.016

Amon, R. M. W. (2003). Dissolved organic carbon distribution and origin in the Nordic Seas: Exchanges with the Arctic Ocean and the North Atlantic. *Journal of Geophysical Research*, *108*(7). https://doi.org/10.1029/2002JC001594

Amon, R. M. W., & Benner, R. (1994). Rapid cycling of high-molecular-weight dissolved organic matter in the ocean. *Nature*, *369*. https://doi.org/10.1038/369549a0

Amon, R. M. W., & Benner, R. (1996). Bacterial utilization of different size classes of dissolved organic matter. *Limnology and Oceanography*, *41*(1). https://doi.org/10.4319/lo.1996.41.1.0041

Amon, R. M. W., & Benner, R. (2003). Combined neutral sugars as indicators of the diagenetic state of dissolved organic matter in the Arctic Ocean. *Deep-Sea Research Part I: Oceanographic Research Papers*, *50*(1). https://doi.org/10.1016/S0967-0637(02)00130-9

Amon, R. M. W., Fitznar, H. P., & Benner, R. (2001). Linkages among the bioreactivity, chemical composition, and diagenetic state of marine dissolved organic matter. *Limnology and Oceanography*, *46*(2). https://doi.org/10.4319/lo.2001.46.2.0287

von Appen, W.-J., Schaffer, J., Rohardt, G., & Wisotzki, A. (2019). *Physical oceanography measured on water bottle samples during POLARSTERN cruise PS114*. https://doi.org/10.1594/PANGAEA.898695

von Appen, W. J., Wekerle, C., Hehemann, L., Schourup-Kristensen, V., Konrad, C., & Iversen, M. H. (2018). Observations of a Submesoscale Cyclonic Filament in the Marginal Ice Zone. *Geophysical Research Letters*, *45*(7). https://doi.org/10.1029/2018GL077897

Ardyna, M., Gosselin, M., Michel, C., Poulin, M., & Tremblay, J. É. (2011). Environmental forcing of phytoplankton community structure and function in the Canadian High arctic: Contrasting oligotrophic and eutrophic regions. *Marine Ecology Progress Series*, *442*. https://doi.org/10.3354/meps09378

Arnosti, C. (2004). Speed bumps and barricades in the carbon cycle: Substrate structural effects on carbon cycling. *Marine Chemistry*, *92*(1–4). https://doi.org/10.1016/j.marchem.2004.06.030

Arnosti, C., Wietz, M., Brinkhoff, T., Hehemann, J. H., Probandt, D., Zeugner, L., & Amann, R. (2021). The Biogeochemistry of Marine Polysaccharides: Sources, Inventories, and Bacterial Drivers of the Carbohydrate Cycle. *Annual Review of Marine Science*, *13*. https://doi.org/10.1146/annurev-marine-032020-012810

Arrigo, K. R. (2014). Sea Ice Ecosystems. *Annual Review of Marine Science*, *6*. https://doi.org/10.1146/annurev-marine-010213-135103

Arrigo, K. R., & van Dijken, G. L. (2015). Continued increases in Arctic Ocean primary production. *Progress in Oceanography*, *136*. https://doi.org/10.1016/j.pocean.2015.05.002

Arrigo, K. R., Perovich, D. K., Pickart, R. S., Brown, Z. W., Van Dijken, G. L., Lowry, K. E., et al. (2012). Massive phytoplankton blooms under arctic sea ice. *Science*. https://doi.org/10.1126/science.1215065

Aslam, S. N., Michel, C., Niemi, A., & Underwood, G. J. C. (2016). Patterns and drivers of carbohydrate budgets in ice algal assemblages from first year Arctic sea ice. *Limnology and Oceanography*, *61*. https://doi.org/10.1002/lno.10260

Azam, F., Fenchel, T., Field, J., Gray, J., Meyer-Reil, L., & Thingstad, F. (1983). The Ecological Role of Water-Column Microbes in the Sea. *Marine Ecology Progress Series*, *10*. https://doi.org/10.3354/meps010257

Baines, S. B., & Pace, M. L. (1991). The production of dissolved organic matter by phytoplankton and its importance to bacteria: Patterns across marine and freshwater systems. *Limnology and Oceanography*, *36*(6). https://doi.org/10.4319/lo.1991.36.6.1078

Bar-Zeev, E., Berman-Frank, I., Girshevitz, O., & Berman, T. (2012). Revised paradigm of aquatic biofilm formation facilitated by microgel transparent exopolymer particles. *Proceedings of the National Academy of Sciences of the United States of America*, *109*(23). https://doi.org/10.1073/pnas.1203708109

Barber, D. G., Hop, H., Mundy, C. J., Else, B., Dmitrenko, I. A., Tremblay, J. E., et al. (2015). Selected physical, biological and biogeochemical implications of a rapidly changing Arctic Marginal Ice Zone. *Progress in Oceanography*, *139*. https://doi.org/10.1016/j.pocean.2015.09.003

Becker, K. W., Collins, J. R., Durham, B. P., Groussman, R. D., White, A. E., Fredricks, H. F., et al. (2018). Daily changes in phytoplankton lipidomes reveal mechanisms of energy storage in the open ocean. *Nature Communications*, *9*(5179). https://doi.org/10.1038/s41467-018-07346-z

Behrenfeld, M. J., & Falkowski, P. G. (1997). Photosynthetic rates derived from satellite-based chlorophyll concentration. *Limnology and Oceanography*, *42*(1). https://doi.org/10.4319/lo.1997.42.1.0001

Benner, R., & Amon, R. M. W. (2015). The size-reactivity continuum of major bioelements in the Ocean. *Annual Review of Marine Science*, *7*. https://doi.org/10.1146/annurev-marine-010213-135126

Benner, R., & Kaiser, K. (2003). Abundance of amino sugars and peptidoglycan in marine particulate and dissolved organic matter. *Limnology and Oceanography*, *48*(1). https://doi.org/10.4319/lo.2003.48.1.0118

Benner, R., Pakulski, J. D., McCarthy, M., Hedges, J. I., & Hatcher, P. G. (1992). Bulk chemical characteristics of dissolved organic matter in the

ocean. *Science*, *255*(5051). https://doi.org/10.1126/science.255.5051.1561

Bercovici, S. K., & Hansell, D. A. (2016). Dissolved organic carbon in the deep Southern Ocean: Local versus distant controls. *Global Biogeochemical Cycles*, *30*(2). https://doi.org/10.1002/2015GB005252

Berman-Frank, I., Spungin, D., Rahav, E., Van Wambeke, F., Turk-Kubo, K., & Moutin, T. (2016). Dynamics of transparent exopolymer particles (TEP) during the VAHINE mesocosm experiment in the New Caledonian lagoon. *Biogeosciences*, *13*(12). https://doi.org/10.5194/bg-13-3793-2016

Bertrand, E. M., McCrow, J. P., Moustafa, A., Zheng, H., McQuaid, J. B., Delmont, T. O., et al. (2015). Phytoplankton-bacterial interactions mediate micronutrient colimitation at the coastal Antarctic sea ice edge. *Proceedings of the National Academy of Sciences of the United States of America*, *112*(32). https://doi.org/10.1073/pnas.1501615112

Beszczynska-Moller, A., Fahrbach, E., Schauer, U., & Hansen, E. (2012). Variability in Atlantic water temperature and transport at the entrance to the Arctic Ocean, 1997-2010. *ICES Journal of Marine Science*, *65*(5). https://doi.org/10.1093/icesjms/fss056

Biddanda, B., & Benner, R. (1997). Carbon, nitrogen, and carbohydrate fluxes during the production of particulate and dissolved organic matter by marine phytoplankton. *Limnology and Oceanography*, *42*(3). https://doi.org/10.4319/lo.1997.42.3.0506

Biersmith, A., & Benner, R. (1998). Carbohydrates in phytoplankton and freshly produced dissolved organic matter. *Marine Chemistry*, *63*(1–2). https://doi.org/10.1016/S0304-4203(98)00057-7

Boetius, A., Albrecht, S., Bakker, K., Bienhold, C., Felden, J., Fernandez-Mendez, M., et al. (2013). Export of Algal Biomass from the Melting Arctic Sea Ice. *Science*, *339*(6126). https://doi.org/10.1126/science.1231346

Boetius, A., Anesio, A. M., Deming, J. W., Mikucki, J. A., & Rapp, J. Z. (2015). Microbial ecology of the cryosphere: Sea ice and glacial habitats. *Nature Reviews Microbiology*, *13*(11). https://doi.org/10.1038/nrmicro3522

Borch, N. H., & Kirchman, D. L. (1997). Concentration and composition of dissolved combined neutral sugars (polysaccharides) in seawater determined by HPLC-PAD. *Marine Chemistry*, *57*(1–2). https://doi.org/10.1016/S0304-4203(97)00002-9

Borchard, C., & Engel, A. (2015). Size-fractionated dissolved primary production and carbohydrate composition of the coccolithophore Emiliania huxleyi. *Biogeosciences*, *12*(4). https://doi.org/10.5194/bg-12-1271-2015

Bouvier, T., Del Giorgio, P. A., & Gasol, J. M. (2007). A comparative study of the cytometric characteristics of High and Low nucleic-acid bacterioplankton cells from different aquatic ecosystems. *Environmental Microbiology*, *9*(8). https://doi.org/10.1111/j.1462-2920.2007.01321.x

Boyd, P. W., & Trull, T. W. (2007). Understanding the export of biogenic particles in oceanic waters: Is there consensus? *Progress in Oceanography*, *72*(4). https://doi.org/10.1016/j.pocean.2006.10.007

Buchan, A., González, J. M., & Moran, M. A. (2005). Overview of the marine

Roseobacter lineage. *Applied and Environmental Microbiology*, *71*(10). https://doi.org/10.1128/AEM.71.10.5665-5677.2005

Buchan, A., LeCleir, G. R., Gulvik, C. A., & González, J. M. (2014). Master recyclers: features and functions of bacteria associated with phytoplankton blooms. *Nature Reviews. Microbiology*, *12*. https://doi.org/10.1038/nrmicro3326

Busch, K., Endres, S., Iversen, M. H., Michels, J., Nöthig, E.-M., & Engel, A. (2017). Bacterial colonization and vertical distribution of marine gel particles (TEP and CSP) in the arctic Fram Strait. *Frontiers in Marine Science*, *4*(166). https://doi.org/10.3389/fmars.2017.00166

Bussmann, I. (1999). Bacterial utilization of humic substances from the Arctic Ocean. *Aquatic Microbial Ecology*, *19*(1). https://doi.org/10.3354/ame019037

Buttigieg, P. L., Fadeev, E., Bienhold, C., Hehemann, L., Offre, P., & Boetius, A. (2018). Marine microbes in 4D — using time series observation to assess the dynamics of the ocean microbiome and its links to ocean health. *Current Opinion in Microbiology*, *43*. https://doi.org/10.1016/j.mib.2018.01.015

Callahan, B. J., McMurdie, P. J., Rosen, M. J., Han, A. W., Johnson, A. J. A., & Holmes, S. P. (2016). DADA2: High-resolution sample inference from Illumina amplicon data. *Nature Methods*, *13*(7). https://doi.org/10.1038/nmeth.3869

Cardman, Z., Arnosti, C., Durbin, A., Ziervogel, K., Cox, C., Steen, A. D., & Teske, A. (2014). Verrucomicrobia are candidates for polysaccharide-degrading bacterioplankton in an Arctic fjord of Svalbard. *Applied and Environmental Microbiology*, *80*(12). https://doi.org/10.1128/AEM.00899-14

Cardozo Mino, M. G., Fadeev, E., Salman-Carvalho, V., & Boetius, A. (2021). Spatial dynamics in Arctic bacterioplankton community densities are strongly linked to distinct physical and biological processes (Fram Strait, 79°N). *Frontiers in Microbiology*, *12*(658803). https://doi.org/10.3389/fmicb.2021.658803

Carlson, C. A., & Ducklow, H. W. (1995). Dissolved organic carbon in the upper ocean of the central equatorial Pacific Ocean, 1992: Daily and finescale vertical variations. *Deep-Sea Research Part II*, *42*(2–3). https://doi.org/10.1016/0967-0645(95)00023-J

Carlson, C. A., & Hansell, D. A. (2014). DOM Sources, Sinks, Reactivity, and Budgets. In *Biogeochemistry of Marine Dissolved Organic Matter: Second Edition* (pp. 65–126). https://doi.org/10.1016/B978-0-12-405940-5.00003-0

Carrias, J. F., Serre, J. P., Sime-Ngando, T., & Amblard, C. (2002). Distribution, size, and bacterial colonization of pico- and nano-detrital organic particles (DOP) in two lakes of different trophic status. *Limnology and Oceanography*, *47*(4). https://doi.org/10.4319/lo.2002.47.4.1202

Cavan, E. L., Le Moigne, F. A. C., Poulton, A. J., Tarling, G. A., Ward, P., Daniels, C. J., et al. (2015). Attenuation of particulate organic carbon flux in the Scotia Sea, Southern Ocean, is controlled by zooplankton fecal pellets. *Geophysical Research Letters*, *42*. https://doi.org/10.1002/2014GL062744

Cavicchioli, R., Ripple, W. J., Timmis, K. N., Azam, F., Bakken, L. R., Baylis,

M., et al. (2019). Scientists' warning to humanity: microorganisms and climate change. *Nature Reviews Microbiology*, *17*(9). https://doi.org/10.1038/s41579-019-0222-5

Cherrier, J., Bauer, J. E., Druffel, E. R. M., Coffin, R. B., & Chanton, J. P. (1999). Radiocarbon in marine bacteria: Evidence for the ages of assimilated carbon. *Limnology and Oceanography*, *44*(3). https://doi.org/10.4319/lo.1999.44.3.0730

Chial, H. J., & Splittgerber, A. G. (1993). A comparison of the binding of Coomassie brilliant blue to proteins at low and neutral pH. *Analytical Biochemistry*, *213*(3). https://doi.org/10.1006/abio.1993.1433

Chin, W. C., Orellana, M. V., & Verdugo, P. (1998). Spontaneous assembly of marine dissolved organic matter into polymer gels. *Nature*, *391*. https://doi.org/10.1038/35345

Chow, J. S., Lee, C., & Engel, A. (2015). The influence of extracellular polysaccharides, growth rate, and free coccoliths on the coagulation efficiency of Emiliania huxleyi. *Marine Chemistry*, *175*. https://doi.org/10.1016/j.marchem.2015.04.010

Ciais, P., Sabine, C., Bala, G., Bopp, L., Brovkin, V., Canadell, J., et al. (2013). Carbon and other biogeochemical cycles. In *Climate Change 2013 the Physical Science Basis: Working Group I Contribution to the Fifth Assessment Report of the Intergovernmental Panel on Climate Change* (pp. 465–570). Cambridge University Press. https://doi.org/10.1017/CBO9781107415324.015

Cisternas-Novoa, C., Lee, C., & Engel, A. (2015). Transparent exopolymer particles (TEP) and Coomassie stainable particles (CSP): Differences between their origin and vertical distributions in the ocean. *Marine Chemistry*, *175*. https://doi.org/10.1016/j.marchem.2015.03.009

Comiso, J. C. (2012). Large decadal decline of the arctic multiyear ice cover. *Journal of Climate*, *25*. https://doi.org/10.1175/JCLI-D-11-00113.1

Cottrell, M. T., & Kirchman, D. L. (2000). Natural assemblages of marine proteobacteria and members of the Cytophaga-flavobacter cluster consuming low- and high-molecular-weight dissolved organic matter. *Applied and Environmental Microbiology*, *66*(4). https://doi.org/10.1128/AEM.66.4.1692-1697.2000

Cowie, G. L., & Hedges, J. I. (1994). Biochemical indicators of diagenetic alteration in natural organic matter mixtures. *Nature*, *369*. https://doi.org/10.1038/369304a0

Cram, J. A., Chow, C. E. T., Sachdeva, R., Needham, D. M., Parada, A. E., Steele, J. A., & Fuhrman, J. A. (2015). Seasonal and interannual variability of the marine bacterioplankton community throughout the water column over ten years. *ISME Journal*, *9*. https://doi.org/10.1038/ismej.2014.153

Crump, B. C., Baross, J. A., & Simenstad, C. A. (1998). Dominance of particle-attached bacteria in the Columbia River estuary, USA. *Aquatic Microbial Ecology*, *14*. https://doi.org/10.3354/ame014007

Crump, B. C., Armbrust, E. V., & Baross, J. A. (1999). Phylogenetic analysis of particle-attached and free-living bacterial communities in the Columbia River, its estuary, and the adjacent coastal ocean. *Applied and Environmental Microbiology*, *65*(7). https://doi.org/10.1128/aem.65.7.3192-3204.1999

Cuevas, L. A., Egge, J. K., Thingstad, T. F., & Töpper, B. (2011). Organic carbon and mineral nutrient limitation of oxygen consumption, bacterial growth and efficiency in the Norwegian Sea. *Polar Biology*, *34*(6). https://doi.org/10.1007/s00300-010-0944-3

Dauwe, B., Middelburg, J. J., Herman, P. M. J., & Heip, C. H. R. (1999). Linking diagenetic alteration of amino acids and bulk organic matter reactivity. *Limnology and Oceanography*, *44*(7). https://doi.org/10.4319/lo.1999.44.7.1809

Davis, J., & Benner, R. (2005). Seasonal trends in the abundance, composition and bioavailability of particulate and dissolved organic matter in the Chukchi/Beaufort Seas and western Canada Basin. *Deep-Sea Research Part II: Topical Studies in Oceanography*, *52*(24–26). https://doi.org/10.1016/j.dsr2.2005.09.006

Davis, J., & Benner, R. (2007). Quantitative estimates of labile and semi-labile dissolved organic carbon in the western Arctic Ocean: A molecular approach. *Limnology and Oceanography*, *52*(6). https://doi.org/10.4319/lo.2007.52.6.2434

Davis, J., Kaiser, K., & Benner, R. (2009). Amino acid and amino sugar yields and compositions as indicators of dissolved organic matter diagenesis. *Organic Geochemistry*, *40*(3). https://doi.org/10.1016/j.orggeochem.2008.12.003

Delmont, T. O., Hammar, K. M., Ducklow, H. W., Yager, P. L., & Post, A. F. (2014). Phaeocystis antarctica blooms strongly influence bacterial community structures in the Amundsen Sea polynya. *Frontiers in Microbiology*, *5*(646). https://doi.org/10.3389/fmicb.2014.00646

Delmont, T. O., Eren, A. M., Vineis, J. H., & Post, A. F. (2015). Genome reconstructions indicate the partitioning of ecological functions inside a phytoplankton bloom in the Amundsen Sea, Antarctica. *Frontiers in Microbiology*, *6*(1090). https://doi.org/10.3389/fmicb.2015.01090

Diepenbroek, M., Glöckner, F. O. F. O., Grobe, P., Güntsch, A., Huber, R., König-Ries, B., et al. (2014). Towards an Integrated Biodiversity and Ecological Research Data Management and Archiving Platform: The German Federation for the Curation of Biological Data (GFBio). *Informatik 2014*.

Dippold, M. A., & Kuzyakov, Y. (2013). Biogeochemical transformations of amino acids in soil assessed by position-specific labelling. *Plant and Soil*, *373*(1–2). https://doi.org/10.1007/s11104-013-1764-3

Dittmar, T., Cherrier, J., & Ludwichowski, K.-U. (2009). The Analysis of Amino Acids in Seawater. In O. Wurl (Ed.), *Practical Guidelines for the Analysis of Seawater* (pp. 67–77). CRC Press, Taylor & Francis Group, FL, USA. https://doi.org/10.1201/9781420073072.ch4

Dong, X., Jochmann, M. A., Elsner, M., Meyer, A. H., Bäcker, L. E., Rahmatullah, M., et al. (2017). Monitoring Microbial Mineralization Using Reverse Stable Isotope Labeling Analysis by Mid-Infrared Laser Spectroscopy. *Environmental Science and Technology*, *51*(20). https://doi.org/10.1021/acs.est.7b02909

Dong, X., Bäcker, L. E., Rahmatullah, M., Schunk, D., Lens, G., & Meckenstock, R. U. (2019). Quantification of microbial degradation activities in biological activated carbon filters by reverse stable isotope labelling. *AMB Express*, *9*(109). https://doi.org/10.1186/s13568-019-0827-0

Doval, M. D., & Hansell, D. A. (2000). Organic carbon and apparent oxygen utilization in the western South Pacific and the central Indian Oceans. *Marine Chemistry*, *68*(3). https://doi.org/10.1016/S0304-4203(99)00081-X

Ducklow, H. W., Schofield, O., Vernet, M., Stammerjohn, S., & Erickson, M. (2012). Multiscale control of bacterial production by phytoplankton dynamics and sea ice along the western Antarctic Peninsula: A regional and decadal investigation. *Journal of Marine Systems*, *98–99*. https://doi.org/10.1016/j.jmarsys.2012.03.003

Engel, A. (2000). The role of transparent exopolymer particles (TEP) in the increase in apparent particle stickiness (alpha) during the decline of a diatom bloom. *Journal of Plankton Research*, *22*(3). https://doi.org/10.1093/plankt/22.3.485

Engel, A. (2009). Determination of Marine Gel Particles. In O. Wirl (Ed.), *Practical Guidelines for the Analysis of Seawater* (pp. 125–142). CRC Press, Taylor & Francis Group, FL, USA. https://doi.org/10.1201/9781420073072.ch7

Engel, A., & Galgani, L. (2016). The organic sea-surface microlayer in the upwelling region off the coast of Peru and potential implications for air-sea exchange processes. *Biogeosciences*, *13*(4). https://doi.org/10.5194/bg-13-989-2016

Engel, A., & Händel, N. (2011). A novel protocol for determining the concentration and composition of sugars in particulate and in high molecular weight dissolved organic matter (HMW-DOM) in seawater. *Marine Chemistry*, *127*(1–4). https://doi.org/10.1016/j.marchem.2011.09.004

Engel, A., Goldthwait, S., Passow, U., & Alldredge, A. (2002). Temporal decoupling of carbon and nitrogen dynamics in a mesocosm diatom bloom. *Limnology and Oceanography*, *47*(3). https://doi.org/10.4319/lo.2002.47.3.0753

Engel, A., Thoms, S., Riabesell, U., Rochelle-Newall, E., & Zondervan, I. (2004). Polysaccharide aggregation as a potential sink of marine dissolved organic carbon. *Nature*, *428*(6986). https://doi.org/10.1038/nature02453

Engel, A., Händel, N., Wohlers, J., Lunau, M., Grossart, H. P., Sommer, U., & Riebesell, U. (2011). Effects of sea surface warming on the production and composition of dissolved organic matter during phytoplankton blooms: Results from a mesocosm study. *Journal of Plankton Research*, *33*(3). https://doi.org/10.1093/plankt/fbq122

Engel, A., Harlay, J., Piontek, J., & Chou, L. (2012). Contribution of combined carbohydrates to dissolved and particulate organic carbon after the spring bloom in the northern Bay of Biscay (North-Eastern Atlantic Ocean). *Continental Shelf Research*, *45*. https://doi.org/10.1016/j.csr.2012.05.016

Engel, A., Borchard, C., Piontek, J., Schulz, K. G., Riebesell, U., & Bellerby, R. (2013). CO2 increases 14C primary production in an Arctic plankton community. *Biogeosciences*, *10*(3). https://doi.org/10.5194/bg-10-1291-2013

Engel, A., Piontek, J., Metfies, K., Endres, S., Sprong, P., Peeken, I., et al. (2017). Inter-annual variability of transparent exopolymer particles in the Arctic Ocean reveals high sensitivity to ecosystem changes.

Scientific Reports, *7*(4129). https://doi.org/10.1038/s41598-017-04106-9

Engel, A., Wagner, H., Le Moigne, F. A. C., & Wilson, S. T. (2017). Particle export fluxes to the oxygen minimum zone of the eastern tropical North Atlantic. *Biogeosciences*, *14*(7). https://doi.org/10.5194/bg-14-1825-2017

Engel, A., Bracher, A., Dinter, T., Endres, S., Grosse, J., Metfies, K., et al. (2019). Inter-Annual Variability of Organic Carbon Concentration in the Eastern Fram Strait During Summer (2009–2017). *Frontiers in Marine Science*, *6*(187). https://doi.org/10.3389/fmars.2019.00187

Engel, A., Endres, S., Galgani, L., & Schartau, M. (2020). Marvelous Marine Microgels: On the Distribution and Impact of Gel-Like Particles in the Oceanic Water-Column. *Frontiers in Marine Science*, *7*(405). https://doi.org/10.3389/fmars.2020.00405

Eppley, R. W., & Peterson, B. J. (1979). Particulate organic matter flux and planktonic new production in the deep ocean. *Nature*, *282*. https://doi.org/10.1038/282677a0

Evans, C. A., O'Reily, J. E., & Thomas, J. P. (1987). *A handbook for measurement of chlorophyll a and primary production*. College Station, TX (USA) Texas A & M University.

Evans, T. W., Könneke, M., Lipp, J. S., Adhikari, R. R., Taubner, H., Elvert, M., & Hinrichs, K. U. (2018). Lipid biosynthesis of Nitrosopumilus maritimus dissected by lipid specific radioisotope probing (lipid-RIP) under contrasting ammonium supply. *Geochimica et Cosmochimica Acta*, *242*. https://doi.org/10.1016/j.gca.2018.09.001

Evans, T. W., Coffinet, S., Könneke, M., Lipp, J. S., Becker, K. W., Elvert, M., et al. (2019). Assessing the carbon assimilation and production of benthic archaeal lipid biomarkers using lipid-RIP. *Geochimica et Cosmochimica Acta*, *265*. https://doi.org/10.1016/j.gca.2019.08.030

Fadeev, E., Salter, I., Schourup-Kristensen, V., Nöthig, E.-M., Metfies, K., Engel, A., et al. (2018). Microbial Communities in the East and West Fram Strait During Sea Ice Melting Season. *Frontiers in Marine Science*, *5*(429). https://doi.org/10.3389/fmars.2018.00429

Fadeev, E., Wietz, M., von Appen, W. J., Iversen, M. H., Nöthig, E. M., Engel, A., et al. (2021). Submesoscale physicochemical dynamics directly shape bacterioplankton community structure in space and time. *Limnology and Oceanography*, *66*(7). https://doi.org/10.1101/2020.09.02.279232

Falkowski, P. G. (2000). Rationalizing elemental ratios in unicellular algae. *Journal of Phycology*, *36*(1). https://doi.org/10.1046/j.1529-8817.2000.99161.x

Fernández-Méndez, M., Wenzhöfer, F., Peeken, I., Sørensen, H. L., Glud, R. N., & Boetius, A. (2014). Composition, buoyancy regulation and fate of ice algal aggregates in the Central Arctic Ocean. *PLoS ONE*, *9*(9). https://doi.org/10.1371/journal.pone.0107452

Filella Lopez de Lamadrid, A. (2020). *Microbial responses to the release of DOC by sea ice and glacier melting in the East Greenland System*. Christian-Albrechts-Universität zu Kiel.

Finkel, Z. V., Follows, M. J., Liefer, J. D., Brown, C. M., Benner, I., & Irwin, A. J. (2016). Phylogenetic diversity in the macromolecular composition of microalgae. *PLoS ONE*, *11*(5).

https://doi.org/10.1371/journal.pone.0155977
Forest, A., Wassmann, P., Slagstad, D., Bauerfeind, E., Nöthig, E.-M., & Klages, M. (2010). Relationships between primary production and vertical particle export at the Atlantic-Arctic boundary (Fram Strait, HAUSGARTEN). *Polar Biology*, *33*(12), 1733–1746. https://doi.org/10.1007/s00300-010-0855-3
Forest, A., Tremblay, J. éric, Gratton, Y., Martin, J., Gagnon, J., Darnis, G., et al. (2011). Biogenic carbon flows through the planktonic food web of the Amundsen Gulf (Arctic Ocean): A synthesis of field measurements and inverse modeling analyses. *Progress in Oceanography*, *91*(4). https://doi.org/10.1016/j.pocean.2011.05.002
Fox, J., & Weisberg, S. (2019). *An R Companion to Applied Regression* (3rd ed.). Thousand Oaks, CA, USA: Sage Publications, CA, USA.
Fukuda, R., Ogawa, H., Nagata, T., & Koike, I. (1998). Direct determination of carbon and nitrogen contents of natural bacterial assemblages in marine environments. *Applied and Environmental Microbiology*, *64*(4). https://doi.org/10.1128/AEM.64.9.3352-3358.1998
Garneau, M. È., Roy, S., Lovejoy, C., Gratton, Y., & Vincent, W. F. (2008). Seasonal dynamics of bacterial biomass and production in a coastal arctic ecosystem: Franklin Bay, western Canadian Arctic. *Journal of Geophysical Research: Oceans*, *113*(7). https://doi.org/10.1029/2007JC004281
Gilbert, J. A., Steele, J. A., Caporaso, J. G., Steinbrück, L., Reeder, J., Temperton, B., et al. (2012). Defining seasonal marine microbial community dynamics. *ISME Journal*, *6*(2). https://doi.org/10.1038/ismej.2011.107
Giovannoni, S. J. (2017). SAR11 Bacteria: The Most Abundant Plankton in the Oceans. *Annual Review of Marine Science*, *9*. https://doi.org/10.1146/annurev-marine-010814-015934
Giovannoni, S. J., Cameron Thrash, J., & Temperton, B. (2014). Implications of streamlining theory for microbial ecology. *ISME Journal*, *8*. https://doi.org/10.1038/ismej.2014.60
Goldberg, S. J., Carlson, C. A., Hansell, D. A., Nelson, N. B., & Siegel, D. A. (2009). Temporal dynamics of dissolved combined neutral sugars and the quality of dissolved organic matter in the Northwestern Sargasso Sea. *Deep Sea Research Part I: Oceanographic Research Papers*, *56*. https://doi.org/10.1016/j.dsr.2008.12.013
Goldberg, S. J., Carlson, C. A., Brzezinski, M., Nelson, N. B., & Siegel, D. A. (2011). Systematic removal of neutral sugars within dissolved organic matter across ocean basins. *Geophysical Research Letters*, *38*(17). https://doi.org/10.1029/2011GL048620
González, J. M., Fernández-Gómez, B., Fernàndez-Guerra, A., Gómez-Consarnau, L., Sánchez, O., Coll-Lladó, M., et al. (2008). Genome analysis of the proteorhodopsin-containing marine bacterium Polaribacter sp. MED152 (Flavobacteria). *Proceedings of the National Academy of Sciences of the United States of America*, *105*(25). https://doi.org/10.1073/pnas.0712027105
Granum, E., Kirkvold, S., & Myklestad, S. M. (2002). Cellular and extracellular production of carbohydrates and amino acids by the marine diatom Skeletonema costatum: Diel variations and effects of N depletion. *Marine Ecology Progress Series*, *242*.

https://doi.org/10.3354/meps242083
Grosse, J., Nöthig, E.-M., Torres-Valdés, S., & Engel, A. (2021). Summertime Amino Acid and Carbohydrate Patterns in Particulate and Dissolved Organic Carbon Across Fram Strait. *Frontiers in Marine Science*, *8*(684675). https://doi.org/10.3389/fmars.2021.684675
Hall, E. K., Neuhauser, C., & Cotner, J. B. (2008). Toward a mechanistic understanding of how natural bacterial communities respond to changes in temperature in aquatic ecosystems. *ISME Journal*, *2*(5). https://doi.org/10.1038/ismej.2008.9
Hansell, D. A., Carlson, C. A., Repeta, D. J., & Schlitzer, R. (2009). Dissolved organic matter in the ocean a controversy stimulates new insights. *Oceanography*, *22*(4). https://doi.org/10.5670/oceanog.2009.109
Hansell, D. A., Carlson, C. A., & Schlitzer, R. (2012). Net removal of major marine dissolved organic carbon fractions in the subsurface ocean. *Global Biogeochemical Cycles*, *26*(1). https://doi.org/10.1029/2011GB004069
Hansman, R. L., Griffin, S., Watson, J. T., Druffel, E. R. M., Ingalls, A. E., Pearson, A., & Aluwihare, L. I. (2009). The radiocarbon signature of microorganisms in the mesopelagic ocean. *Proceedings of the National Academy of Sciences of the United States of America*, *106*(16). https://doi.org/10.1073/pnas.0810871106
Hartigan, J. A., & Wong, M. A. (1979). Algorithm AS 136: A K-Means Clustering Algorithm. *Applied Statistics*, *28*(1). https://doi.org/10.2307/2346830
Hedges, J. I., Baldock, J. A., Gélinas, Y., Lee, C., Peterson, M. L., & Wakeham, S. G. (2002). The biochemical and elemental compositions of marine plankton: A NMR perspective. *Marine Chemistry*. https://doi.org/10.1016/S0304-4203(02)00009-9
Hothorn, T., Bretz, F., & Westfall, P. (2008). Simultaneous Inference In General Parametric Models. *Biometrical Journal*, *50*(3). https://doi.org/10.1002/bimj.200810425
Hsieh, T. C., Ma, K. H., & Chao, A. (2016). iNEXT: an R package for rarefaction and extrapolation of species diversity (Hill numbers). *Methods in Ecology and Evolution*, *7*(12). https://doi.org/10.1111/2041-210X.12613
Husson, F., Josse, J., Le, S., & Mazet, J. (2008). Multivariate exploratory data analysis and data mining with R. *Journal of Statistical Software*, *25*(1).
Ihaka, R., & Gentleman, R. (1996). R: A Language for Data Analysis and Graphics. *Journal of Computational and Graphical Statistics*, *5*(3). https://doi.org/10.2307/1390807
Ingalls, A. E., Shah, S. R., Hansman, R. L., Aluwihare, L. I., Santos, G. M., Druffel, E. R. M., & Pearson, A. (2006). Quantifying archaeal community autotrophy in the mesopelagic ocean usinq natural radiocarbon. *Proceedings of the National Academy of Sciences of the United States of America*, *103*(17). https://doi.org/10.1073/pnas.0510157103
IPCC. (2019). IPCC Special Report on the Ocean and Cryosphere in a Changing Climate. *Intergovernmental Panel on Climate Change*.
Ittekkot, V., Brockmann, U., Michaelis, W., & Degens, E. (1981). Dissolved

Free and Combined Carbohydrates During a Phytoplankton Bloom in the Northern North Sea. *Marine Ecology Progress Series*, *4*. https://doi.org/10.3354/meps004299

Iversen, K. R., & Seuthe, L. (2011). Seasonal microbial processes in a high-latitude fjord (Kongsfjorden, Svalbard): I. Heterotrophic bacteria, picoplankton and nanoflagellates. *Polar Biology*, *34*(5). https://doi.org/10.1007/s00300-010-0929-2

von Jackowski, A., & Engel, A. (2019). *Physical oceanography measured on water bottle samples during Maria S. Merian cruise MSM77*. https://doi.org/10.1594/PANGAEA.907467

von Jackowski, A., Grosse, J., Nöthig, E.-M., & Engel, A. (2020a). *Bacterial production and organic matter of POLARSTERN cruise PS114 and Maria S. Merian cruise MSM77*. https://doi.org/10.1594/PANGAEA.915751

von Jackowski, A., Grosse, J., Nöthig, E.-M., & Engel, A. (2020b). Dynamics of organic matter and bacterial activity in the Fram Strait during summer and autumn. *Philosophical Transactions. Series A, Mathematical, Physical, and Engineering Sciences*, *378*(20190366). https://doi.org/10.1098/rsta.2019.0366

Jain, A., Krishnan, K. P., Begum, N., Singh, A., Thomas, F. A., & Gopinath, A. (2020). Response of bacterial communities from Kongsfjorden (Svalbard, Arctic Ocean) to macroalgal polysaccharide amendments. *Marine Environmental Research*, *155*(104874). https://doi.org/10.1016/j.marenvres.2020.104874

Janse, I., Van Rijssel, M., Van Hall, P. J., Gerwig, G. J., Gottschal, J. C., & Prins, R. A. (1996). The storage glucan of Phaeocystis globosa (Prymnesiophyceae) cells. *Journal of Phycology*. https://doi.org/10.1111/j.0022-3646.1996.00382.x

Jansson, B. P. M., Malandrin, L., & Johansson, H. E. (2000). Cell cycle arrest in archaea by the hypusination inhibitor N1-guanyl-1,7-diaminoheptane. *Journal of Bacteriology*, *182*(4). https://doi.org/10.1128/JB.182.4.1158-1161.2000

Jorgensen, N. O. G., Kroer, N., Coffin, R. B., Xiao-Hua Yang, & Lee, C. (1993). Dissolved free amino acids, combined amino acids, and DNA as sources of carbon and nitrogen to marine bacteria. *Marine Ecology Progress Series*. https://doi.org/10.3354/meps098135

Kaiser, K., & Benner, R. (2000). Determination of amino sugars in environmental samples with high salt content by high-performance anion-exchange chromatography and pulsed amperometric detection. *Analytical Chemistry*, *72*(11). https://doi.org/10.1021/ac991407t

Kaiser, K., & Benner, R. (2009). Biochemical composition and size distribution of organic matter at the Pacific and Atlantic time-series stations. *Marine Chemistry*, *113*(1–2). https://doi.org/10.1016/j.marchem.2008.12.004

Kaiser, P., Hagen, W., von Appen, W. J., Niehoff, B., Hildebrandt, N., & Auel, H. (2021). Effects of a Submesoscale Oceanographic Filament on Zooplankton Dynamics in the Arctic Marginal Ice Zone. *Frontiers in Marine Science*, *8*(625395). https://doi.org/10.3389/fmars.2021.625395

Kana, T. M., & Glibert, P. M. (1987). Effect of irradiances up to 2000 μE m-2 s-1 on marine Synechococcus WH7803-I. Growth, pigmentation, and cell composition. *Deep Sea Research Part A, Oceanographic Research*

Papers, *94*(4). https://doi.org/10.1016/0198-0149(87)90001-X
Karner, M. B., Delong, E. F., & Karl, D. M. (2001). Archaeal dominance in the mesopelagic zone of the Pacific Ocean. *Nature*, *409*(6819). https://doi.org/10.1038/35054051
Kashiwase, H., Ohshima, K. I., Nihashi, S., & Eicken, H. (2017). Evidence for ice-ocean albedo feedback in the Arctic Ocean shifting to a seasonal ice zone. *Scientific Reports*, *7*(8170). https://doi.org/10.1038/s41598-017-08467-z
Kawasaki, N., & Benner, R. (2006). Bacterial release of dissolved organic matter during cell growth and decline: Molecular origin and composition. *Limnology and Oceanography*, *51*(5). https://doi.org/10.4319/lo.2006.51.5.2170
Keil, R. G., & Kirchman, D. L. (1999). Utilization of dissolved protein and amino acids in the northern Sargasso Sea. *Aquatic Microbial Ecology*, *18*. https://doi.org/10.3354/ame018293
Kellermann, M. Y., Yoshinaga, M. Y., Wegener, G., Krukenberg, V., & Hinrichs, K. U. (2016). Tracing the production and fate of individual archaeal intact polar lipids using stable isotope probing. *Organic Geochemistry*, *95*. https://doi.org/10.1016/j.orggeochem.2016.02.004
Kharbush, J. J., Close, H. G., Van Mooy, B. A. S., Arnosti, C., Smittenberg, R. H., Le Moigne, F. A. C., et al. (2020). Particulate Organic Carbon Deconstructed: Molecular and Chemical Composition of Particulate Organic Carbon in the Ocean. *Frontiers in Marine Science*, *7*(518). https://doi.org/10.3389/fmars.2020.00518
Kim, J. M., Lee, K., Shin, K., Yang, E. J., Engel, A., Karl, D. M., & Kim, H. C. (2011). Shifts in biogenic carbon flow from particulate to dissolved forms under high carbon dioxide and warm ocean conditions. *Geophysical Research Letters*, *38*(8). https://doi.org/10.1029/2011GL047346
Kirchman, D. L., Meon, B., Ducklow, H. W., Carlson, C. A., Hansell, D. A., & Steward, G. F. (2001). Glucose fluxes and concentrations of dissolved combined neutral sugars (polysaccharides) in the Ross Sea and Polar Front Zone, Antarctica. *Deep-Sea Research Part II: Topical Studies in Oceanography*, *48*(19–20). https://doi.org/10.1016/S0967-0645(01)00085-6
Kirchman, D. L., Malmstrom, R. R., & Cottrell, M. T. (2005). Control of bacterial growth by temperature and organic matter in the Western Arctic. *Deep-Sea Research Part II: Topical Studies in Oceanography*, *52*(24–26). https://doi.org/10.1016/j.dsr2.2005.09.005
Kirchman, D. L., Morán, X. A. G., & Ducklow, H. (2009). Microbial growth in the polar oceans - Role of temperature and potential impact of climate change. *Nature Reviews Microbiology*, *7*(6). https://doi.org/10.1038/nrmicro2115
Kirchman, D. L., Hill, V., Cottrell, M. T., Gradinger, R., Malmstrom, R. R., & Parker, A. (2009). Standing stocks, production, and respiration of phytoplankton and heterotrophic bacteria in the western Arctic Ocean. *Deep Sea Research Part II: Topical Studies in Oceanography*, *56*(17). https://doi.org/10.1016/j.dsr2.2008.10.018
Kirchman, D. L., Cottrell, M. T., & Lovejoy, C. (2010). The structure of bacterial communities in the western Arctic Ocean as revealed by pyrosequencing of 16S rRNA genes. *Environmental Microbiology*,

12(5). https://doi.org/10.1111/j.1462-2920.2010.02154.x
Krembs, C., & Engel, A. (2001). Abundance and variability of microorganisms and transparent exopolymer particles across the ice-water interface of melting first-year sea ice in the Laptev Sea (Arctic). *Marine Biology*, *138*(1). https://doi.org/10.1007/s002270000396
Krishna, M. S., Prasad, V. R., Sarma, V. V. S. S., Reddy, N. P. C., Hemalatha, K. P. J., & Rao, Y. V. (2015). Fluxes of dissolved organic carbon and nitrogen to the northern Indian Ocean from the Indian monsoonal rivers. *Journal of Geophysical Research: Biogeosciences*, *120*(10). https://doi.org/10.1002/2015JG002912
Kwok, R. (2009). Outflow of Arctic Ocean sea ice into the Greenland and Barent Seas: 1979-2007. *Journal of Climate*, *22*(9). https://doi.org/10.1175/2008JCLI2819.1
Laber, C. P., Hunter, J. E., Carvalho, F., Collins, J. R., Hunter, E. J., Schieler, B. M., et al. (2018). Coccolithovirus facilitation of carbon export in the North Atlantic. *Nature Microbiology*, *3*(5). https://doi.org/10.1038/s41564-018-0128-4
Laird, N. M., & Ware, J. H. (1982). Random-Effect Models for Longitudinal Data. *Biometrics*, *38*(4). https://doi.org/10.2307/2529876
Lampe, V., Nöthig, E.-M., & Schartau, M. (2021). Spatio-Temporal Variations in Community Size Structure of Arctic Protist Plankton in the Fram Strait. *Frontiers in Marine Science*, *7*(579880). https://doi.org/10.3389/fmars.2020.579880
Law, K. L. (2017). Plastics in the Marine Environment. *Annual Review of Marine Science*, *9*. https://doi.org/10.1146/annurev-marine-010816-060409
Laws, E. A. (1991). Photosynthetic quotients, new production and net community production in the open ocean. *Deep Sea Research Part A. Oceanographic Research Papers*, *38*(1). https://doi.org/10.1016/0198-0149(91)90059-O
Lee, Y. J., Matrai, P. A., Friedrichs, M. A. M., Saba, V. S., Antoine, D., Ardyna, M., et al. (2015). An assessment of phytoplankton primary productivity in the Arctic Ocean from satellite ocean color/in situ chlorophyll-a based models. *Journal of Geophysical Research: Oceans*, *120*(9). https://doi.org/10.1002/2015JC011018
Lefcheck, J. S. (2016). piecewiseSEM: Piecewise structural equation modelling in r for ecology, evolution, and systematics. *Methods in Ecology and Evolution*, *7*(5). https://doi.org/10.1111/2041-210X.12512
Lenth, R. V. (2016). Least-squares means: The R package lsmeans. *Journal of Statistical Software*, *69*(1). https://doi.org/10.18637/jss.v069.i01
Lin, P., & Guo, L. (2015). Spatial and vertical variability of dissolved carbohydrate species in the northern Gulf of Mexico following the Deepwater Horizon oil spill, 2010-2011. *Marine Chemistry*, *174*. https://doi.org/10.1016/j.marchem.2015.04.001
Lindh, M. V., Sjöstedt, J., Andersson, A. F., Baltar, F., Hugerth, L. W., Lundin, D., et al. (2015). Disentangling seasonal bacterioplankton population dynamics by high-frequency sampling. *Environmental Microbiology*, *17*(7). https://doi.org/10.1111/1462-2920.12720
Lindroth, P., & Mopper, K. (1979). High Performance Liquid Chromatographic Determination of Subpicomole Amounts of Amino

Acids by Precolumn Fluorescence Derivatization with o-Phthaldialdehyde. *Analytical Chemistry*, *51*(11). https://doi.org/10.1021/ac50047a019

Ling, S. C., & Alldredge, A. L. (2003). Does the marine copepod Calanus pacificus consume transparent exopolymer particles (TEP)? *Journal of Plankton Research*, *25*(5). https://doi.org/10.1093/plankt/25.5.507

Liu, Q., Parrish, C. C., & Helleur, R. (1998). Lipid class and carbohydrate concentrations in marine colloids. *Marine Chemistry*, *60*. https://doi.org/10.1016/S0304-4203(97)00103-5

Logan, B. E., Grossart, H. P., & Simon, M. (1994). Direct observation of phytoplankton, TEP and aggregates on polycarbonate filters using brightfield microscopy. *Journal of Plankton Research*. https://doi.org/10.1093/plankt/16.12.1811

Logan, B. E., Passow, U., Alldredge, A. L., Grossartt, H. P., & Simont, M. (1995). Rapid formation and sedimentation of large aggregates is predictable from coagulation rates (half-lives) of transparent exopolymer particles (TEP). *Deep-Sea Research Part II*, *42*(1). https://doi.org/10.1016/0967-0645(95)00012-F

Loginova, A. N., Thomsen, S., Dengler, M., Lüdke, J., & Engel, A. (2019). Diapycnal dissolved organic matter supply into the upper Peruvian oxycline. *Biogeosciences*, *16*(9). https://doi.org/10.5194/bg-16-2033-2019

Lønborg, C., Álvarez–Salgado, X. A., Letscher, R. T., & Hansell, D. A. (2018). Large Stimulation of Recalcitrant Dissolved Organic Carbon Degradation by Increasing Ocean Temperatures. *Frontiers in Marine Science*, *4*. https://doi.org/10.3389/fmars.2017.00436

Long, R. A., & Azam, F. (1996). Abundant protein-containing particles in the sea. *Aquatic Microbial Ecology*, *10*. https://doi.org/10.3354/ame010213

Love, M. I., Huber, W., & Anders, S. (2014). Moderated estimation of fold change and dispersion for RNA-seq data with DESeq2. *Genome Biology*, *15*(12). https://doi.org/10.1186/s13059-014-0550-8

Mabeau, S., & Kloareg, B. (1987). Isolation and analysis of the cell walls of brown algae: Fucus spiralis, F. ceranoides, F. vesiculosus, F. serratus, Bifurcaria bifurcata and Laminaria digitata. *Journal of Experimental Botany*. https://doi.org/10.1093/jxb/38.9.1573

Maranger, R., Vaqué, D., Nguyen, D., Hébert, M. P., & Lara, E. (2015). Pan-Arctic patterns of planktonic heterotrophic microbial abundance and processes: Controlling factors and potential impacts of warming. *Progress in Oceanography*, *139*. https://doi.org/10.1016/j.pocean.2015.07.006

Mari, X. (1999). Carbon content and C:N ratio of transparent exopolymeric particles (TEP) produced by bubbling exudates of diatoms. *Marine Ecology Progress Series*, *183*(2). https://doi.org/10.3354/meps183059

Mari, X., & Burd, A. (1998). Seasonal size spectra of transparent exopolymeric particles (TEP) in a coastal sea and comparison with those predicted using coagulation theory. *Marine Ecology Progress Series*, *163*. https://doi.org/10.3354/meps163063

Mari, X., & Kiørboe, T. (1996). Abundance, size distribution and bacterial colonization of transparent exopolymeric particles (TEP) during spring in the Kattegat. *Journal of Plankton Research*, *18*(6). https://doi.org/10.1093/plankt/18.6.969

Mari, X., Rochelle-Newall, E., Torréton, J. P., Pringault, O., Jouon, A., & Migon, C. (2007). Water residence time: A regulatory factor of the DOM to POM transfer efficiency. *Limnology and Oceanography*. https://doi.org/10.4319/lo.2007.52.2.0808

Martin, J. H., Knauer, G. A., Karl, D. M., & Broenkow, W. W. (1987). VERTEX: carbon cycling in the northeast Pacific. *Deep Sea Research Part A, Oceanographic Research Papers*. https://doi.org/10.1016/0198-0149(87)90086-0

Martin, M. (2011). Cutadapt removes adapter sequences from high-throughput sequencing reads. *EMBnet.Journal*, *17*(1). https://doi.org/10.14806/ej.17.1.200

Martiny, A. C., Pham, C. T. A., Primeau, F. W., Vrugt, J. A., Moore, J. K., Levin, S. A., & Lomas, M. W. (2013). Strong latitudinal patterns in the elemental ratios of marine plankton and organic matter. *Nature Geoscience*, *6*. https://doi.org/10.1038/ngeo1757

Maslanik, J., Stroeve, J., Fowler, C., & Emery, W. (2011). Distribution and trends in Arctic sea ice age through spring 2011. *Geophysical Research Letters*. https://doi.org/10.1029/2011GL047735

Maßmig, M., Lüdke, J., Krahmann, G., & Engel, A. (2020). Bacterial degradation activity in the eastern tropical South Pacific oxygen minimum zone. *Biogeosciences*, *17*(1). https://doi.org/10.5194/bg-17-215-2020

Masson-Delmotte, V., Pörtner, H.-O., Skea, J., Pirani, A., Pidcock, R., Chen, Y., et al. (2018). *Global warming of 1.5°C: an IPCC special report on the impacts of global warming of 1.5°C above pre-industrial levels and related global greenhouse gas emission pathways, in the context of strengthening the global response to the threat of climate change*.

McCarren, J., Becker, J. W., Repeta, D. J., Shi, Y., Young, C. R., Malmstrom, R. R., et al. (2010). Microbial community transcriptomes reveal microbes and metabolic pathways associated with dissolved organic matter turnover in the sea. *Proceedings of the National Academy of Sciences*, *107*(38). https://doi.org/10.1073/pnas.1010732107

McCarthy, M., Hedges, J., & Benner, R. (1996). Major biochemical composition of dissolved high molecular weight organic matter in seawater. *Marine Chemistry*, *55*(3–4). https://doi.org/10.1016/S0304-4203(96)00041-2

McMurdie, P. J., & Holmes, S. (2013). Phyloseq: An R Package for Reproducible Interactive Analysis and Graphics of Microbiome Census Data. *PLoS ONE*, *8*(4). https://doi.org/10.1371/journal.pone.0061217

Meiners, K., Brinkmeyer, R., Granskog, M. A., & Lindfors, A. (2004). Abundance, size distribution and bacterial colonization of exopolymer particles in Antarctic sea ice (Bellingshausen Sea). *Aquatic Microbial Ecology*, *35*. https://doi.org/10.3354/ame035283

Meng, S., & Liu, Y. (2016). New insights into transparent exopolymer particles (TEP) formation from precursor materials at various Na+/Ca 2+ ratios. *Scientific Reports*, *6*(19747). https://doi.org/10.1038/srep19747

Meon, B., & Amon, R. M. W. (2004). Heterotrophic bacterial activity and fluxes of dissolved free amino acids and glucose in the Arctic rivers Ob,

Yenisei and the adjacent Kara Sea. *Aquatic Microbial Ecology*, *37*(2). https://doi.org/10.3354/ame037121

Le Moigne, F. A. C. (2019). Pathways of Organic Carbon Downward Transport by the Oceanic Biological Carbon Pump. *Frontiers in Marine Science*, *6*(634). https://doi.org/10.3389/fmars.2019.00634

Murphy, J., & Riley, J. P. (1962). A modified single solution method for the determination of phosphate in natural waters. *Analytica Chimica Acta*, *27*. https://doi.org/10.1016/S0003-2670(00)88444-5

Myklestad, S. M., & Børsheim, K. Y. (2007). Dynamics of carbohydrates in the Norwegian Sea inferred from monthly profiles collected during 3 years at 66°N, 2°E. *Marine Chemistry*, *107*. https://doi.org/10.1016/j.marchem.2007.09.002

Nakagawa, S., & Schielzeth, H. (2013). A general and simple method for obtaining R2 from generalized linear mixed-effects models. *Methods in Ecology and Evolution*, *4*(2). https://doi.org/10.1111/j.2041-210x.2012.00261.x

National Snow Snow Ice Data Center. (2018). Arctic sea ice at minimum extent for 2018. Retrieved from https://nsidc.org/news/newsroom/arctic-sea-ice-2018-minimum-extent

Nghiem, S. V., Chao, Y., Neumann, G., Li, P., Perovich, D. K., Street, T., & Clemente-Colón, P. (2006). Depletion of perennial sea ice in the East Arctic Ocean. *Geophysical Research Letters*, *33*(174). https://doi.org/10.1029/2006GL027198

Nguyen, D., Maranger, R., Tremblay, J. É., & Gosselin, M. (2012). Respiration and bacterial carbon dynamics in the Amundsen Gulf, western Canadian Arctic. *Journal of Geophysical Research: Oceans*, *117*(C9). https://doi.org/10.1029/2011JC007343

Norman, L., Thomas, D. N., Stedmon, C. A., Granskog, M. A., Papadimitriou, S., Krapp, R. H., et al. (2011). The characteristics of dissolved organic matter (DOM) and chromophoric dissolved organic matter (CDOM) in Antarctic sea ice. *Deep-Sea Research Part II: Topical Studies in Oceanography*, *58*(9–10). https://doi.org/10.1016/j.dsr2.2010.10.030

Nöthig, E.-M., Bracher, A., Engel, A., Metfies, K., Niehoff, B., Peeken, I., et al. (2015). Summertime plankton ecology in Fram Strait - a compilation of long- and short-term observations. *Polar Research*, *34*(1). https://doi.org/10.3402/polar.v34.23349

Nöthig, E.-M., Ramondenc, S., Haas, A., Hehemann, L., Walter, A., Bracher, A., et al. (2020). Summertime Chlorophyll a and Particulate Organic Carbon Standing Stocks in Surface Waters of the Fram Strait and the Arctic Ocean (1991–2015). *Frontiers in Marine Science*, *7*(350). https://doi.org/10.3389/fmars.2020.00350

Notz, D., & Stroeve, J. (2016). Observed Arctic sea-ice loss directly follows anthropogenic CO 2 emission. *Science*, *354*(6313). https://doi.org/10.1126/science.aag2345

Ogawa, H., & Tanoue, E. (2003). Dissolved organic matter in oceanic waters. *Journal of Oceanography*, *59*(2). https://doi.org/10.1023/A:1025528919771

Oksanen, J., Blanchet, F. G., Friendly, M., Kindt, R., Legendre, P., Mcglinn, D., et al. (2019). Package “vegan” Community Ecology Package Version 2.5-6.

Orellana, M. V., & Leck, C. (2015). Marine Microgels. In *Biogeochemistry of Marine Dissolved Organic Matter: Second Edition* (pp. 451–480). https://doi.org/10.1016/B978-0-12-405940-5.00009-1

Orkney, A., Platt, T., Narayanaswamy, B. E., Kostakis, I., & Bouman, H. A. (2020). Bio-optical evidence for increasing Phaeocystis dominance in the Barents Sea. *Philosophical Transactions. Series A, Mathematical, Physical, and Engineering Sciences*. https://doi.org/10.1098/rsta.2019.0357

Ortega-Retuerta, E., Fichot, C. G., Arrigo, K. R., Van Dijken, G. L., & Joux, F. (2014). Response of marine bacterioplankton to a massive under-ice phytoplankton bloom in the Chukchi Sea (Western Arctic Ocean). *Deep-Sea Research Part II: Topical Studies in Oceanography*, *105*. https://doi.org/10.1016/j.dsr2.2014.03.015

Ortega-Retuerta, E., Marrasé, C., Muñoz-Fernández, A., Sala, M. M., Simó, R., & Gasol, J. M. (2018). Seasonal dynamics of transparent exopolymer particles (TEP) and their drivers in the coastal NW Mediterranean Sea. *Science of the Total Environment*, *631–632*. https://doi.org/10.1016/j.scitotenv.2018.02.341

Pakulski, J. D., & Benner, R. (1994). Abundance and distribution of carbohydrates in the ocean. *Limnology and Oceanography*, *39*(4). https://doi.org/10.4319/lo.1994.39.4.0930

Panagiotopoulos, C., & Sempéré, R. (2005). Analytical methods for the determination of sugars in marine samples: A historical perspective and future directions. *Limnology and Oceanography: Methods*, *3*(10). https://doi.org/10.4319/lom.2005.3.419

Panagiotopoulos, C., Sempéré, R., Jacq, V., & Charrière, B. (2014). Composition and distribution of dissolved carbohydrates in the Beaufort Sea Mackenzie margin (Arctic Ocean). *Marine Chemistry*, *166*. https://doi.org/10.1016/j.marchem.2014.09.004

Parada, A. E., Needham, D. M., & Fuhrman, J. A. (2016). Every base matters: assessing small subunit rRNA primers for marine microbiomes with mock communities, time series and global field samples. *Environmental Microbiology*, *18*(5). https://doi.org/10.1111/1462-2920.13023

Parker, B. C., & Diboll, A. G. (1966). Alcian Stains for Histochemical Localization of Acid and Sulfated Polysaccharides in Algae. *Phycologia*, *6*. https://doi.org/10.2216/i0031-8884-6-1-37.1

Passow, U. (2002). Transparent exopolymer particles (TEP) in aquatic environments. *Progress in Oceanography*, *55*(3–4). https://doi.org/10.1016/S0079-6611(02)00138-6

Paulsen, M. L., Doré, H., Garczarek, L., Seuthe, L., Müller, O., Sandaa, R.-A., et al. (2016). Synechococcus in the Atlantic Gateway to the Arctic Ocean. *Frontiers in Marine Science*, *3*(191). https://doi.org/10.3389/fmars.2016.00191

PEBCAO. (2020). Retrieved from https://www.awi.de/en/science/biosciences/polar-biological-oceanography/main-research-focus/arctic-plankton-ecology-and-related-sedimentary-flux/pebcao.html

Piechura, J., & Walczowski, W. (2009). Warming of the West Spitsbergen Current and sea ice north of Svalbard. *Oceanologia*. https://doi.org/10.5697/oc.51-2.147

Pinheiro, J., Bates, D., DebRoy, S., Deepayan, S. and, & Team, R. C. (2020). nlme: Linear and Nonlinear Mixed Effects Models. Retrieved from https://cran.r-project.org/web/packages/nlme/nlme.pdf

Piontek, J., Händel, N., De Bodt, C., Harlay, J., Chou, L., & Engel, A. (2011). The utilization of polysaccharides by heterotrophic bacterioplankton in the Bay of Biscay (North Atlantic Ocean). *Journal of Plankton Research*, *33*(11). https://doi.org/10.1093/plankt/fbr069

Piontek, J., Sperling, M., Nöthig, E.-M., & Engel, A. (2014). Regulation of bacterioplankton activity in Fram Strait (Arctic Ocean) during early summer: The role of organic matter supply and temperature. *Journal of Marine Systems*, *132*. https://doi.org/10.1016/j.jmarsys.2014.01.003

Piontek, J., Sperling, M., Nöthig, E.-M., & Engel, A. (2015). Multiple environmental changes induce interactive effects on bacterial degradation activity in the arctic ocean. *Limnology and Oceanography*, *60*(4). https://doi.org/10.1002/lno.10112

Piontek, J., Galgani, L., Nöthig, E.-M., Peeken, I., & Engel, A. (2020). Organic matter composition and heterotrophic bacterial activity at declining summer sea ice in the central Arctic Ocean. *Limnology and Oceanography*, *66*(S1). https://doi.org/10.1002/lno.11639

Polyakov, I. V., Pnyushkov, A. V., Alkire, M. B., Ashik, I. M., Baumann, T. M., Carmack, E. C., et al. (2017). Greater role for Atlantic inflows on sea-ice loss in the Eurasian Basin of the Arctic Ocean. *Science*, *356*(6335). https://doi.org/10.1126/science.aai8204

Pomeroy, L. R. (1974). The Ocean's Food Web, A Changing Paradigm. *BioScience*, *24*(9). https://doi.org/10.2307/1296885

Pomeroy, L. R., & Deibel, D. (1986). Temperature regulation of bacterial activity during the spring bloom in Newfoundland coastal waters. *Science*, *233*(4761). https://doi.org/10.1126/science.233.4761.359

Pomeroy, L. R., & Wiebe, W. J. (2001). Temperature and substrates as interactive limiting factors for marine heterotrophic bacteria. *Aquatic Microbial Ecology*, *23*(2). https://doi.org/10.3354/ame023187

Popendorf, K. J., Koblížek, M., & Van Mooy, B. A. S. (2020). Phospholipid turnover rates suggest that bacterial community growth rates in the open ocean are systematically underestimated. *Limnology and Oceanography*, *65*(8). https://doi.org/10.1002/lno.11424

Popova, E. E., Yool, A., Coward, A. C., Aksenov, Y. K., Alderson, S. G., De Cuevas, B. A., & Anderson, T. R. (2010). Control of primary production in the Arctic by nutrients and light: Insights from a high resolution ocean general circulation model. *Biogeosciences*, *7*(11). https://doi.org/10.5194/bg-7-3569-2010

Popova, E. E., Yool, A., Coward, A. C., Dupont, F., Deal, C., Elliott, S., et al. (2012). What controls primary production in the Arctic Ocean? Results from an intercomparison of five general circulation models with biogeochemistry. *Journal of Geophysical Research: Oceans*, *117*(C8). https://doi.org/10.1029/2011JC007112

Poulin, M., Underwood, G. J. C., & Michel, C. (2014). Sub-ice colonial Melosira arctica in Arctic first-year ice. *Diatom Research*, *29*(2). https://doi.org/10.1080/0269249X.2013.877085

Qian, J., & Mopper, K. (1996). Automated High-Performance, High-Temperature Combustion Total Organic Carbon Analyzer. *Analytical Chemistry*, *68*(18). https://doi.org/10.1021/ac960370z

Quigg, A., Finkel, Z. V., Irwin, A. J., Rosenthal, Y., Ho, T. Y., Reinfelder, J. R., et al. (2003). The evolutionary inheritance of elemental stoichiometry in marine phytoplankton. *Nature*, *425*. https://doi.org/10.1038/nature01953

Quigg, A., Irwin, A. J., & Finkel, Z. V. (2011). Evolutionary inheritance of elemental stoichiometry in phytoplankton. *Proceedings of the Royal Society B: Biological Sciences*, *278*(1705). https://doi.org/10.1098/rspb.2010.1356

Randelhoff, A., Reigstad, M., Chierici, M., Sundfjord, A., Ivanov, V., Cape, M., et al. (2018). Seasonality of the Physical and Biogeochemical Hydrography in the Inflow to the Arctic Ocean Through Fram Strait. *Frontiers in Marine Science*, *5*(224). https://doi.org/10.3389/fmars.2018.00224

Rapp, J. Z., Fernández-Méndez, M., Bienhold, C., & Boetius, A. (2018). Effects of Ice-Algal Aggregate Export on the Connectivity of Bacterial Communities in the Central Arctic Ocean. *Frontiers in Microbiology*, *9*(1035). https://doi.org/10.3389/fmicb.2018.01035

Read, D. S., Bowes, M. J., Newbold, L. K., & Whiteley, A. S. (2014). Weekly flow cytometric analysis of riverine phytoplankton to determine seasonal bloom dynamics. *Environmental Sciences: Processes and Impacts*, *16*(3). https://doi.org/10.1039/c3em00657c

Reid, P. C., Lancelot, C., Gieskes, W. W. C., Hagmeier, E., & Weichart, G. (1990). Phytoplankton of the North Sea and its dynamics: A review. *Netherlands Journal of Sea Research*. https://doi.org/10.1016/0077-7579(90)90094-W

Reigstad, M., & Wassmann, P. (2007). Does Phaeocystis spp. contribute significantly to vertical export of organic carbon? *Biogeochemistry*, *83*(1). https://doi.org/10.1007/s10533-007-9093-3

Reintjes, G., Arnosti, C., Fuchs, B. M., & Amann, R. (2017). An alternative polysaccharide uptake mechanism of marine bacteria. *ISME Journal*, *11*(7). https://doi.org/10.1038/ismej.2017.26

Reintjes, G., Arnosti, C., Fuchs, B., & Amann, R. (2019). Selfish, sharing and scavenging bacteria in the Atlantic Ocean: a biogeographical study of bacterial substrate utilisation. *ISME Journal*, *13*. https://doi.org/10.1038/s41396-018-0326-3

Rich, J., Gosselin, M., Sherr, E., Sherr, B., & Kirchman, D. L. (1997). High bacterial production, uptake and concentrations of dissolved organic matter in the Central Arctic Ocean. *Deep-Sea Research Part II: Topical Studies in Oceanography*, *44*(8). https://doi.org/10.1016/S0967-0645(97)00058-1

Riedel, A., Michel, C., Gosselin, M., & LeBlanc, B. (2007). Enrichment of nutrients, exopolymeric substances and microorganisms in newly formed sea ice on the Mackenzie shelf. *Marine Ecology Progress Series*, *342*. https://doi.org/10.3354/meps342055

Robertson, B. R., & Button, D. K. (1989). Characterizing aquatic bacteria according to population, cell size, and apparent DNA content by flow cytometry. *Cytometry*, *10*(1). https://doi.org/10.1002/cyto.990100112

Sabine, C. L., Heimann, M., Artaxo, P., Bakker, D. C. E., Chen, C.-T., Field, C. B., et al. (2004). Current Status and Past Trends of the Global Carbon Cycle. In *The Global Carbon Cycle: Integrating Humans, Climate, and the Natural World* (pp. 17–44).

Sakshaug, E. (2004). Primary and Secondary Production in the Arctic Seas. In *The Organic Carbon Cycle in the Arctic Ocean* (pp. 55–81). https://doi.org/10.1007/978-3-642-18912-8_3

Sala, M. M., Terrado, R., Lovejoy, C., Unrein, F., & Pedrós-Alió, C. (2008). Metabolic diversity of heterotrophic bacterioplankton over winter and spring in the coastal Arctic Ocean. *Environmental Microbiology*, *10*(4). https://doi.org/10.1111/j.1462-2920.2007.01513.x

Sala, M. M., Arrieta, J. M., Boras, J. A., Duarte, C. M., & Vaqué, D. (2010). The impact of ice melting on bacterioplankton in the Arctic Ocean. *Polar Biology*, *33*(12). https://doi.org/10.1007/s00300-010-0808-x

Sarmiento, J. L., & Gruber, N. (2006). *Ocean Biogeochemical Dynamics*. *Princeton University Press*. Princeton University Press. https://doi.org/10.2307/j.ctt3fgxqx

Schauer, U., Beszczynska-Möller, A., Walczowski, W., Fahrbach, E., Piechura, J., & Hansen, E. (2008). Variation of Measured Heat Flow Through the Fram Strait Between 1997 and 2006. In *Arctic–Subarctic Ocean Fluxes* (pp. 65–85). Dordrecht: Springer Netherlands. https://doi.org/10.1007/978-1-4020-6774-7_4

Schuster, S., & Herndl, G. J. (1995). Formation and significance of trasparent exopolymeric particles in the northern Adriatic Sea. *Marine Ecology Progress Series*, *124*(1–3). https://doi.org/10.3354/meps124227

Seifert, M., Hoppema, M., Burau, C., Friedrichs, A., Geuer, J. K., John, U., et al. (2019). Influence of glacial meltwater on summer biogeochemical cycles in Scoresby Sund, East Greenland. *Frontiers in Marine Science*. https://doi.org/10.3389/fmars.2019.00412

Serreze, M. C., Barrett, A. P., Slater, A. G., Woodgate, R. A., Aagaard, K., Lammers, R. B., et al. (2006). The large-scale freshwater cycle of the Arctic. *Journal of Geophysical Research: Oceans*, *111*(C11). https://doi.org/10.1029/2005JC003424

Serreze, M. C., Holland, M. M., & Stroeve, J. (2007). Perspectives on the Arctic's Shrinking Sea-Ice Cover. *Science*, *315*.

Sharp, J. H. (1974). Improved analysis for "particulate" organic carbon and nitrogen from seawater. *Limnology and Oceanography*, *19*(6). https://doi.org/10.4319/lo.1974.19.6.0984

Shen, Y., Fichot, C. G., & Benner, R. (2012). Dissolved organic matter composition and bioavailability reflect ecosystem productivity in the Western Arctic Ocean. *Biogeosciences*, *9*(7). https://doi.org/10.5194/bg-9-4993-2012

Shen, Y., Benner, R., Kaiser, K., Fichot, C. G., & Whitledge, T. E. (2018). Pan-Arctic Distribution of Bioavailable Dissolved Organic Matter and Linkages With Productivity in Ocean Margins. *Geophysical Research Letters*, *45*(3). https://doi.org/10.1002/2017GL076647

Sherr, B., & Sherr, E. (2003). Community respiration/production and bacterial activity in the upper water column of the central Arctic Ocean. *Deep Sea Research Part I: Oceanographic Research Papers*, *50*(4). https://doi.org/10.1016/S0967-0637(03)00030-X

Sherr, E., Sherr, B., Wheeler, P. A., & Thompson, K. (2003). Temporal and spatial variation in stocks of autotrophic and heterotrophic microbes in the upper water column of the central Arctic Ocean. *Deep-Sea Research Part I: Oceanographic Research Papers*, *50*(5).

https://doi.org/10.1016/S0967-0637(03)00031-1
Sherr, E., Sherr, B., & Longnecker, K. (2006). Distribution of bacterial abundance and cell-specific nucleic acid content in the Northeast Pacific Ocean. *Deep-Sea Research Part I: Oceanographic Research Papers*, *53*(4). https://doi.org/10.1016/j.dsr.2006.02.001
Simon, M., & Azam, F. (1989). Protein content and protein synthesis rates of planktonic marine bacteria. *Marine Ecology Progress Series*, *51*. https://doi.org/10.3354/meps051201
Sipler, R. E., Kellogg, C. T. E., Connelly, T. L., Roberts, Q. N., Yager, P. L., & Bronk, D. A. (2017). Microbial community response to terrestrially derived dissolved organic matter in the coastal Arctic. *Frontiers in Microbiology*, *8*(1018). https://doi.org/10.3389/fmicb.2017.01018
Skoog, A., & Benner, R. (1997). Aldoses in various size fractions of marine organic matter: Implications for carbon cycling. *Limnology and Oceanography*, *42*(8). https://doi.org/10.4319/lo.1997.42.8.1803
Smetacek, V. (2000). The giant diatom dump. *Nature*, *406*(6796). https://doi.org/10.1038/35020665
Smith, D. C., & Azam, F. (1992). A simple, economical method for measuring bacterial protein synthesis rates in seawater using 3H-leucine. *Marine Microbial Food Webs*, *6*(2).
Soltwedel, T., Portnova, D., Kolar, I., Mokievsky, V., & Schewe, I. (2005). The small-sized benthic biota of the Håkon Mosby Mud Volcano (SW Barents Sea slope). *Journal of Marine Systems*. https://doi.org/10.1016/j.jmarsys.2004.09.001
Soltwedel, T., Schauer, U., Boebel, O., Nothig, E.-M., Bracher, A., Metfies, K., et al. (2013). FRAM - FRontiers in Arctic marine Monitoring Visions for permanent observations in a gateway to the Arctic Ocean. *OCEANS 2013 MTS/IEEE Bergen: The Challenges of the Northern Dimension*. https://doi.org/10.1109/OCEANS-Bergen.2013.6608008
Soltwedel, T., Bauerfeind, E., Bergmann, M., Bracher, A., Budaeva, N., Busch, K., et al. (2016). Natural variability or anthropogenically-induced variation? Insights from 15 years of multidisciplinary observations at the arctic marine LTER site HAUSGARTEN. *Ecological Indicators*, *65*. https://doi.org/10.1016/j.ecolind.2015.10.001
Spring, S., Bunk, B., Spröer, C., Schumann, P., Rohde, M., Tindall, B. J., & Klenk, H. P. (2016). Characterization of the first cultured representative of Verrucomicrobia subdivision 5 indicates the proposal of a novel phylum. *ISME Journal*, *10*(12). https://doi.org/10.1038/ismej.2016.84
Ssekagiri, A., & Ijaz, U. Z. (2020). microbiomeSeq: Microbial community analysis in an environmental context. Retrieved from www.github.com/umerijaz/microbiomeSeq
de Steur, L., Hansen, E., Gerdes, R., Karcher, M., Fahrbach, E., & Holfort, J. (2009). Freshwater fluxes in the East Greenland Current: A decade of observations. *Geophysical Research Letters*, *36*(23). https://doi.org/10.1029/2009gl041278
Stocker, R. (2012). Marine microbes see a sea of gradients. *Science*, *338*(6107). https://doi.org/10.1126/science.1208929
Sugimura, Y., & Suzuki, Y. (1988). A high-temperature catalytic oxidation method for the determination of non-volatile dissolved organic carbon in seawater by direct injection of a liquid sample. *Marine Chemistry*, *24*(2). https://doi.org/10.1016/0304-4203(88)90043-6

Swan, B. K., Martinez-Garcia, M., Preston, C. M., Sczyrba, A., Woyke, T., Lamy, D., et al. (2011). Potential for chemolithoautotrophy among ubiquitous bacteria lineages in the dark ocean. *Science*, *333*(6047). https://doi.org/10.1126/science.1203690

Teeling, H., Fuchs, B. M., Becher, D., Klockow, C., Gardebrecht, A., Bennke, C. M., et al. (2012). Substrate-controlled succession of marine bacterioplankton populations induced by a phytoplankton bloom. *Science*, *336*(6081). https://doi.org/10.1126/science.1218344

Teira, E., Pazó, M. J., Serret, P., & Fernández, E. (2001). Dissolved organic carbon production by microbial populations in the Atlantic Ocean. *Limnology and Oceanography*, *46*(6). https://doi.org/10.4319/lo.2001.46.6.1370

Teira, E., Abalde, J., Álvarez-Ossorio, M. T., Bode, A., Cariño, C., Cid, Á., et al. (2003). Plankton carbon budget in a coastal wind-driven upwelling station off a Coruña (NW Iberian Peninsula). *Marine Ecology Progress Series*, *265*. https://doi.org/10.3354/meps265031

Thingstad, T. F., Bellerby, R. G. J., Bratbak, G., Børsheim, K. Y., Egge, J. K., Heldal, M., et al. (2008). Counterintuitive carbon-to-nutrient coupling in an Arctic pelagic ecosystem. *Nature*, *455*. https://doi.org/10.1038/nature07235

Thornton, D. C. O. (2014). Dissolved organic matter (DOM) release by phytoplankton in the contemporary and future ocean. *European Journal of Phycology*, *49*(1). https://doi.org/10.1080/09670262.2013.875596

Thornton, D. C. O. (2018). Coomassie Stainable Particles (CSP): Protein containing exopolymer particles in the ocean. *Frontiers in Marine Science*, *5*(206). https://doi.org/10.3389/fmars.2018.00206

Tippenhauer, S., Janout, M., Chouksey, M., Torres-Valdes, S., Fong, A., & Wulff, T. (2021). Substantial Sub-Surface Chlorophyll Patch Sustained by Vertical Nutrient Fluxes in Fram Strait Observed With an Autonomous Underwater Vehicle. *Frontiers in Marine Science*, *8*(605225). https://doi.org/10.3389/fmars.2021.605225

Torres-Valdés, S., Tsubouchi, T., Bacon, S., Naveira-Garabato, A. C., Sanders, R., McLaughlin, F. A., et al. (2013). Export of nutrients from the Arctic Ocean. *Journal of Geophysical Research: Oceans*, *118*(4). https://doi.org/10.1002/jgrc.20063

Underwood, G. J. C., Michel, C., Meisterhans, G., Niemi, A., Belzile, C., Witt, M., et al. (2019). Organic matter from Arctic sea-ice loss alters bacterial community structure and function. *Nature Climate Change*, *9*(2). https://doi.org/10.1038/s41558-018-0391-7

Vaqué, D., Guadayol, Ò., Peters, F., Felipe, J., Angel-Ripoll, L., Terrado, R., et al. (2008). Seasonal changes in planktonic bacterivory rates under the ice-covered coastal Arctic Ocean. *Limnology and Oceanography*, *53*(6). https://doi.org/10.4319/lo.2008.53.6.2427

Verbeke, G., & Molenberghs, G. (2000). *Linear Mixed Models for Longitudinal Data*. *Springer Series in Statistics*. NY, USA: Springer.

Verdugo, P. (2012). Marine Microgels. *Annual Review of Marine Science*, *4*(1). https://doi.org/10.1146/annurev-marine-120709-142759

Verdugo, P., Alldredge, A. L., Azam, F., Kirchman, D. L., Passow, U., & Santschi, P. H. (2004). The oceanic gel phase: A bridge in the DOM-POM continuum. *Marine Chemistry*, *92*(1–4). https://doi.org/10.1016/j.marchem.2004.06.017

Vernet, M., Richardson, T. L., Metfies, K., Nöthig, E.-M., & Peeken, I. (2017). Models of Plankton Community Changes during a Warm Water Anomaly in Arctic Waters Show Altered Trophic Pathways with Minimal Changes in Carbon Export. *Frontiers in Marine Science*, *4*(160). https://doi.org/10.3389/fmars.2017.00160

Vernet, M., Ellingsen, I. H., Seuthe, L., Slagstad, D., Cape, M. R., & Matrai, P. A. (2019). Influence of Phytoplankton Advection on the Productivity Along the Atlantic Water Inflow to the Arctic Ocean. *Frontiers in Marine Science*, *6*(583). https://doi.org/10.3389/fmars.2019.00583

Vihtakari, M. (2020). PlotSvalbard: PlotSvalbard - Plot research data from Svalbard on maps. Retrieved from https://github.com/MikkoVihtakari/PlotSvalbard

Volk, T., & Hoffert, M. I. (1985). Ocean carbon pumps: analysis of relative strengths and efficiencies in ocean-driven atmospheric CO2 changes. *The Carbon Cycle and Atmospheric CO*, *32*. https://doi.org/10.1029/gm032p0099

Wagner, S., Schubotz, F., Kaiser, K., Hallmann, C., Waska, H., Rossel, P. E., et al. (2020). Soothsaying DOM: A Current Perspective on the Future of Oceanic Dissolved Organic Carbon. *Frontiers in Marine Science*, *7*(341). https://doi.org/10.3389/fmars.2020.00341

Walczowski, W., Beszczynska-Möller, A., Wieczorek, P., Merchel, M., & Grynczel, A. (2017). Oceanographic observations in the Nordic Sea and Fram Strait in 2016 under the IO PAN long-term monitoring program AREX. *Oceanologia*, *59*(2). https://doi.org/10.1016/j.oceano.2016.12.003

Ward, C. S., Yung, C. M., Davis, K. M., Blinebry, S. K., Williams, T. C., Johnson, Z. I., & Hunt, D. E. (2017). Annual community patterns are driven by seasonal switching between closely related marine bacteria. *ISME Journal*, *11*. https://doi.org/10.1038/ismej.2017.4

Wassmann, P., Duarte, C. M., Agustí, S., & Sejr, M. K. (2011). Footprints of climate change in the Arctic marine ecosystem. *Global Change Biology*, *17*(2). https://doi.org/10.1111/j.1365-2486.2010.02311.x

Wassmann, P., Carmack, E. C., Bluhm, B. A., Duarte, C. M., Berge, J., Brown, K., et al. (2020). Towards a unifying pan-arctic perspective: A conceptual modelling toolkit. *Progress in Oceanography*, *189*. https://doi.org/10.1016/j.pocean.2020.102455

Wauthy, M., Rautio, M., Christoffersen, K. S., Forsström, L., Laurion, I., Mariash, H. L., et al. (2018). Increasing dominance of terrigenous organic matter in circumpolar freshwaters due to permafrost thaw. *Limnology and Oceanography Letters*, *3*(3). https://doi.org/10.1002/lol2.10063

Weber, T., & Deutsch, C. (2012). Oceanic nitrogen reservoir regulated by plankton diversity and ocean circulation. *Nature*, *489*. https://doi.org/10.1038/nature11357

Weber, T. S., & Deutsch, C. (2010). Ocean nutrient ratios governed by plankton biogeography. *Nature*. https://doi.org/10.1038/nature09403

Wegener, G., Bausch, M., Holler, T., Thang, N. M., Prieto Mollar, X., Kellermann, M. Y., et al. (2012). Assessing sub-seafloor microbial activity by combined stable isotope probing with deuterated water and 13C-bicarbonate. *Environmental Microbiology*, *14*(6). https://doi.org/10.1111/j.1462-2920.2012.02739.x

Wegener, G., Kellermann, M. Y., & Elvert, M. (2016). Tracking activity and function of microorganisms by stable isotope probing of membrane lipids. *Current Opinion in Biotechnology*, *41*. https://doi.org/10.1016/j.copbio.2016.04.022

Wickham, H. (2016). tidyverse: Easily Install and Load “Tidyverse” Packages. Retrieved from https://cran.r-project.org/package=tidyverse

Wiebe, W. J., Sheldon, W. M., & Pomeroy, L. R. (1992). Bacterial growth in the cold: Evidence for an enhanced substrate requirement. *Applied and Environmental Microbiology*, *58*(1).

Wietz, M., Bienhold, C., Metfies, K., Torres-Valdés, S., von Appen, W.-J., Salter, I., & Boetius, A. (2021). The polar night shift: seasonal dynamics and drivers of Arctic Ocean microbiomes revealed by autonomous sampling. *ISME Communications*, *1*(76). https://doi.org/10.1038/s43705-021-00074-4

Wilson, B., Müller, O., Nordmann, E.-L., Seuthe, L., Bratbak, G., & Øvreås, L. (2017). Changes in Marine Prokaryote Composition with Season and Depth Over an Arctic Polar Year. *Frontiers in Marine Science*, *4*(95). https://doi.org/10.3389/fmars.2017.00095

Wohlers, J., Engel, A., Zöllner, E., Breithaupt, P., Jürgens, K., Hoppe, H. G., et al. (2009). Changes in biogenic carbon flow in response to sea surface warming. *Proceedings of the National Academy of Sciences of the United States of America*, *106*(17). https://doi.org/10.1073/pnas.0812743106

Worden, A. Z., Nolan, J. K., & Palenik, B. (2004). Assessing the dynamics and ecology of marine picophytoplankton: The importance of the eukaryotic component. *Limnology and Oceanography*, *49*(1). https://doi.org/10.4319/lo.2004.49.1.0168

Wright, K. (2018). corrgram: Plot a Correlogram. Retrieved from https://cran.r-project.org/package=corrgram

Yelton, A. P., Acinas, S. G., Sunagawa, S., Bork, P., Pedrós-Alió, C., & Chisholm, S. W. (2016). Global genetic capacity for mixotrophy in marine picocyanobacteria. *ISME Journal*, *10*. https://doi.org/10.1038/ismej.2016.64

Yilmaz, P., Kottmann, R., Field, D., Knight, R., Cole, J. R., Amaral-Zettler, L., et al. (2011). Minimum information about a marker gene sequence (MIMARKS) and minimum information about any (x) sequence (MIxS) specifications. *Nature Biotechnology*, *29*(5). https://doi.org/10.1038/nbt.1823

Zäncker, B., Engel, A., & Cunliffe, M. (2019). Bacterial communities associated with individual transparent exopolymer particles (TEP). *Journal of Plankton Research*, *41*(4). https://doi.org/10.1093/plankt/fbz022

Zhong, H., Zhong, H., Lehtovirta-Morley, L., Liu, J., Liu, J., Zheng, Y., et al. (2020). Novel insights into the Thaumarchaeota in the deepest oceans: Their metabolism and potential adaptation mechanisms. *Microbiome*, *8*(78). https://doi.org/10.1186/s40168-020-00849-2

Acknowledgments

My time as a doctoral researcher in Anja's group was exhilarating, challenging, and filled with many learning opportunities that make me look back very fondly on the past four years.

I would like to express my fullest gratitude to Prof. Dr. Anja Engel! Thank you for offering me the opportunity to pursue my scientific aspirations and giving me the opportunity to participate in five expeditions to the Arctic Ocean.

I am very grateful to Prof. Dr. Ute Hentschel Humeida for being the second reviewer and co-supervising my thesis. Thank you for your helpful comments during the ISOS committee meetings and your continued support throughout my thesis.

I would like to thank Prof. Dr. Hermann Bange for examining this thesis and being part of my defense committee.

I would like to thank Dr. Judith Piontek for co-supervising my thesis. Thank you for attending the bi-annual ISOS committee meetings via skype when online conferences were still an irregularity, and we never thought that they would take over our lives. Thank you for the helpful advice you have given me throughout my thesis.

I would like to thank everyone who was part of or affiliated with the BMBF NERC Changing Arctic Ocean MicroARC project. I really enjoyed the positive and enthusiastic conversations held throughout this successful project, whether in Plymouth or online. In particular, I would like to thank Vanessa, who was such a wonderful officemate, the best PhD twin I could have asked for, and a genuinely great friend!

Thank you to:

- Anni, Lindsay, Alba, Carolina, Quentin, Sasha, Helmke, Vivienne, Monika, and Cathleen for all the kind support and conversations we had during my PhD
- Ruth, Jon, Tania, and Sandra for analyzing many of the samples that were used in this thesis.
- Kevin for being so supportive and helping me so much to write the second paper, along with the numerous cups of coffee we downed in discussing how cool science is. I don't know what my PhD would have been without you!
- All the friends I made during the expeditions (PS114, MSM77, AL519, PS121, PS126, ArcticCentury).
- PS121 Mädels for being the coolest group of girls that I could have asked for to make PS121 expedition so memorable.
- Theresa for figuring out how to tackle PhD hurdles together and I am grateful for taking the time to read my manuscript draft and thesis when I didn't know how to move forward.
- Sonja for having my back and being my true pandemic buddy and I am so thankful for our facetime calls.

- Sandra for being so positive, encouraging, and a great friend.
- Vero for the incredible friendship we have built since we got assigned to be hobby physical oceanographers during PS121.
- David for proofreading, cooking for me, and being so patient with me.
- my parents, my sister (“duuuuude”), and my brother. I cannot begin to express how grateful I am for your support throughout this.

Eidesstattliche Erklärung

Hiermit bestätige ich, dass die vorliegende Arbeit mit dem Titel:

“Seasonal Dynamics of Organic Matter Turnover in the Arctic Ocean”

von mir selbstständig verfasst worden ist und hat, abgesehen von der Beratung durch die Betreuerin, keine weiteren Hilfsmittel verwendet. Die vorliegende Arbeit ist unter Einhaltung der Regeln guter wissenschaftlicher Praxis der Deutschen Forschungsgemeinschaft entstanden und wurde nicht im Rahmen eines Prüfungsverfahrens an anderer Stelle vorgelegt. Veröffentlichte oder zur Veröffentlichung eingereichte Manuskripte wurden kenntlich gemacht. Ich erkläre mich einverstanden, dass diese Arbeit an die Bibliothek des GEOMAR Helmholtz-Zentrum für Ozeanforschung Kiel und die Universitätsbibliothek der Christian-Albrechts-Universität zu Kiel weitergeleitet wird.

_____	_____
Ort, Datum	Anabel Charlott von Jackowski